地震研究所彙報別冊
Bull. Earthq. Res. Inst.
Univ. Tokyo
Suppl. Vol. IX (1997) 1-93

Characteristic Seismograms —Part 2—

Masaru TSUJIURA*

Preface

The purpose of this paper is to demonstrate useful seismograms to better understand seismic phenomena and to clarify the structure of the Earth's interior. Accordingly, in 1988, the seismogram collection entitled "Characteristic Seismograms" was published. This collection mainly made use of medium-period (MP), long-period (LP) and wide-band (WB) seismographs at Dodaira Seismological Observatory (DDR), and 100 sample seismograms with characteristic waveforms are collected.

For this paper, the seismograms were collected mainly at a point of "phase" using short-period vertical seismographs (SP-Z) of five stations belonging to the Dodaira Seismological network. Data for the period from 1968 to 1984 are re-examined, and 38 samples including some special seismograms related to the source process of an earthquake were selected for the present study.

In general, the waveforms in seismograms, especially an appearance of phase, differ from region to region, even for an event with similar epicentral distances, source depths and earthquake sizes. Moreover, earthquake occurrences in a specific region are another factor for study. It is, therefore, necessary to collect data over a long period.

Seismograms are separated into seismic regions and are arranged by epicentral distance or source depth within the region. Among these samples, some of them are already well known, however, some new phases were obtained in this study. Seismograms contain a great variety of information. We hope that this collection will be useful to provide a better understanding of seismic phenomena and also new facts will be found.

* ; No. 33 Yaraicho Shinjuku-ku Tokyo, 162-0805, Japan

1. Introduction

In the previous paper of this series (TSUJIURA, 1988), seismograms with characteristic waveforms were collected using data from seismic stations belonging to the Dodaira network, Kanto District, Japan. One hundred samples with characteristic seismograms selecting in each seismic region, source depth, and epicentral distance were collected.

In general, the complexity of the Earth's structure provides seismograms with a great variety of waveforms. The waveform of the seismogram, especially the appearance of "phase" differs from region to region, even for events with similar epicentral distances, source depths and earthquake sizes, and such complexity gives clues for the study of the Earth's structure.

Another purpose of this paper is to demonstrate seismogram features relating to the source process of some event groups, such as foreshocks, main shock, aftershocks and earthquake swarms.

Recently, a new type of seismograph, *i.e.*, " STS " with wide-band and high-dynamic range, developed by WIELANDT and STRECKEISEN (1982) has been used world wide. Although our seismograms used here were obtained with conventional seismographs having a limited dynamic range and frequency band, they are still useful for detecting seismic phase and detailed studies of waveform features of earthquakes.

This seismogram collection demonstrates the following point :

1) Characteristic seismograms including phase and spectrum of earthquakes from local to world-wide scale.
2) The characteristic phase in a given seismic region and its relation to source depth.
3) Spatial behavior of seismic waves along the epicentral distance from 120 to 145 degrees.
4) Special features of seismograms of some event groups including foreshocks, main shocks, aftershocks and earthquake swarms.
5) The use of the same purpose of data as shown previously is avoided in this study, except for a few figures.

Thirty-eight samples were collected. In the former group (Figs. 1-30) are seismic phases, and in the latter group we show waveform features of the event groups mentioned above.

2. Data

The seismograms selected here were compiled from data of Dodaira Microearthquake Observatory (DDR) and its satellite stations. The locations of stations with their geological formations are shown in Figure A and Table 1.

Table 1. List of seismographic stations with local geology.

Station	Code	Location N			E			Altitude m	Formation
Dodaira	DDR	35°	59′	54″.0	139°	11′	36″.2	800	Chart
Tsukuba	TSK	36	12	39.0	140	06	35.0	280	Granite
Kiyosumi	KYS	35	11	51.6	140	08	53.6	180	Sandstone
Ohyama	OYM	35	25	12.3	139	14	34.9	600	Andesite
Shiroyama	SRY	35	30	30.0	139	16	27.0	254	Slate

All seismic signals were recorded at the Earthquake Research Institute (ERI), Tokyo by a telemetering system. DDR is the main station of our seismic network where various kinds of seismograph are operating. Detailed description of the system is given in the previous study of this series (TSUJIURA, 1988).

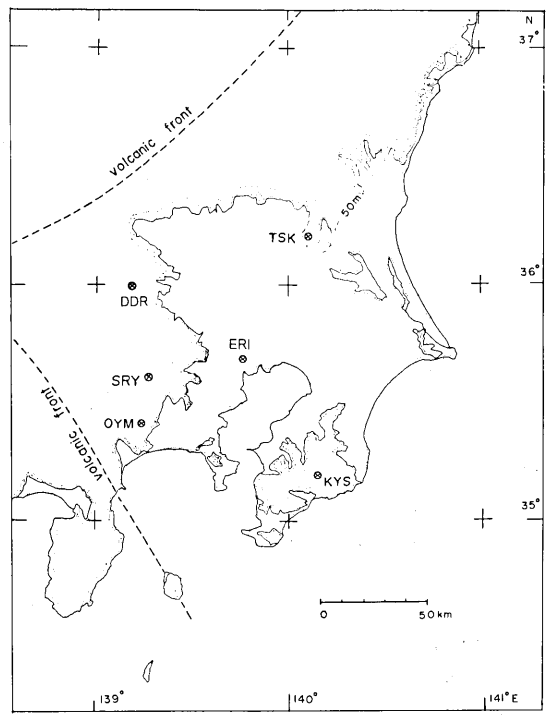

Fig. A. Distribution of seismographic stations.

Figure B shows the displacement magnification curves of the seismographs at DDR. The frequency characteristics of SP seismographs at other stations are almost the same for that of DDR, except for magnification for which there is a difference by a factor of five among the stations.

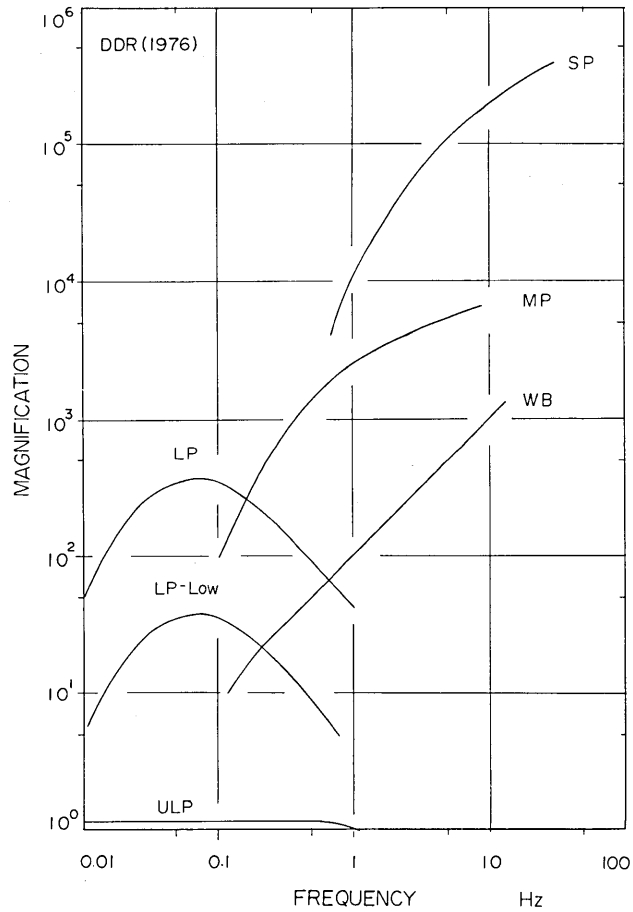

Fig. B. Displacement magnification curves of seismographs. Detailed description of the system has already been published (TSUJIURA, 1988).

In this collection, data from short-period vertical component seismographs (SP-Z) were re-examined during the period from 1968 to 1984. After 1985, the original data were recorded by the heat pen. These data cannot be used for the present study, because their records comprise thin traces. The paper speed of the original seismograms was 60 mm/min. The measured time of the phase for local earthquakes is, therefore, somewhat uncertain.

The seismograms are classified mainly according to region, as proposed by FLINN and ENGDAHL (1965), except for local earthquakes within an area of a few hundred kilometers. The source information e.g., epicenter, source depth (h) and magnitude

(M) for local earthquakes is obtained from the List of Earthquakes in the Kanto Area and its Vicinity provided by MATSU'URA *et al.* (1988), and the Bulletin of the International Seismological Centre (ISC) are used for near, regional and teleseismic events. The criterion of these events is followed to their epicentral distances as indicated in the Table 2.

A brief comments with a title are presented for each set of seismograms to emphasize the features of seismograms, and known phases are indicated when their arrival times agree to within a few seconds of the computed travel times given by JEFFREYS and BULLEN (1967). Phases with the label of "X" are unidentified arrivals, however, they are still useful for new studies. Finally, a few seismograms having characteristic waveforms are added to provide a better understanding of seismic phenomena.

3. Arrangement of seismograms

Seismograms with characteristic phases are arranged according to epicentral distance. Thirty-eight sets of seismograms including seismograms with special features were prepared for the present paper.

Table 2 lists the 38 sets with title, name of region and epicentral distance in degrees (Δ).

Table 2. List of seismograms.

No.*	Title	Region	Δ	Page
1	X phase, Local earthquakes (1)	Kanto	1	11
2	X phase, Local earthquakes (2)	Kanto	1	13
3	X phase, Near earthquakes (1)	E.C. Honshu	3-4	16
4	X phase, Near earthquakes (2)	E.C. Honshu S. Honshu	4-5	20
5	X phase, Near earthquakes (3)	S. Honshu	2-4	23
6	Comparison of seismograms	N., S. Honshu	3.5-4	25
7	T wave	S. Honshu	2-7.5	27
8	Reflected wave, Near earthq.	S. Honshu	3.7	29

* ; The symbol of No. corresponds to Figure number.

Table 2. List of seismograms (continued).

No.*	Title	Region	Δ	Page
9	Unidentified wave, Near earthq.	E.C. Honshu	2-3	
	Regional Eq.	S. Honshu	6.6	31
10	*X* phase, Regional earthq. (1)	Bonin Is.	7-8	33
11	*X* phase, Regional earthq. (2)	Bonin Is.	9	35
12	*X* phase, three regions Eq.	Marianas	17	
		E. Russia	11	
		Bonin Is.	9	37
13	*X* phase, Regional earthq.	Marianas	18	39
14	*X* phase, Regional earthq.	Okhotsk	18	41
15	*X* phase, Distant earthq.	Mindanao	32	43
16	*X* phase, Regional earthq.	Taiwan	18	45
17	Waveforms, *PcP*, *ScP*	Philippine-		
		Flores Sea	21-26	47
18	Waveforms, *ScS*, *ScP*	E. Russia-		
		Santa Cruz	11-54	49
19	*P*-Later phase, three regions	Solomon Is.	43-50	
		Fiji Is.	69-71	
		S. Italy	89	51
20	*P*-Later phase	Fiji Is.	66-72	53
21	*pP* phase	Alaska	45	55
22	Double phase, *pP*	Fiji Is.	68	57
23	Double phase, *pP*, three regions	S. Fiji Is.	71	
		Kermadec	79	
		Fiji Is.	70	59
24	*P3KP*, Near, Regional Eq.	N. Honshu	3	
		Kurile Is.	10	
		Philippine	22	61
25	*P3KP*, *P'P'* waves	S. Honshu		
		S. Fiji	3-72	63
26	*P'P'* wave	Solomon-		
		Samoa	45-70	65
27	*X* phase, Near-Distant Eq.	E. Honshu-		

Table 2. (continued)

No.*	Title	Region	Δ	Page
		Mindanao	3-28	67
28	*X* phase, Distant Eq.	Band Sea	45	69
29	*PKP* waves	Peru-	125-146	71
30	*PKP* waves (deep)	Colombia	135	75
31	*P* waveforms, large Eq. (1)	Solomon-	21-68	77
32	*P* waveforms, large Eq. (1)	Solomon Is.	49-50	79
33	*P* waveforms, moderate Eq.	Santa Cruz-	46-69	81
34	*P* waveforms, moderate Eq.	Taiwan-	20-77	83
35	Recurrent occurrence, Eq.Family	Miyakejima	2	85
36	Characteristic freq. Eq.Family	Kanto	0.1	87
37	Spectrum, Foreshocks	Kanto	2	89
38	Spectrum, Ordinary Eq.	Kanto	2	91

1. Seismograms with X phase from local earthquakes (1)

Many studies of later phases from local earthquakes have been performed, and their results are summarized by MATSUZAWA (1989). Most studies of these phases relate to converted or reflected wave at the upper boundary of a descending oceanic plate, and the locations of the upper boundary of the plate are estimated.

Local phases are seen on seismograms obtained from a short period vertical component seismograph (SP-Z) at Tsukuba station (TSK) for events in the Kanto area. Their epicenters and seismograms are shown in Figs. 1a and 1b, respectively. The source information taken from the List of Earthquakes in the Kanto Area and its Vicinity, edited by MATSU'URA *et al.* (1988), are summarized in Table 3. In this Table, No. is the event number corresponding to Fig. 1a. Origin time is Japanese Standard Time, h is source depth in km and M is magnitude determined from total duration time of the signal, respectively.

Table 3. List of source information.

No.	Origin Time					Epicenter		h	M
	y	d	h	m	s	N	E	km	
1	1978 Sept.	26	20	30	00.9	36°09′28″.4	141°27′38″.2	31.4	3.0
2	1980 Feb.	1	09	02	39.9	36 05 56.4	141 18 43.6	47.5	2.9
3	1972 Nov.	4	08	34	56.7	36 16 01.9	141 51 10.1	66.3	3.4
4	1977 Jan.	17	09	27	42.8	36 11 02.8	141 56 00.2	46.8	3.4
5	1978 Sept.	1	04	07	00.5	34 48 10.1	140 08 31.6	55.4	3.3
6	1979 Feb.	16	14	22	15.1	34 48 41.8	140 00 20.9	34.8	3.3
7	1975 Feb.	20	01	47	49.3	37 25 26.4	141 28 40.8	54.1	3.6
8	1977 Sept.	30	14	49	40.9	37 12 34.6	141 28 43.7	103.8	2.9

Origin Time ; JST, h ; source depth in km, M ; magnitude by total duration time.

As shown in Fig. 1b, all seismograms are accompanied with X phases. From waveforms and X_1-P or X_2-S times their seismograms are classified into four groups, *i.e.*, G_1-G_4, although the G_4 seismograms are not shown here.

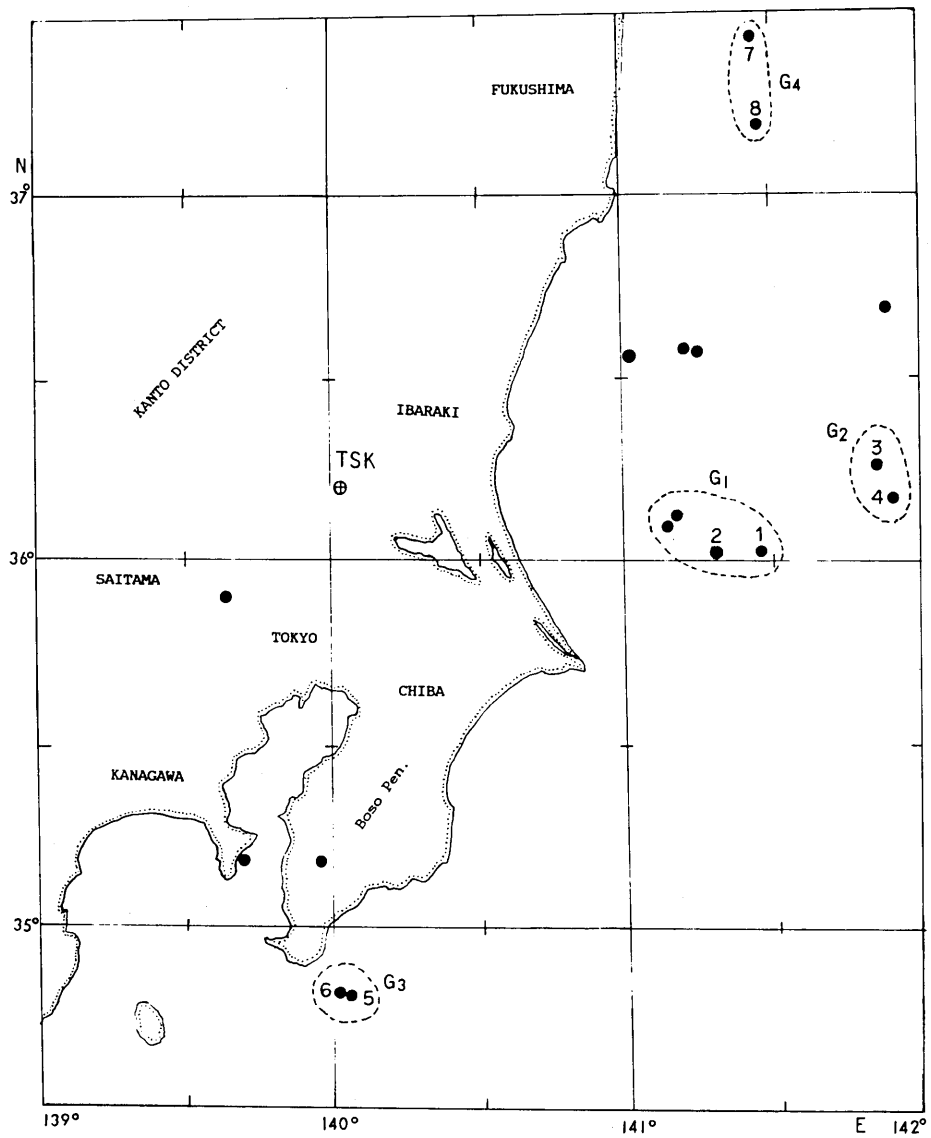

Fig. 1a. Epicentral location of earthquakes used here. Numbers from 1 to 8 correspond to Table 3. Symbols G_1-G_4 show the group number of seismograms with similar X-P times, respectively.

Comments ;

1) G 1 indicates only X_2 phase, and X_2-S time is 15 sec for both events.
2) G 2 indicates X_1 and X_2 phases. The time interval between X_1 and P is about 11 sec and that of X_2 and S is 13-15 sec, respectively.
3) G 3 also indicates X_1 and X_2 phases, but X_1-P time is different from that of G 2. The X_1-P time of G 3 is 8 sec and X_2-S time is 15 sec, respectively.
4) G 4 indicates only X_1 phase, and X_1-P time is 11-12 sec.
5) The amplitude of X_1 phase is larger than that of P wave, except for No. 3 event.

The source depth of events in each group varies within a range of a few tens of kilometers. Considering waveforms and S-P times, the source depth in each group will be probably the same.

The X_2-S times of G 1 and G 3 are the same at 15 sec, and the X_1-P times of G 2 and G 4 are approximately 11 sec, although that of G 3 is slightly less (8 sec).

From the results mentioned above, the X_2 phase of G 1 and G 3 are reflected waves from S to S at the lower boundary of the double seismic zone of a descending Pacific plate. Conversely, the X_1 phase of the three groups is the converted phase from S to P at the same boundary which is similar to that shown by KATSUMATA *et al.* (1983).

The tick near the P wave indicates minute, and numerals attached to each mark show the time in hours and minutes, and this convention is applied consistently for all seismograms in this paper.

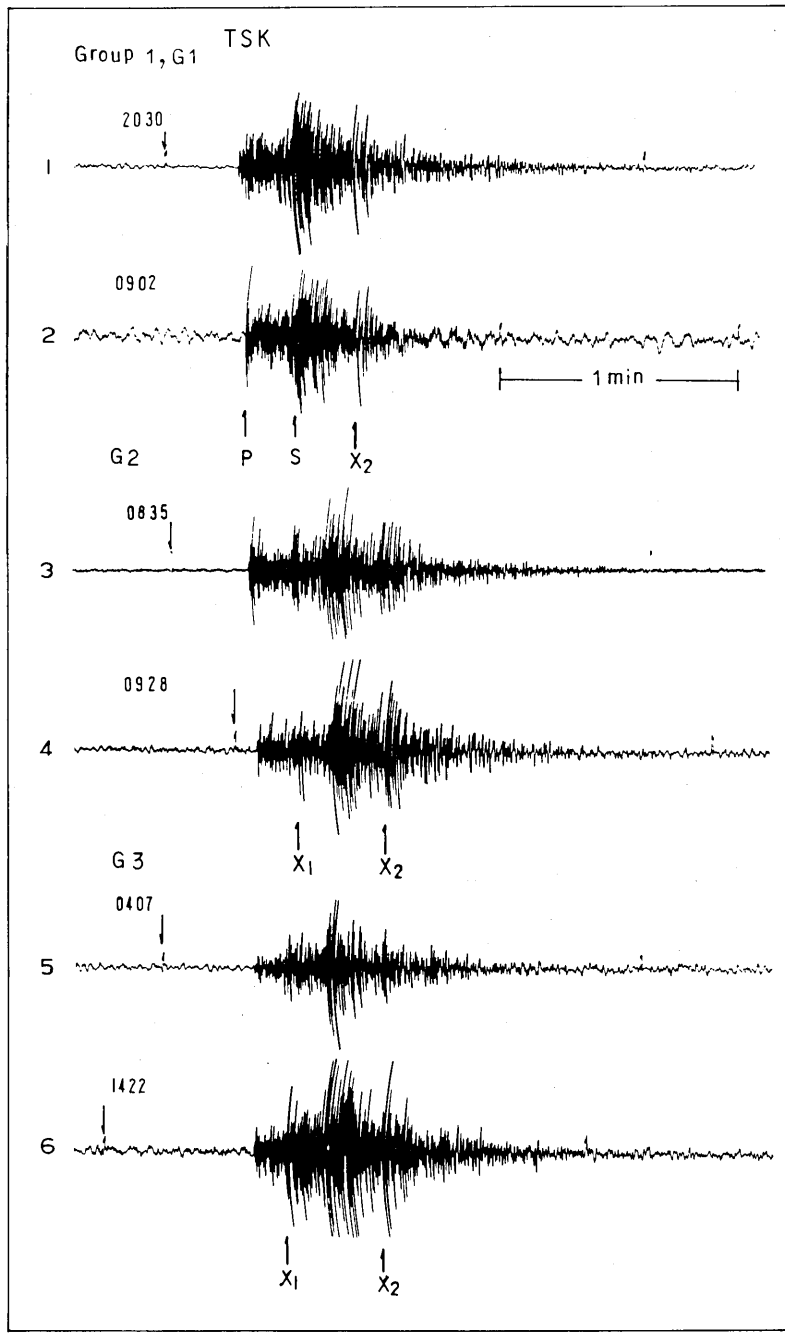

Fig. 1b. Seismograms shown in Table 3. The number to the left hand corresponds to Table 3. Tick mark near the *P* shows the time in minute, and numerals attached to each mark show the time in hour and minute. This is the same for all seismograms in this paper.

2. Seismograms with *X* phase from local earthquakes (2)

Seismograms accompanied with *X* phase from local earthquakes obtained by a SP-Z seismograph at Dodaira station (DDR) are presented. Figure 2 shows typical examples of the seismograms. Their source parameters taken from MATSU'URA *et al.* (1988) are also shown in Table 4. Two broken lines show isodepths of the deep seismic zone roughly 85 km and 150 km, respectively.

Table 4. Source imformation of earthquakes.

No.	Origin Time					Epicenter		*h*	*M*
	y	d	h	m	s	N	E	km	
1	1973 June	14	19	59	50.8	36°38′44″.9	140°13′31″.8	120.7	3.4
2	1977 Jan.	16	22	31	31.1	36 07 36.1	140 05 14.6	69.3	2.8
3	1978 Sept.	23	21	19	34.2	35 39 17.6	139 15 33.5	154.3	2.8
4	1973 Jan.	7	13	56	33.6	35 32 29.4	140 16 44.4	82.0	2.9
5	1971 Nov.	20	07	27	07.1	35 01 30.0	139 59 50.6	65.8	3.5
6	1976 June	22	10	40	01.4	34 49 23.2	140 07 22.8	85.1	3.2

Comments ;

A sharp *X* phase appears on all seismograms, but the appearance of phase is different from that of TSK. The phase appearance at DDR can be seen on the seismograms with a deep source, and no *S*-later phase appears. The seismic area is also different, and the event from Off Ibaraki and Fukushima Prefecture does not have the phase.

The *X*-*P* times varied from event to event between 6-11 sec, and are proportional to the source depth rather than the epicentral distance.

A detailed study is needed to identify *X* phase, however, this phase is in part the converted wave from *S* to *P* at the upper boundary of the descending Pacific plate. The apparent velocity of *X* phase of events Nos. 1, 3 and 6 is almost the same as that of *P* wave, independent of epicentral distance, but the others show too much variability. More data are needed to reach a conclusion.

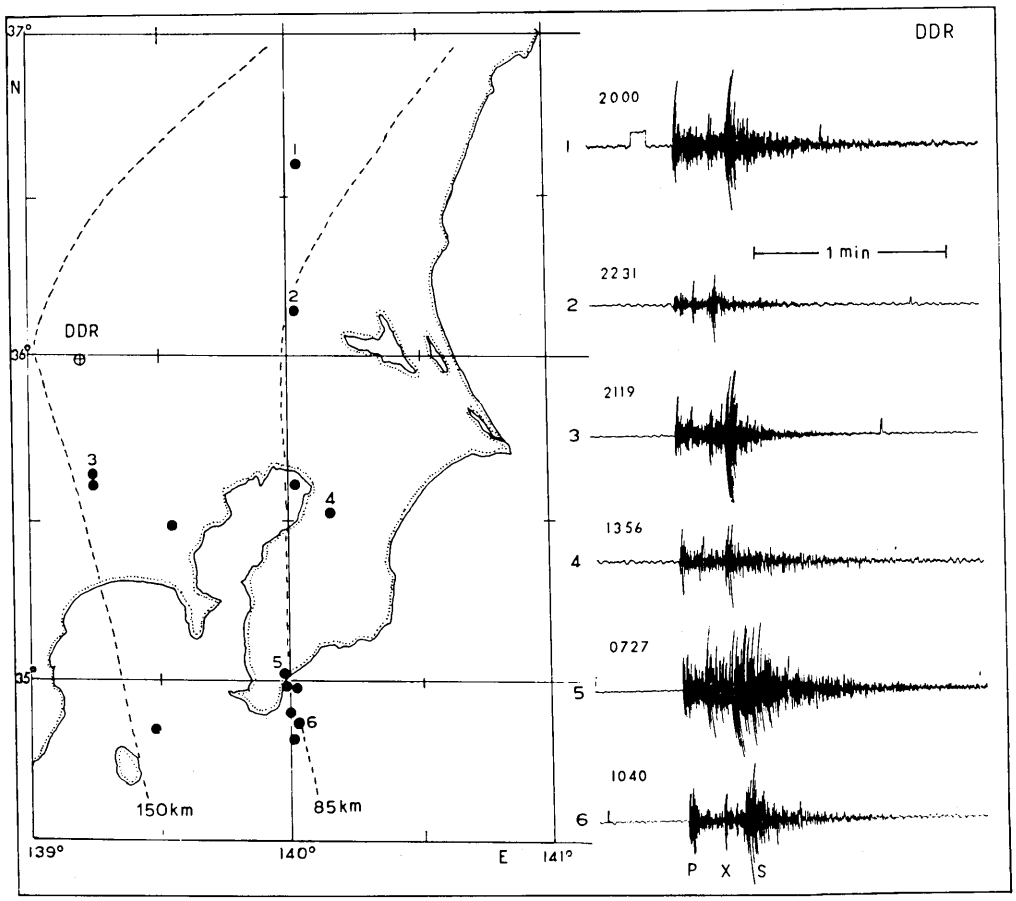

Fig. 2. Seismograms with *X* phase obtained at DDR. Two broken lines show isodepths of deep seismic zone of roughly 85 km and 150 km, respectively. The number in each seismogram corresponds to Table 4.

3. Seismograms with X phases from near earthquakes (1)

Seismograms accompanied with X phase from near earthquakes obtained by the SP-Z seismograph at TSK are presented. Fig. 3a shows the epicenters of the events used here, and Fig. 3b shows typical examples of the seismograms. Table 5 shows the focal parameters of these events by ISC and their X-P times.

Table 5. Focal parameters by ISC and X-P time.

No.	Origin Time					Epicenter		h	Mb	X-P*
	y		d	h	m s	N	E	km		s
8	1980	June	6	10	05 33.4	38°.67	142°.24	64	4.4	9
7	1979	June	24	08	01 17.5	39.02	142.51	69	4.1	9
5	1977	Mar.	17	05	12 14.3	39.20	141.37	104	4.0**	9
9	1981	Mar.	18	07	55 04.1	39.83	143.21	46	4.7	11
1	1972	Aug.	4	05	47 53.8	39.44	144.01	70	4.1	11
14	1979	Feb.	13	17	28 26.6	41.18	143.72	45	4.7	10

No. ; event number corresponds to Fig. 3a, h ; source depth in km, Mb ; body wave magnitude, * ; X-P time in sec, ** ; by JMA

Comments ;

1) Most events accompanied with the X phase are located at the Off East Coast of Honshu.
2) The X-P times are not related to source depth or water depth.
3) The epicentral distance is correlated to the X-P time by 1-2 sec.
4) The No. 5 seismogram is accompanied with S_XS phase together with X phase.

From the combined features, the X phase is probably the converted phase from P to S (P_XS) at the upper boundary of the descending Pacific slab beneath the station, similar to that shown by IIDAKA *et al.* (1989), and S_XS phase is the reflected wave from S to S at the lower boundary of the same slab.

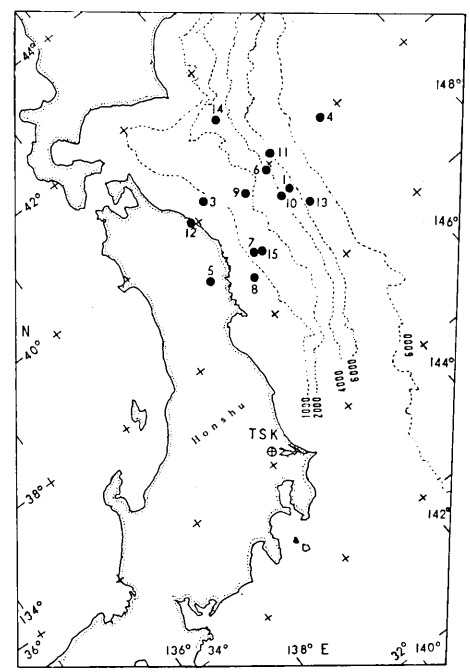

Fig. 3a. Epicentral location of earthquakes with X phase obtained at TSK. The number attached to each circle corresponds to Table 5. Broken lines show isobaths in meters.

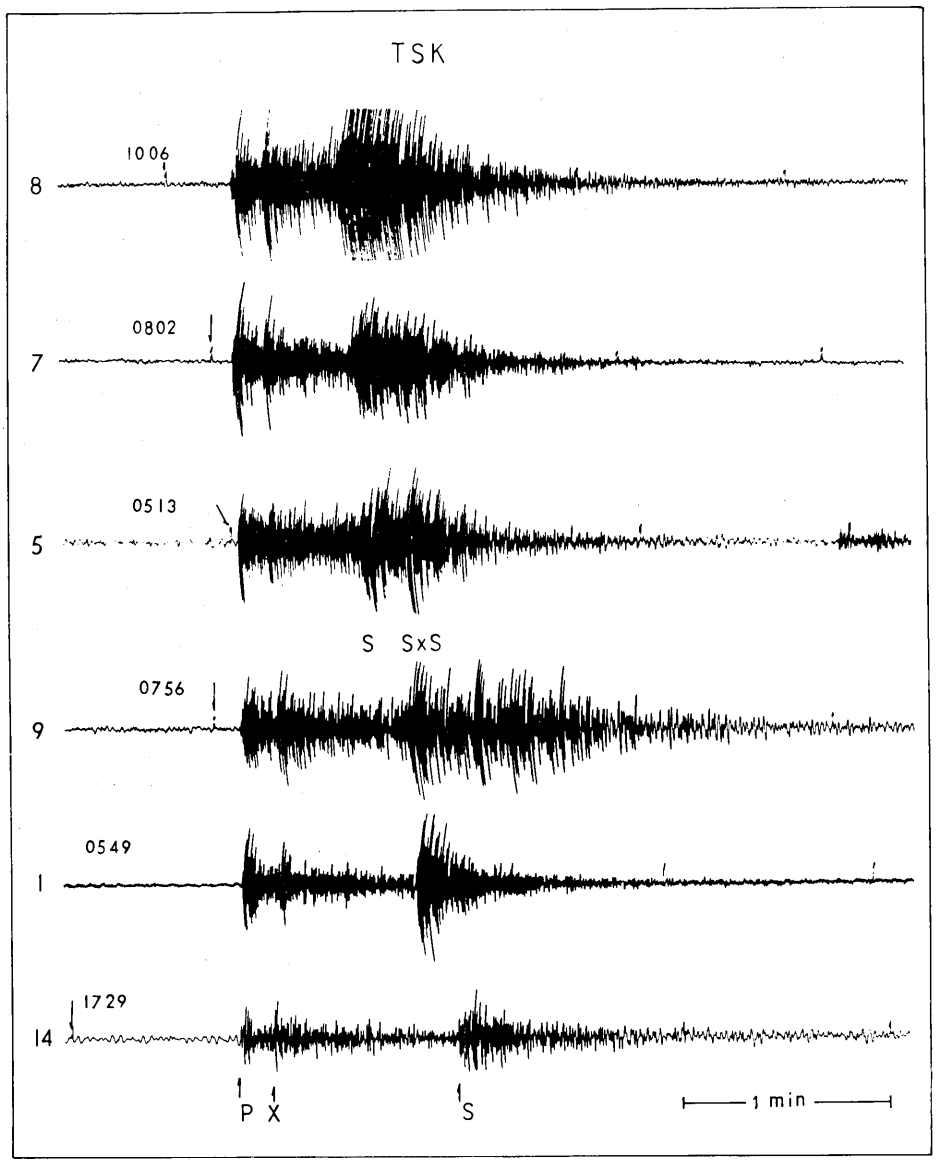

Fig. 3b. Seismograms with *X* and *SxS* phases were obtained at TSK. The number to the left corresponds to Table 5. The *X*–*P* time lies between 9 and 11 s.

4. Seismograms with *X* phase from near earthquakes (2)

Seismograms accompanied with *X* phase from near earthquakes obtained at DDR are presented. Fig. 4a shows the epicenters of events (closed circle) used here. The number attached to each circle is chronological, except for event 12, which is discussed in Fig. 6. Typical examples of seismograms are shown in Fig. 4b. Table 6 shows the focal parameters of these events by ISC and *X*-*P* time obtained here.

Table 6. Focal parameters by ISC and *X*-*P* time.

No.	Origin Time					Epicenter		*h*	*Mb*	*X*-*P*
	y		d	h	m	s	N	E	km		s
1	1972	Aug.	4	05	47	53.8	39°.44	144°.01	70	4.5	11
4	1974	Aug.	26	14	32	16.0	30.54	142.00	21	4.6	13.5
9	1976	Mar.	30	03	32	39.0	40.19	143.99	30*	4.3**	10
14	1977	Nov.	24	22	30	16.0	39.94	143.80	40	4.6	10
18	1981	Mar.	1	03	44	46.5	40.10	142.10	97	4.3	15
22	1983	May	16	21	39	51.2	38.63	144.51	20	4.9	9
12	1977	May	2	05	05	24.4	31.14	138.73	33	—	22

Mb ; body wave magnitude, * ; 60 in JMA, ** ; 4.7 in JMA.

Comments ;

1) The *X* phase accompanies all events, and such events are located over a wide area compared to that of TSK shown in Fig. 3.
2) The frequency content of *X* phase differs among events. Events 1 and 18 contain high-frequency components. In particular, *X* phase of event No. 22 is very sharp and impulsive. Such phenomena relate to the epicentral location. Events near the trench contained high-frequency components, and this tendency is the same as in the previous study as shown in Fig. 9 (TSUJIURA, 1988).
3) The *X*-*P* time relates to epicentral location and source depth. Event No. 18 with a deep source shows the maximum value, although the *S*-*P* time is almost the same as that of event No. 22.

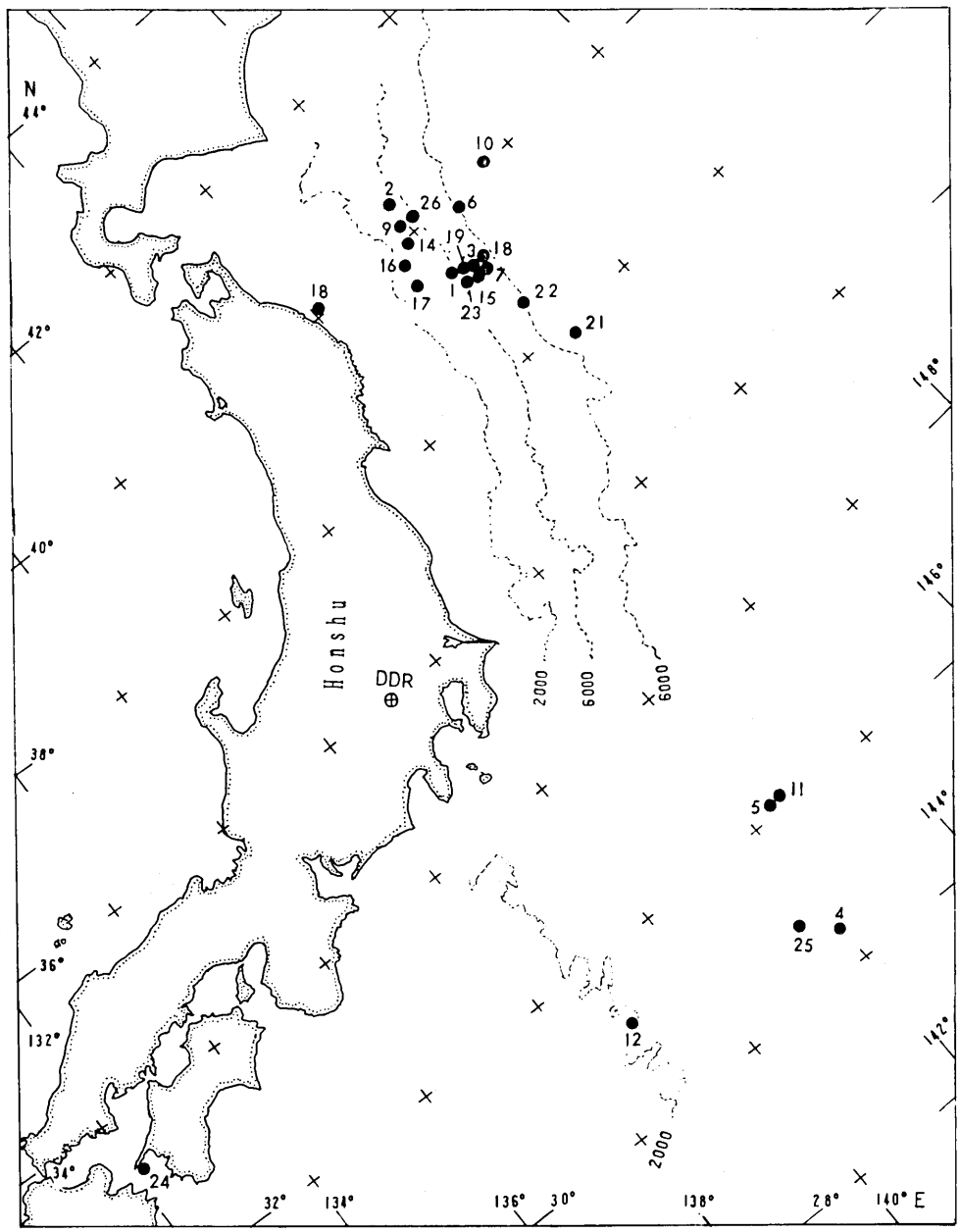

Fig. 4a. Epicentral locations of seismograms accompanied with *X* phase obtained at DDR. The number attached to each circle corresponds to Table 6. Broken lines show isobaths in meters.

4) The amplitude of X phase is equal to or larger than that of P wave.

There is a variety of X-P times. Here, we consider three events (Nos. 1, 9, 14) with almost the same X-P times lying between 10 and 11 sec.

Considering X-P and S-P times, the X phase is the converted phase from P to S near the station. If we assume that the average velocity of P wave is 8 km/s and that of S wave is 4.5 km/s, the converted point locates at a point about 100 km from the station. This point corresponds to 37° N, where the upper boundary of the descending Pacific plate is about 90 km depth (IIDAKA *et al.*, 1989).

OBARA (1989) reports that a strong reflecting plain of S wave exists at the upper plane of the descending Pacific plate between 35° and 37° N. However, the large amplitude of X phase cannot be explained from the above conclusion.

The apparent velocity of Nos. 18 and 22 events is about 1.5 km/s earlier than that of the others. It must be considered that there are several converted points. Considering the waveform of No. 22 event, it is expected that the source is deeper than 20 km. However, we have no explanation of such a travelling path.

The phase appearance of the seismogram of No. 24 event (July 16, 1981) is different compared with other events. The X-P time varies systematically among stations with a value of 3 and 12 sec. The study of events in this area is useful for estimating the Philippine Sea plate. However, no more data are available for the present study. The X phase of No. 12 event is discussed in Fig. 6.

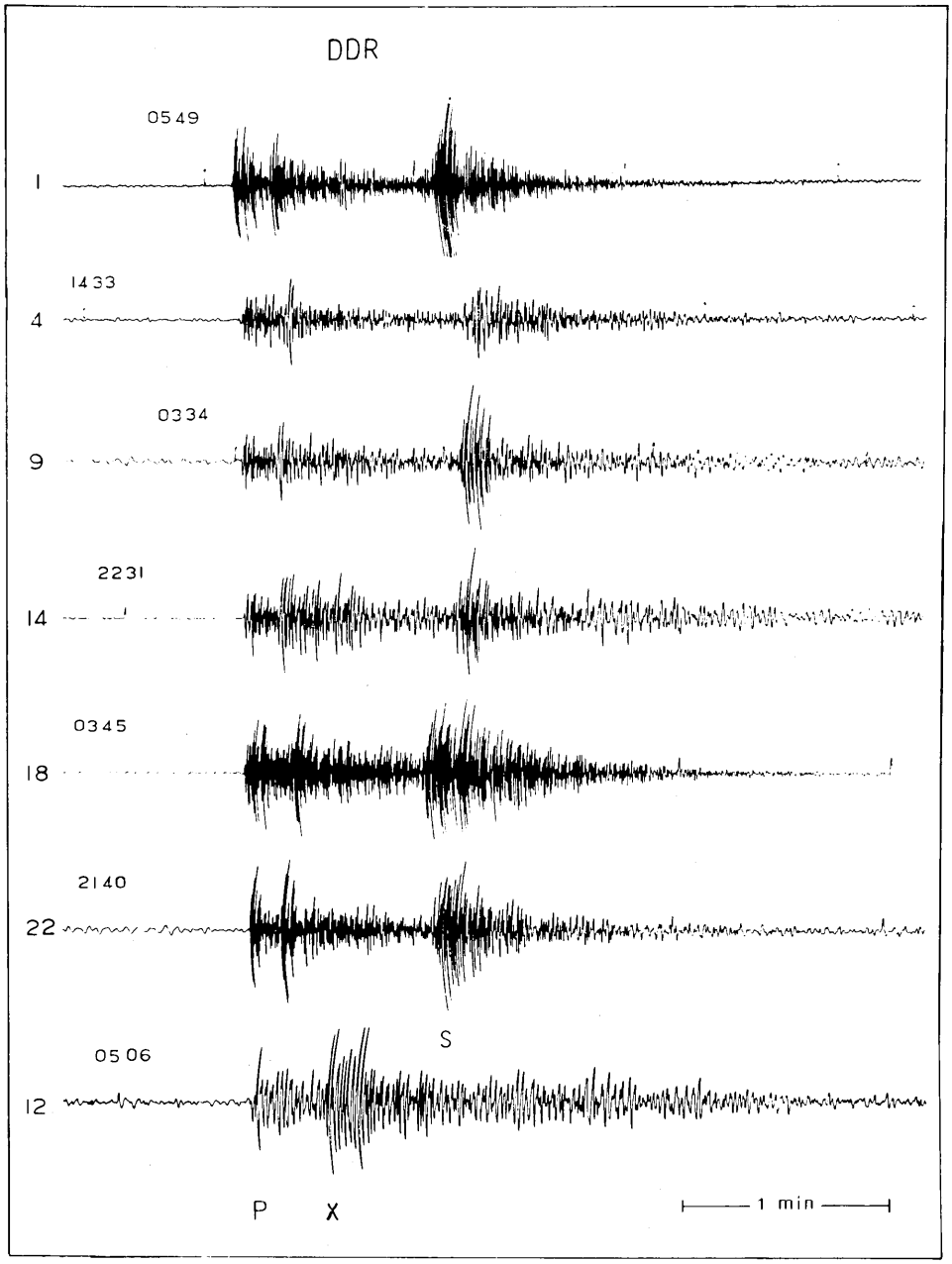

Fig. 4b. Seismograms accompanied with *X* phase obtained at DDR. Numeral at left shows event number, and it corresponds to that in Fig. 4a. Note that frequency-components differ among the events.

5. Seismograms with *X* phase from near earthquakes (3)

Seismograms accompanied with *X* phase from near earthquakes obtained at OYM are presented. Fig. 5a shows the epicenters of events used here. The number attached to each circle is chronological, except for events shown in an open circle (Nos. 9, 10) as no *X* phases are available.

Typical examples of seismograms for events in Fig. 5a are shown in Fig. 5b, and they are arranged according to the length of *S*-*P* times. The focal parameters of these events by ISC and *S*-*X* time are shown in Table 7.

Table 7. Focal parameters by ISC and *S*-*X* time.

No.	Origin Time					Epicenter		*h*	*Mb*	*S*-*X*
	y		d	h	m s	N	E	km		s
1	1973	Nov.	24	19	47 34.5	33°.71	137°.30	366	—	17
5	1977	Aug.	8	18	26 15.5	33.66	137.6	333	—	17.5
7	1981	Apr.	19	20	09 31.8	31.46	138.39	380	4.8	25
4	1976	Oct.	6	08	13 13.5	30.79	137.83	474	4.7	22
3	1976	May	18	17	21 06.1	30.21	138.53	455	5.0	25
8*	1977	May	2	05	05 24.4	31.14	138.73	33	—	22

*; No. 8 is the same event as No. 12 in Fig. 4b.

Comments;

1) All events are accompanied with *X* phase, but their source depths and locations differ from those of previous figures. The events accompanied with *X* phase are located only south of Honshu and are deeper than 300 km. The events of Nos. 9 and 10 are not accompanied with the *X* phase.
2) The waveform of *X* phase is different from those of previous figures (Figs. 3b and 4b), and the amplitude of *X* phase is continued until *S* waves.

The combined features mentioned above suggest that the inclined discontinuities, *i.e.*, Pacific and Philippine Sea plates, are descending beneath the station (ISHIDA, 1992). This phase therefore is for converted waves from *S* to *P* at these boundaries.

Another explanation of *X* phase is that the descending slab is heterogeneous, and this heterogeneity causes a scattering converted waves. This is consistent with the results of OBARA (1996).

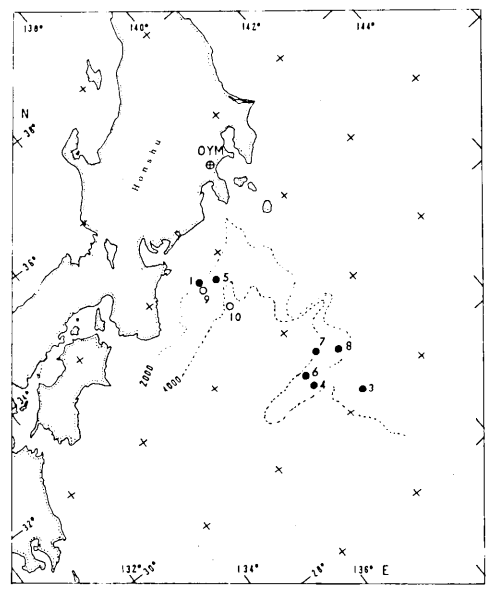

Fig. 5a. Epicentral locations of events accompanied with *X* phase obtained at OYM. Broken lines show isobaths in meters. No *X* phase on the seismogram is shown by open circles.

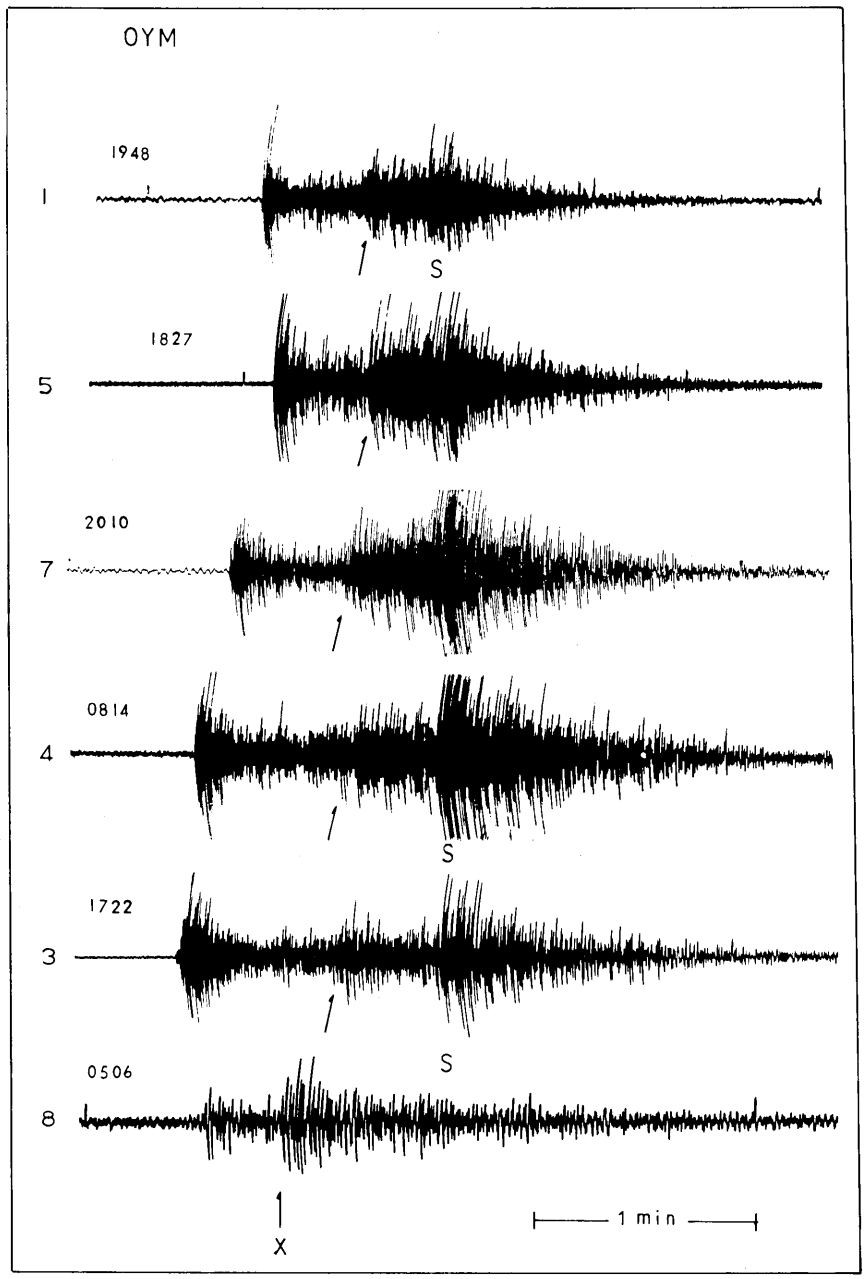

Fig. 5b. Typical example of seismograms accompanied with *X* phase obtained at OYM. It is noted that the amplitude of *X* phase is not impulsive.

6. Comparison of seismograms for events N. and S. of Honshu

Comparison of seismograms for two events are presented. One is located in north Honshu (1) and the other in south Honshu (2) obtained at SRY, OYM and DDR. Fig. 6 shows the epicenters of the two events and their seismograms. Focal parameters and X-P times are shown in Table 8.

Table 8. Focal parameters by ISC and X-P time.

No.	Origin Time						Epicenter		h	Mb	X-P
	y		d	h	m	s	N	E	km		s
1	1977	Jan.	26	04	05	17.1	39°.89	141°.06	103*	4.7	25
2	1977	May	2	05	05	24.4	31.14	138.73	33	—	22

*; h=90 (JMA)

Comments ;

1) Large amplitudes of X phases are observed for both events, although the X-P time is different.
2) The apparent velocity of X phase is the same as that of P.
3) The S wave is not clear, except for event 1 at OYM, and no S waves are observed for event 2.
4) The frequency component is different for the two events : Event 1 abounds in high-frequency components compared to that of No. 2.

Considering the X-P times of both events and large amplitudes of X phase, the X phase may be converted waves from S to P at the lower boundary of the subducting Pacific plate.

The difference in the frequency component between the two events may be due to the path effect and the different source depths (TSUJIURA, 1988).

Another explanation for the large amplitude of the X phase of No. 2 event may be that the inclined discontinuity plane exists beneath the epicenter, and the X phase is the converted wave from S to P at this discontinuity. A similar X phase can be seen on the seismogram of the event located south-east of Shikoku on Dec. 21, 1977. In both cases, these conclusions are tentative. More data from different stations are needed (under collection).

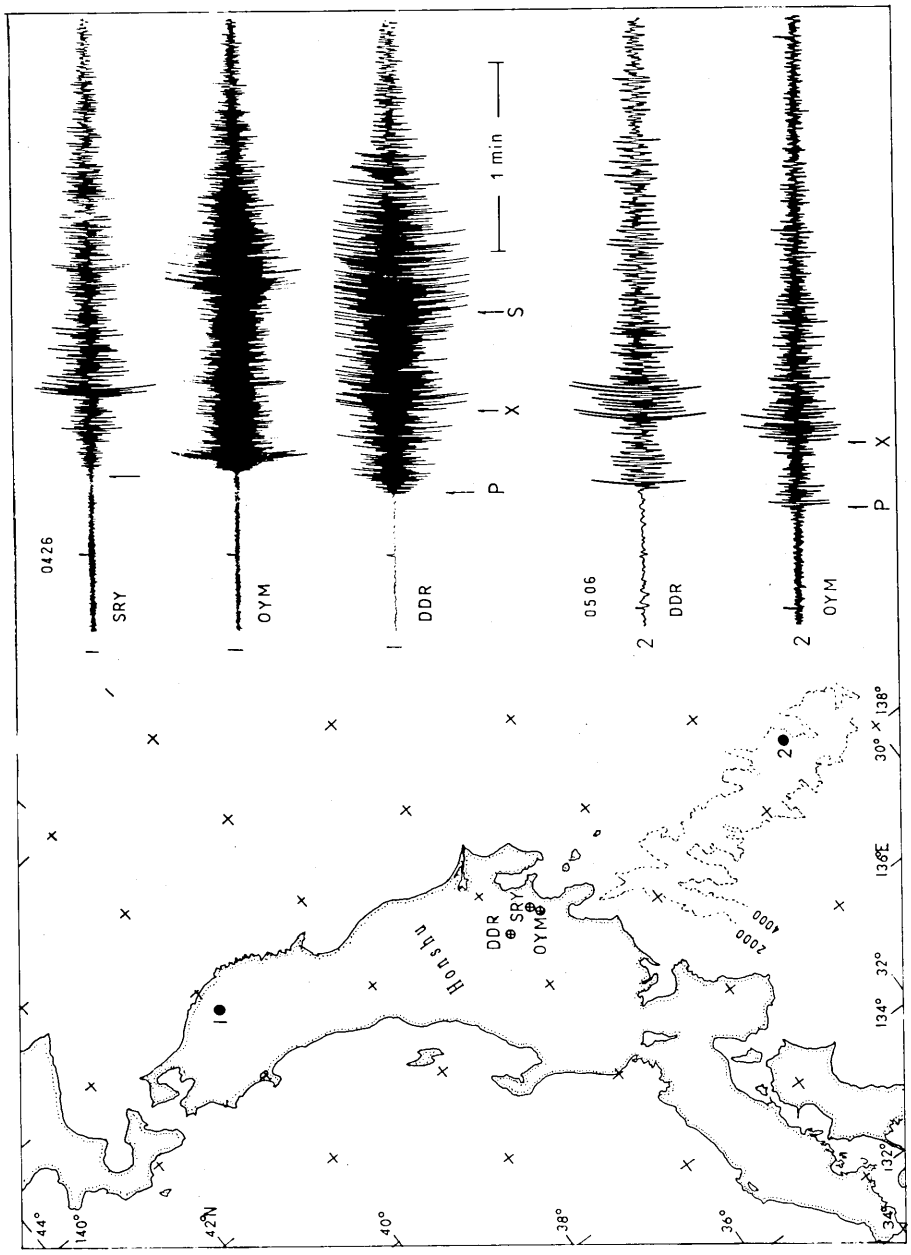

Fig. 6. Comparison of seismograms for the events No. 1 and No. 2. The difference of frequency components is noticeable. Broken lines show isobaths in meters.

7. *T* wave from earthquakes in south Honshu

The existence of the *T* wave is well known. Among our observatories, KYS station often observed the *T* wave in events located at south Honshu. Fig. 7a shows the distribution of events accompanied with the *T* phase (closed circles). The open circles are not accompanied with the *T* phase at KYS. Fig. 7b shows a typical example of seismograms accompanied with *T* phase. The focal parameters of this event are shown in Table 9.

Table 9. Focal parameters by ISC.

No.	Origin Time						Epicenter		*h*	*Mb*	*Δ*
	y		d	h	m	s	N	E	km		deg
4	1983	Aug.	20	13	08	32.9	27°.94	141°.91	44	5.7	7.39

Comments ;

1) The clear *T* wave is observed at KYS, although the initial motion is not clear, and its continued about three minutes.
2) The *T* wave at SRY and OYM is very small compared to that of KYS. Most of travelling path to KYS is a deep oceanic zone.
3) The events indicated by closed circles occurred along the deep water depths (6,000 m). Two events, Nos. 7 and 10, are not accompanied with *T* phase. This may be probably due to small events (no data of magnitude on ISC).
4) The velocity of *T* wave obtained here is 1.5 km/s.

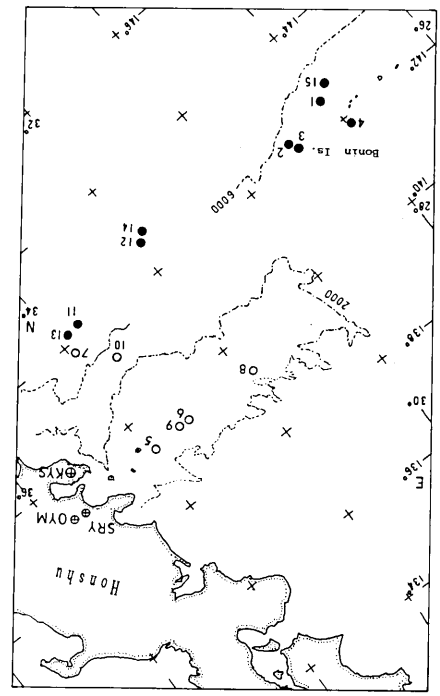

Fig. 7a. Distribution of epicentral locations of events accompanied with *T* phase (closed circles). Broken lines show isobaths in meters.

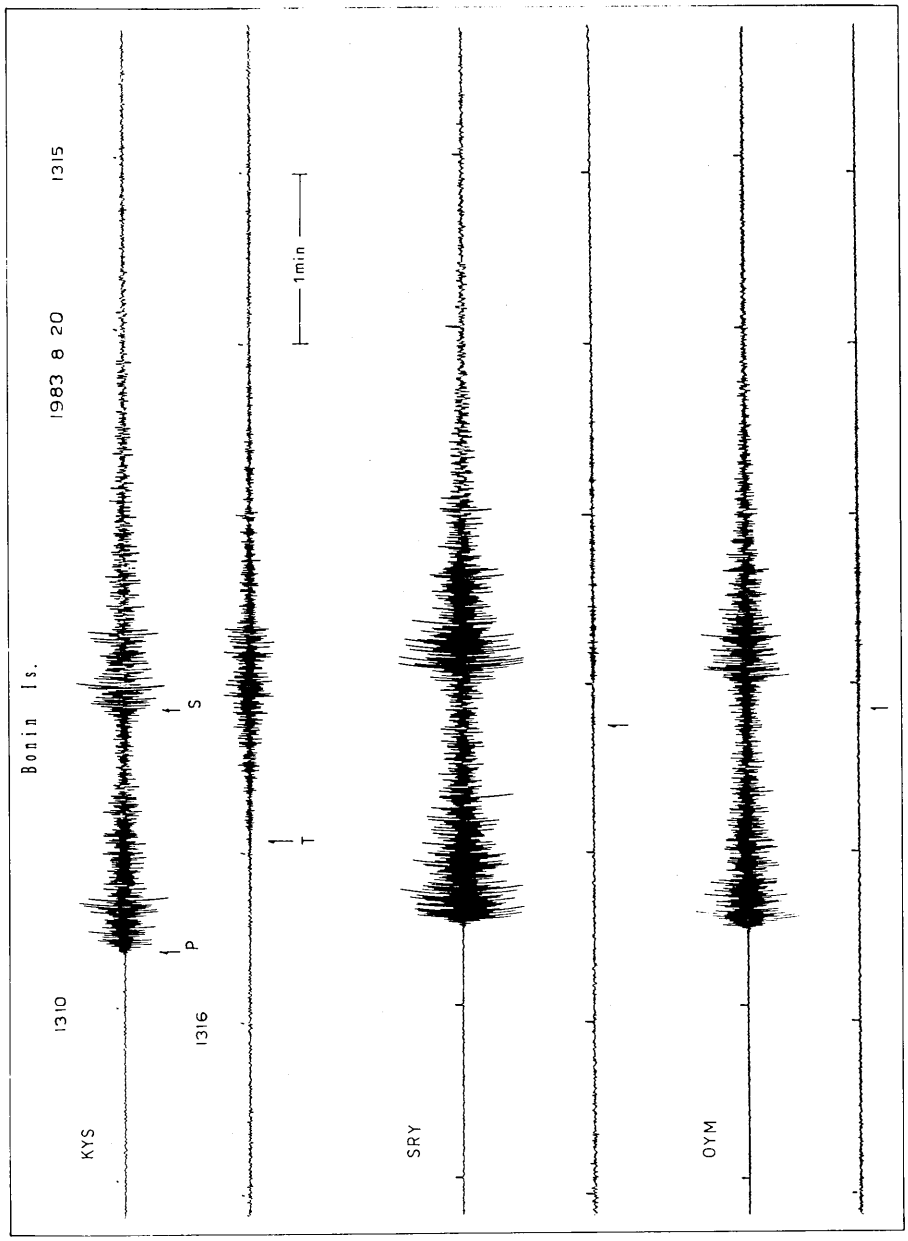

Fig. 7b. Seismograms of No. 4 event obtained at three stations, KYS, SRY and OYM. The *T* phase is clearly demonstrated on the seismogram at KYS.

8. Reflected wave from near earthquake

The small event (E 2) appears about 4 m 43 s after the earthquake which occurred south of Honshu (E 1). Figure 8 shows seismograms obtained at five stations. E 2 is very small, but it can be seen clearly at all stations. E 2 consists of two phases. The time interval of the two phases is about 4 s. From this figure, it is not clear that the E 2 event is an earthquake or a later phase of E 1. The difference of arrival times among stations (ΔT) for E 1 and E 2 gives a clue to understanding the difference in both cases. Table 10a shows focal parameters of E 1.

Table 10a. Focal parameters of E1 by ISC.

Origin Time					Epicenter		h	Mb	Δ
y	d	h	m	s	N	E	km		deg
1982 Jan.	8	14	58	34.0	32°.41	140°.31	110	4.1	3.70*

*; at DDR, 2.79 at KYS

The arrival times (AT) and time differences among stations (ΔT) for both events are shown in Table 10b. In this Table, ΔT_1 shows the difference in arrival times for E1, and ΔT_2 shows similar time differences for E 2 event.

Table 10b. Arrival times of E1 and E2 at five stations.

Code	A T (E 1)			ΔT_1	A T (E 2)			ΔT_2
	h	m	s	s	h	m	s	s
KYS	14	59	16.0	0	15	03	59.0	0
OYM	14	59	21.0	5.0	15	04	03.0	4.0
SRY	14	59	23.0	7.0	15	04	04.5	5.5
DDR	14	59	28.5	12.5	15	04	08.5	9.5
TSK	14	59	28.5	12.5	15	04	08.5	9.5

The maximum time difference for E 1 is 12.5 sec and that of E 2 is 9.5 sec, respectively. From the difference of ΔT for both events, E 2 will be the later phase of E 1. The time difference of 4 m 43 s for both events may be due to the existence of a discontinuity underlying the station and the epicenter of E 1. If we assume that the velocity of P wave of 9 km/s for E1 and that of S wave is 5 km/s for E 2, their results agree with the time differences shown in Table 10b. Therefore, E 2 is probably a reflected wave from S to S at the discontinuity. If this assumption is correct its depth corresponds to 700 km.

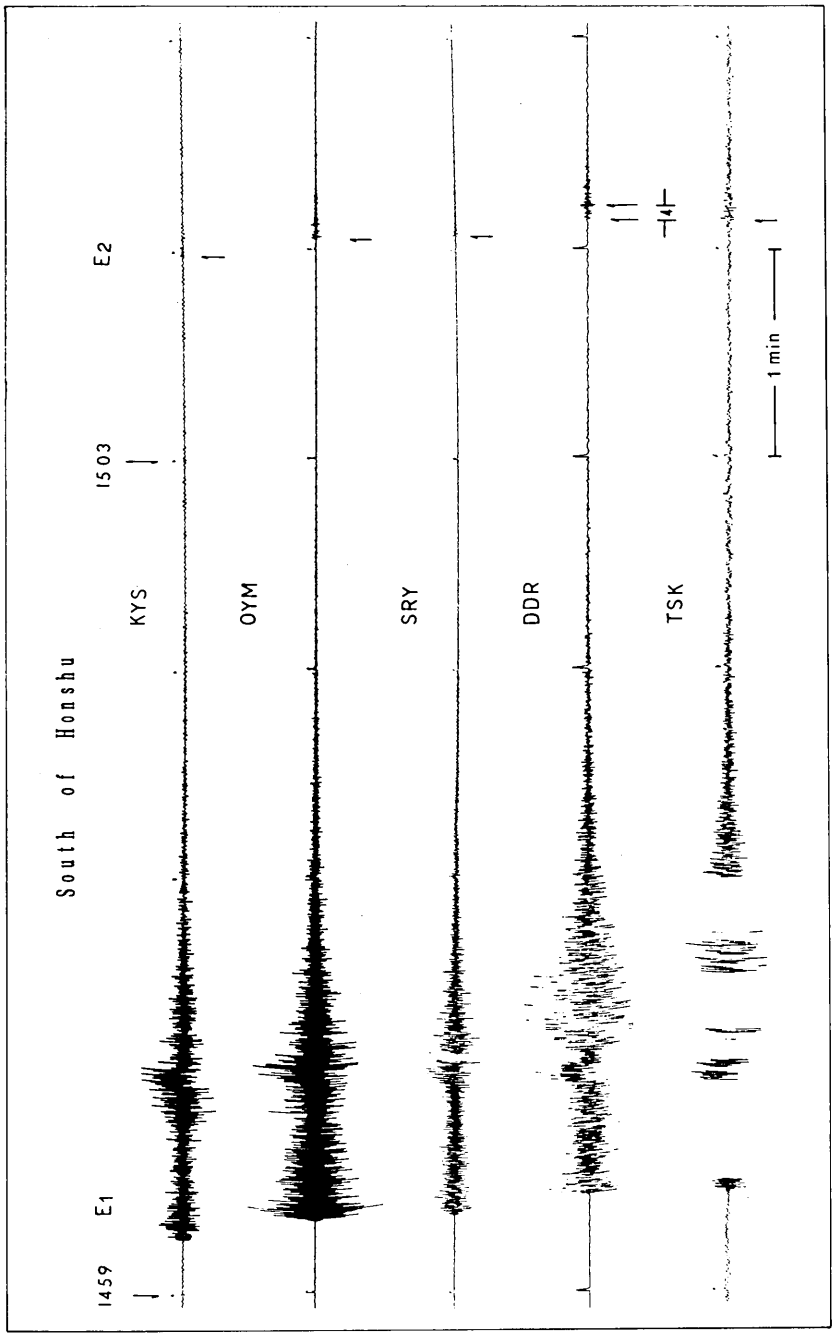

Fig. 8. The reflected wave from near earthquake. Small, but clear later phase (E2) can be seen for all stations.

9. Unidentified wave from near and regional earthquakes

The regional seismograms are rarely accompanied with an unusual wave. Figure 9 shows three samples accompanied with an unusual wave (*X*). The focal parameters of these events are shown in Table 11.

Table 11. Focal parameters by ISC.

No.	Origin Time						Epicenter		*h*	*Mb*	*Δ*
	y		d	h	m	s	N	E	km		deg
1	1973	July	10	23	25	32.1	37°.64	142°.37	42	5.2	3.03
2	1982	Sept.	6	01	47	03.2	29.40	140.43	179	6.4	6.66
3	1982	Aug.	16	01	13	21.0	36.56	140.71	29	4.4	2.12

Comments ;

1) The epicenter of event No. 1 is located at Off East Coast of Honshu, and this event is accompanied with *X* wave after about 21 m 07 s from the origin time at DDR station.
2) The epicenter of event No. 2 is located at south Honshu. This event is accompanied with two phases indicated by X_1 and X_2. The epicentral distance at DDR is 6.66 degrees. The *X* waves of three stations are also shown for comparison. The arrival time of the X_1 phase from the origin time is 30 m 31 s at SRY. Similarly, the later arrival of the *X* wave can be seen for the other events e.g., Taiwan earthquake on July 23, 1978.
3) The epicenter of event No. 3 is located at Off East Coast of Honshu, and this figure shows the waveforms of *P* wave group and *X* phase obtained at TSK. The arrival time of the *X* phase from the origin time is about 9 m 30 s. If we considered this phase to be *PcP*, the arrival time of this phase is about 1 m 25 s later than the time expected from *J-B* Table.

The *X* waves shown in seismograms Nos. 1 and 2 are neither aftershocks nor other events as inferred from ISC. However, we have no explanation of the *X* waves from the present data.

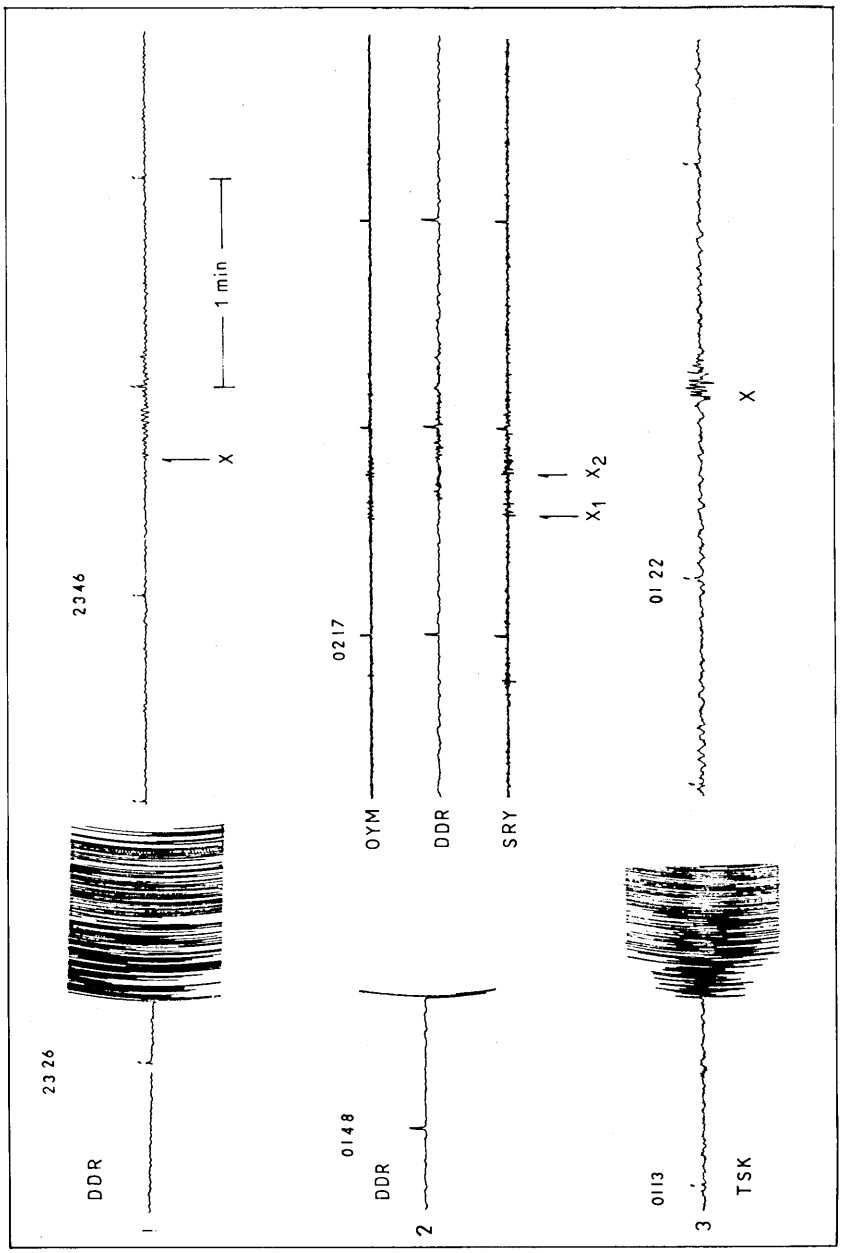

Fig. 9. Seismograms of *P* wave part of three events and their later phase (*X*). The epicenter ; 1) Off East Coast of Honshu, 2) south Honshu, 3) Off East Coast of Honshu.

10. *X* phase from deep Bonin Is. earthquake (1)

The deep earthquakes occur frequently in the Bonin Islands region, and some of them are accompanied with a special phase (*X*) between *P* and *S* waves. Figure 10 shows four examples of seismograms with a *X* phase. The seismograms are arranged chronologically.

The focal parameters of these events and their *X*-*P* times are shown in Table 12.

Table 12. Focal parameters by ISC and *X*-*P* time.

No.	Origin Time						Epicenter		*h*	*Mb*	*Δ*	*X*-*P*
	y		d	h	m	s	N	E	km		deg	s
1	1972	Sept.	10	20	12	36.2	27°.96	139°.50	518	—	8.02	39
2	1973	Jan.	15	11	19	50.1	27.06	140.13	470	4.8	8.94	49
3	1980	Jan.	17	09	21	55.2	28.30	138.91	523	5.2	7.68	39
4	1982	May	17	20	32	12.7	28.35	138.89	531	4.5	7.63	38

Comments ;

A common phase indicated by *X* can be seen on the seismograms, and their *X*-*P* times are almost the same, except for event No. 2 where the source depth is shallower than in other events.

The values of 38–39 sec are common values as the *X*-*P* time of events with a source depth of about 520 km and epicentral distance of about 8 degrees.

The *X*-*P* times obtained here are in good agreement with the results of BARLEY *et al.* (1982) and FUKAO *et al.* (1988). They interpret this *X* phase as the converted wave from *S* to *P* at the surface of discontinuity existing at a depth of about 700 km.

The *X* phase of event No. 2 will also be a similar converted wave, if the difference of source depth is considered.

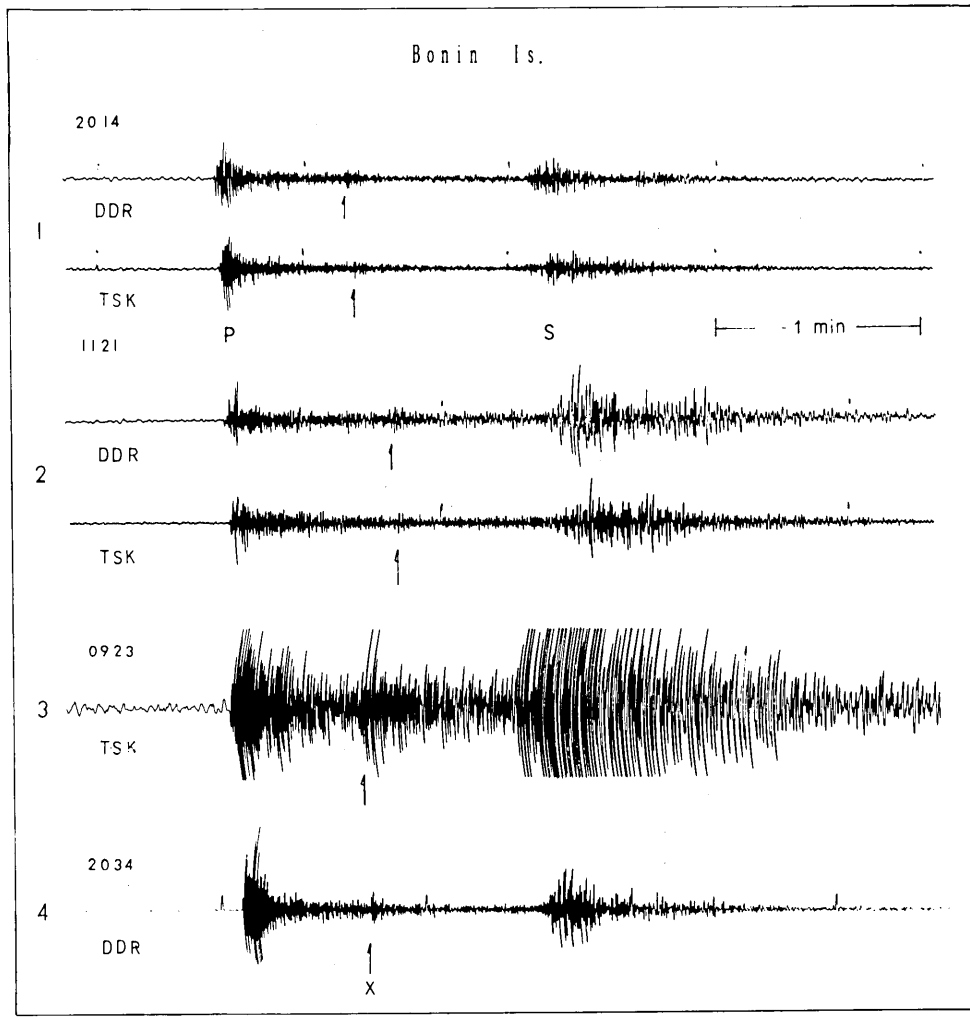

Fig. 10. Example of seismograms with *X* phase obtained at DDR and TSK for the deep events of Bonin Islands region.

11. *X* phase from deep Bonin Is. earthquake (2)

Another example of a seismogram accompanied with *X* phase from Bonin Islands region is provided. Figure 11 shows seismograms obtained at five stations of the DDR network. The *X* phase can be seen clearly between *P* and *S* waves for all seismograms. The focal parameters and *X*-*P* time are shown in Table 13.

Table 13. Focal parameters by ISC and *X*-*P* time.

Origin Time					Epicenter		*h*	*Mb*	*Δ*	*X*-*P*
y	d	h	m	s	N	E	km		deg	s
1983 Dec.	25	11	28	48.7	28°.09	139°.43	536	4.6	7.89*	19

* ; DDR.

Comments ;

1) The *X*-*P* times of these seismograms lie between 18.5 and 19 s.
2) The *X*-*P* time obtained here is shorter than that of previous seismograms, although their epicentral distance and source depth are almost the same.
3) The amplitude of the *X* phase is almost the same for that of the *P* wave.
4) The *X*-*P* time is examined for seismograms of the Wakayama network, located about 500 km west of the DDR network. In Wakayama, the *X*-*P* times also lie between 18 and 18.5 s.

Events with similar *X*-*P* times are observed at the Australian network for deep events in the Tonga subduction zone (BOCK and HA, 1984). They interpret this phase as the converted phase from *S* to *P* at a depth of nearly 700 km.

Considering the results obtained by the two networks, the later phase (*X*) obtained here is probably the 2 nd shock, which occurred about 18 sec after the first event. Because the amplitude of the *X* phase has a similar size as the *P* wave. No *S* wave is seen for the 2 nd shock. This may be due to a different mechanism?

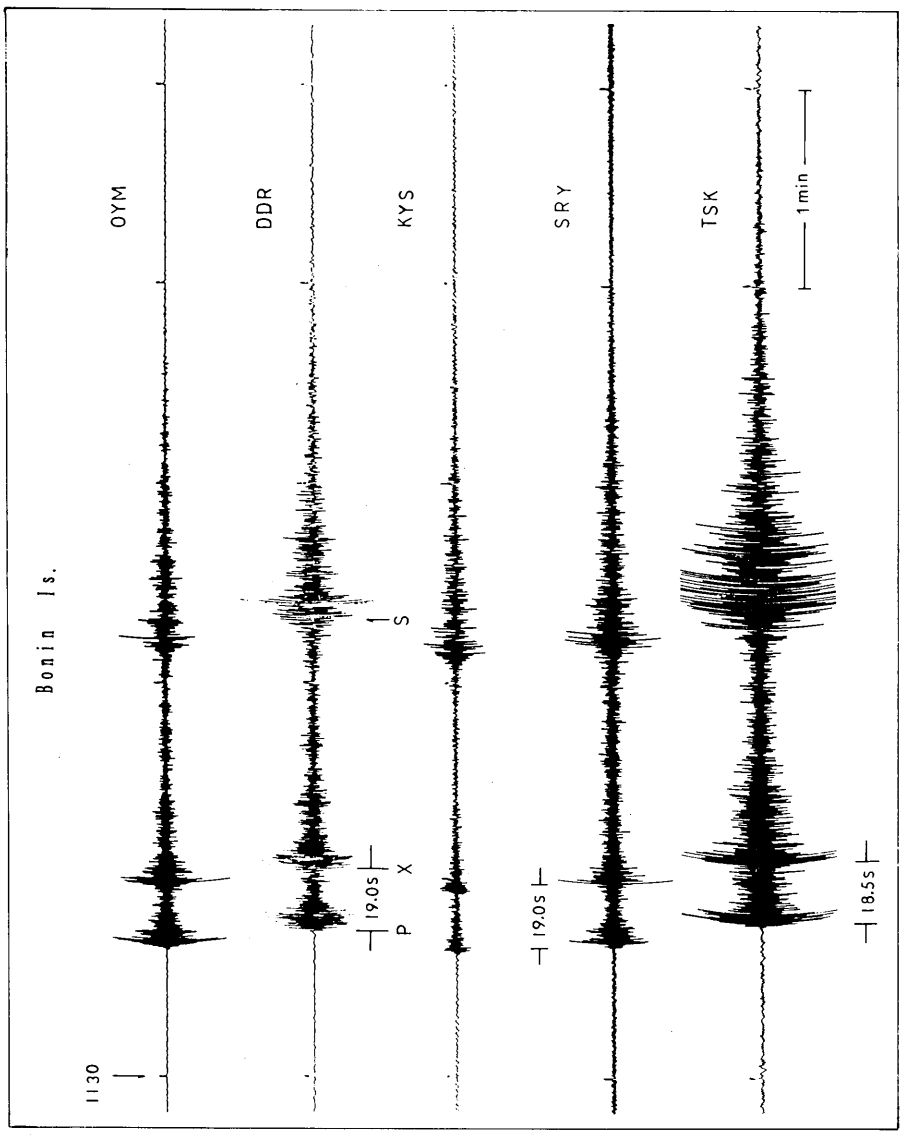

Fig. 11. Seismograms obtained at five stations for the deep event of Bonin Islands region. Clear *P*-later phase (*X*) is seen for the seismograms of all stations. It is noted that the amplitudes of *X* phase are almost the same for those of *P* wave.

12. *X* phase of deep earthquakes from three regions

An *X* phase similar to that shown in Fig. 10 can be seen on the seismograms of different regions. Fig. 12 shows seismograms from Marianas (1), E. Russia-N. E. Chaina Border (2), and Bonin Islands (3) regions. The No. 3 seismogram is the same as event No. 2 shown in Fig. 10. The common phase indicated by *X* exists on all seismograms. The focal parameters of the three events and *X*-*P* times are shown in Table 14.

Table 14. Focal parameters by ISC and *X*-*P* time.

No.	Origin Time					Epicenter		*h*	*Mb*	*Δ*	*X*-*P*
	y		d	h	m s	N	E	km		deg	s
1	1978	Aug.	15	21	47 15.8	19°.71	144°.41	502	5.4	16.86*	48
2	1983	Oct.	8	07	45 26.3	44.21	130.74	551	5.6	10.94	46
3	1973	Jan.	15	11	19 50.1	27.06	140.13	470	4.8	8.94	49

*; DDR

Comments;

1) Epicentral distance is distributed over a wide range of 9~17 degrees. In spite of a wide range of distances and source depths, the *X*-*P* times are almost the same within a range of 46~49 sec.
2) The apparent velocity of *P* wave for the three events is almost the same at 11 km/s, however, that of the *X* phase is different among the events. The apparent velocity of the *X* phase of No. 1 event is 13 km/s and those of Nos. 2 and 3 are 15 km/s.

As explained in Fig. 10, the *X* phase of No. 3 seismogram (Bonin Is.) is the converted wave from *S* to *P* at a discontinuity of 720 km depth.

The combined data mentioned above suggest that the depths of discontinuity in the three regions are almost the same as that of the Bonin Is. region. The difference in apparent velocity of *X* phase may be due to the difference in epicentral distance.

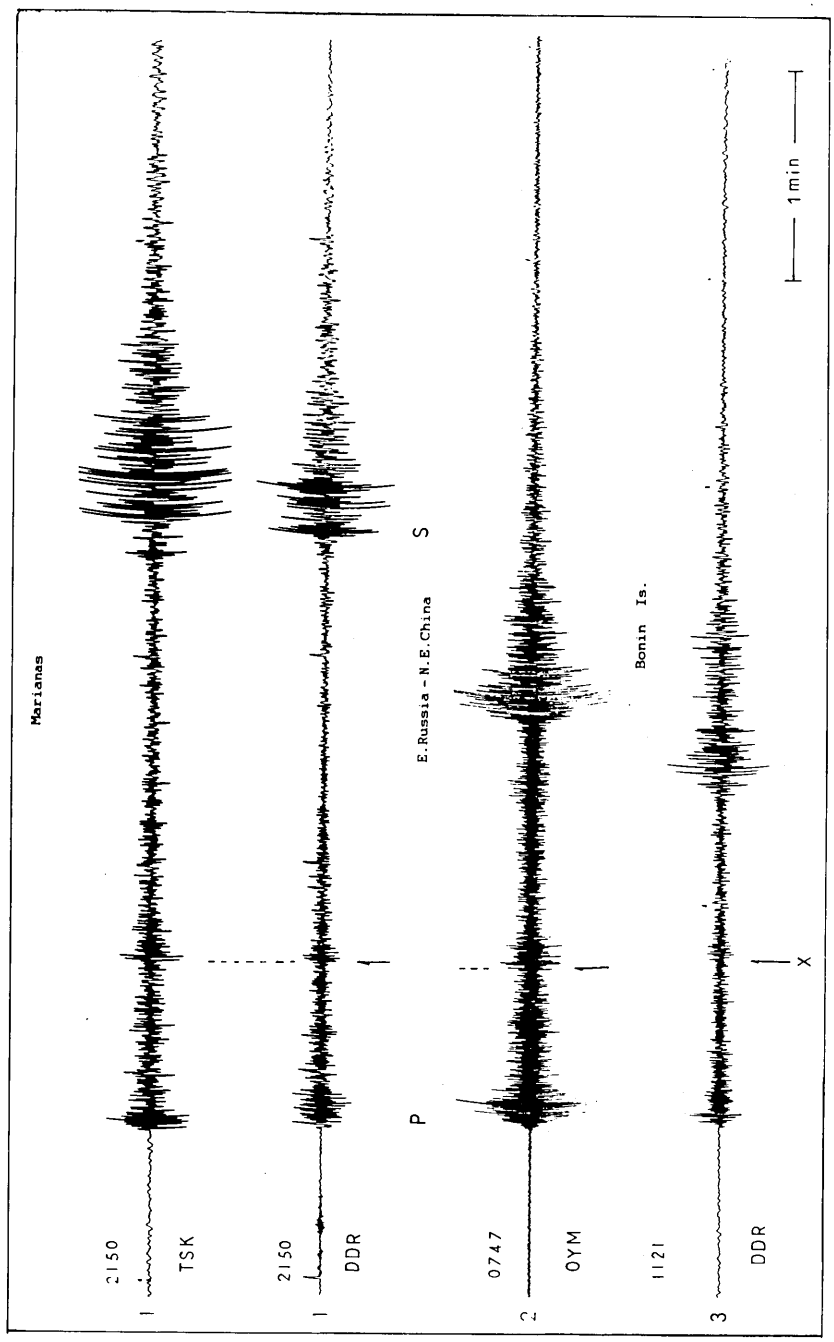

Fig. 12. Seismograms accompanied with X phase for the events from three regions. It is noted that the X-P times are almost the same, in spite of different source depth and epicentral distance.

13. *X* phase from deep Marianas earthquakes

Through Figs. 10 to 12, it is confirmed that the seismograms from Bonin Is.-Marianas regions are accompanied with the *X* phase, although the *X*-*P* times depend on seismic regions. The seismograms from the deep Marianas region are also accompanied with the *X* phase. The focal parameters of four events and *X*-*P* times are shown in Table 15. Figure 13 shows a typical example of seismograms with *X* phase for three events. The seismogram of event No. 4 is not shown here because its amplitude is too small.

Table 15. Focal parameters by ISC and *X*-*P* time.

No.	Origin Time					Epicenter		*h*	*Mb*	*Δ*	*X*-*P*
	y	d	h	m	s	N	E	km		deg	s
1	1970 June	6	12	59	54.1	18°.61	145°.28	601	5.0	17.74*	80
2	1977 Feb.	17	18	34	09.5	18.61	145.26	594	4.9	17.74	80
3	1982 Jan.	4	06	15	15.9	18.03	145.50	603	5.4	18.36	82
4	1973 July	17	14	17	43.8	18.72	145.38	600	4.2	18.06	79

*; SRY

Comments;

1) The source depth and the epicentral distance are large compared to those of events shown in Figs. 10 to 12. The *X*-*P* times are also large.
2) Similar seismograms are seen frequently for events with similar epicentral distance and depth.
3) The expected time of *PP* phase is 62 sec after arrival of the *P* wave, and such a phase can be seen rarely only on LP seismograms (Fig. 25, TSUJIURA, 1988).

In Figs. 10~13, the *X*-*P* times increase with epicentral distance and source depth. The source depth and the *X*-*P* time obtained here are about 600 km and about 80 sec, respectively.

If we assume that the *X* phase is a similar converted phase from *S* to *P* at the discontinuity, the converted point corresponds to a depth of 920 km.

Recently, the existence of 920 km depth discontinuity has been proposed by KAWAKATSU and NIU (1994) using stacking data of J Array. It is noted that the *X* phase can be seen directly if selection of data is adequate.

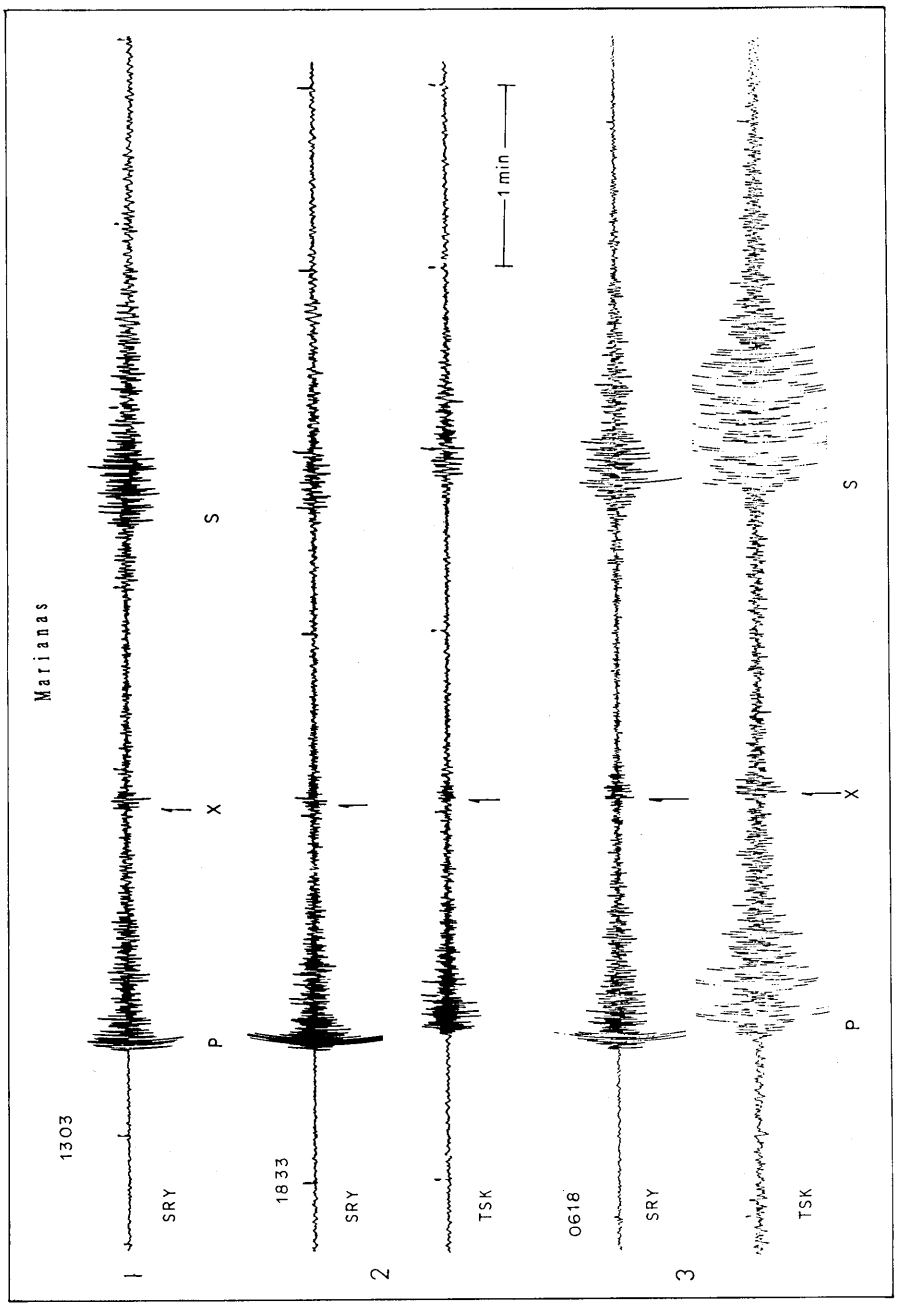

Fig. 13. Seismograms accompanied with X phase for the events of Marianas region. Note that the source depth and epicentral distance are larger than those of previous Figures (Figs. 10~12).

14. *X* phase from deep Okhotsk earthquakes

The seismograms of deep earthquakes from south Honshu including the Bonin Is.-Marianas regions are accompanied with the *X* phase, although the *X*-*P* times differ by source depth and epicentral distance or by seismic region. A similar *X* phase can be seen also for seismograms from the Okhotsk Sea region.

Figure 14 shows seismograms from deep earthquakes of the Sea of Okhotsk region obtained by a long-period seismograph (LP) at DDR. No data of SP seismograph are available because all seismograms are saturated. The focal parameters and *X*-*P* time are shown in Table 16.

Table 16. Focal parameters by ISC and *X*-*P* time.

No.	Origin Time					Epicenter		*h*	*Mb*	*Δ*	*X*-*P*
	y		d	h	m	s	N	E	km		deg	s
1	1970	Sep.	5	07	52	27.2	52°.28	151°.49	560	5.7	18.47	38.0
2	1971	Jan.	29	21	58	03.2	51.69	150.97	515	6.0	17.81	37.5
3	1975	Dec.	21	10	54	17.2	51.93	151.57	546	6.0	18.19	36.2
4	1970	Aug.	30	17	46	08.9	52.36	151.64	643	6.5	18.59	52.0

Comments ;

1) The *X* phase also appears on the seismograms of deep Okhotsk earthquakes, although their amplitudes are small. The sizes of the bars at the end of seismogram show relative differences of the magnification of a seismograph.
2) The arrival time of *X* phase measured on the LP seismogram is somewhat uncertain compared to that of SP seismogram. Even considering the uncertain reading of *X* phase, the *X*-*P* times obtained here are smaller than those of Marianas events with similar depths and distances, except for event No. 4.

Considering the facts mentioned above, there is two kinds of discontinuity. The depth of the former group (Nos. 1～3) is probably 720 km and the latter (No. 4) is deeper than 720 km. It is interesting to note that the depth of a discontinuity is different between the Marianas and Okhotsk regions.

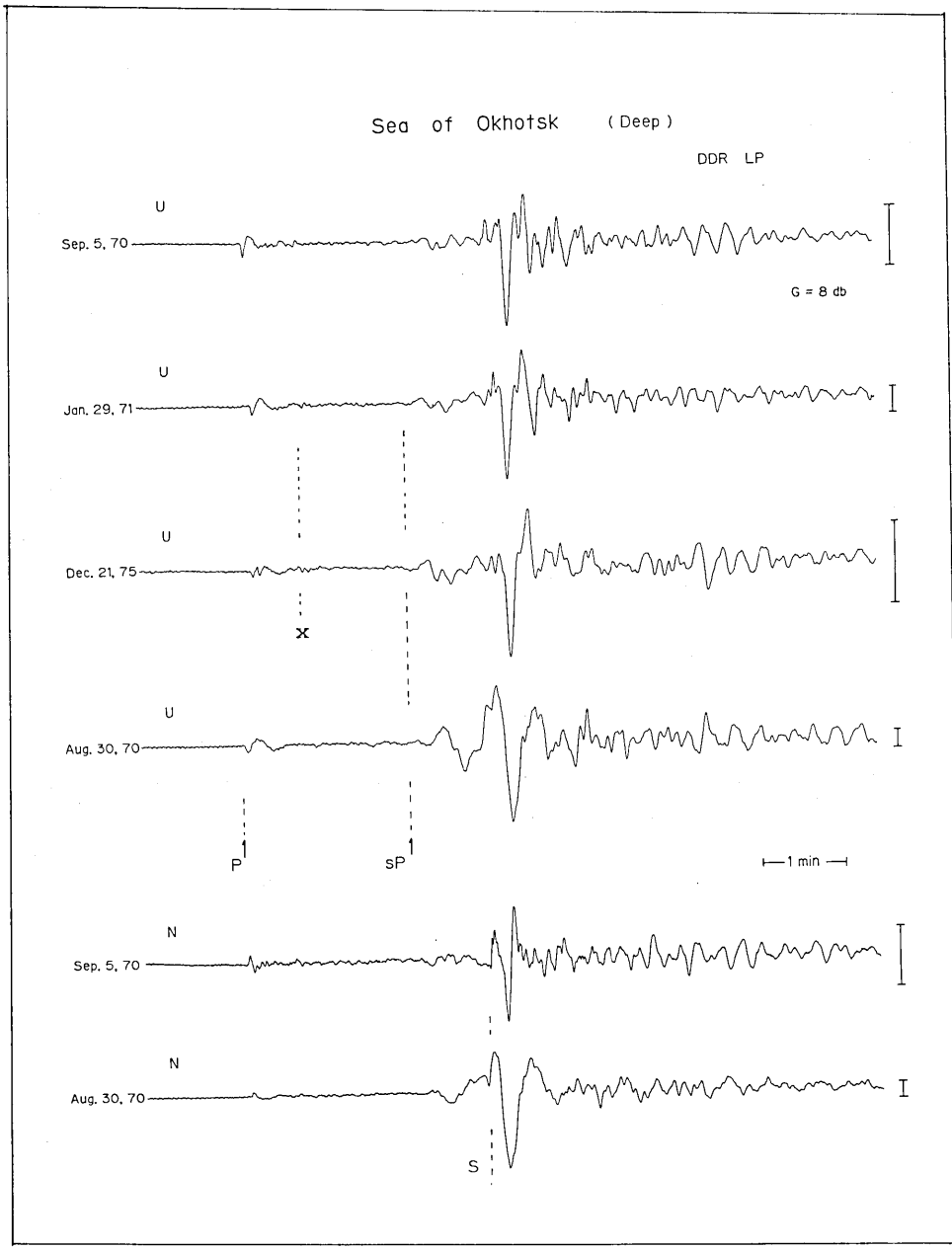

Fig. 14. Seismograms obtained by LP seismograph at DDR. These seismograms are reproduced from magnetic tape. The length of bars show relative difference of magnification. Small *X* phase is observed for all vertical component (U) seismograms.

15. *X* phase from deep Mindanao earthquakes

In the previous Figures (Figs. 10～14), *X* phases are found between *P* and *S* phases in regional deep earthquakes ($\Delta=8°\sim18°$). Similar phases are found also in deep tele-seismic events.

Figure 15 shows seismograms of two events on the Mindanao Islands, Philippine region, and their focal parameters and *X*-*P* times are shown in Table 17.

Table 17. Focal parameters by ISC and *X*-*P* time.

No.	Origin Time					Epicenter		*h*	*Mb*	Δ	*X*-*P*
	y		d	h	m	s	N	E	km		deg	s
1	1972	Oct.	1	23	49	37.5	07°.46	123°.77	632	6.0	31.71*	31.7
2	1977	Nov.	21	11	39	40.4	06.82	123.58	603	5.7	32.37*	31.1

*; DDR

Comments ;

1) A clear *X* phase is seen between *P* and *pP* phases for event No. 1, but no *pP* phase is observed for event No. 2.
2) The time interval of *P* and *X* phases is 31.7 sec for event No. 1 and 31.1 sec for event No. 2, respectively.
3) The source depths of both events are about 600 km, and this value is the same for that of Marianas events (Fig. 13).
4) An apparent velocity of *P* waves is 13 km/s, and that of *X* phase is 13.5 km/s.

Although the *X* phase is obtained here in only two samples, the *X* phase will probably be a reflected wave from *P* to *P* at the discontinuity located at a depth of about 1,200 km, because the deepest point of the event at a depth of 600 km and epicentral distance with 32 degrees is 893 km. However, there is no evidence supporting the above conclusion.

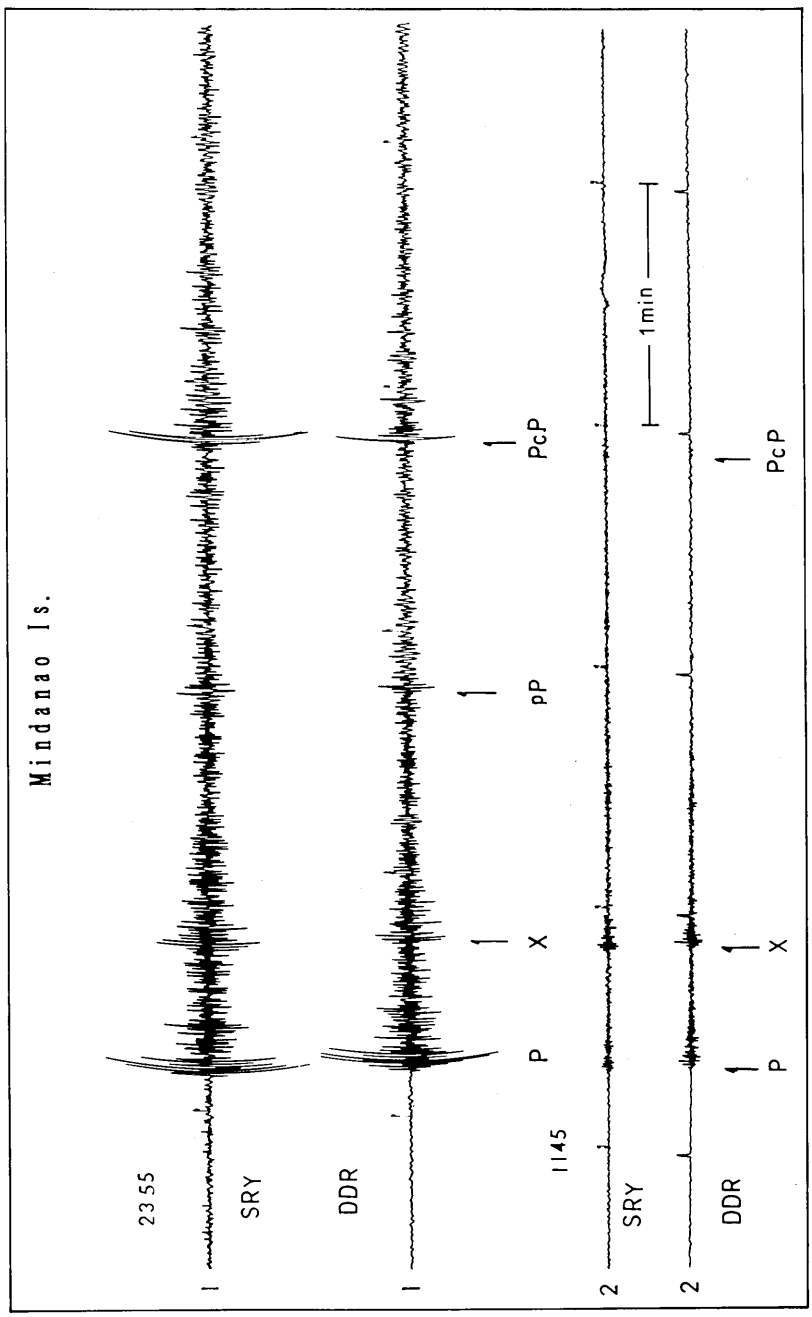

Fig. 15. Seismograms accompanied with *X* phase from deep events of Mindanao region obtained at SRY and DDR. A similar phase can be seen for the other stations.

16. *X* phase from Taiwan earthquake

In Figures 10~15, the *X* phase is found between *P* and *S* waves from a deep earthquake (500 km). A similar *X* phase is found for a Taiwan earthquake of an intermediate source depth.

Figure 16 shows seismograms from Taiwan region obtained at SRY, DDR and TSK stations, and focal parameters of this event are shown in Table 18a.

Table 18a. Focal parameters by ISC.

Origin Time					Epicenter		*h*	*Mb*	*Δ*
y	d	h	m	s	N	E	km		deg
1976 June	2	10	24	32.5	25°.27	122°.18	223	5.3	17.95*

*; SRY

In this figure, a clear *X* phase is seen about 40 sec after the *P* wave arrives. Table 18b shows the arrival times of *P* and *X* phases and *X-P* times obtained at three stations.

Table 18b. Arrival times of *P* and *X* phases.

Code	*P*			*X*			*Δ*	*X-P*
	h	m	s	h	m	s	deg	s
SRY	10	28	26.5	10	29	05.8	17.95	39.3
DDR	10	28	28.8	10	29	08.8	18.10	40.0
TSK	10	28	33.0	10	29	13.8	18.84	40.8

Comments ;

1) The difference in arrival times of *X* and *P* waves is about 40 sec.
2) The difference in arrival times of *P* and *X* waves among the stations is 6.5 sec and 8.0 sec, respectively.

The time difference among the stations for the *X* phase is larger than that of the *P* wave. The *X* phase therefore is the *pP* wave, although there are no data on the *J-B* Table for an epicentral distance shorter than 20 degrees and for a source depth of 225 km. Our value of *X-P* times, however, agrees within a few seconds for the *pP* phase when the *J-B* Table is extended to 18 degrees.

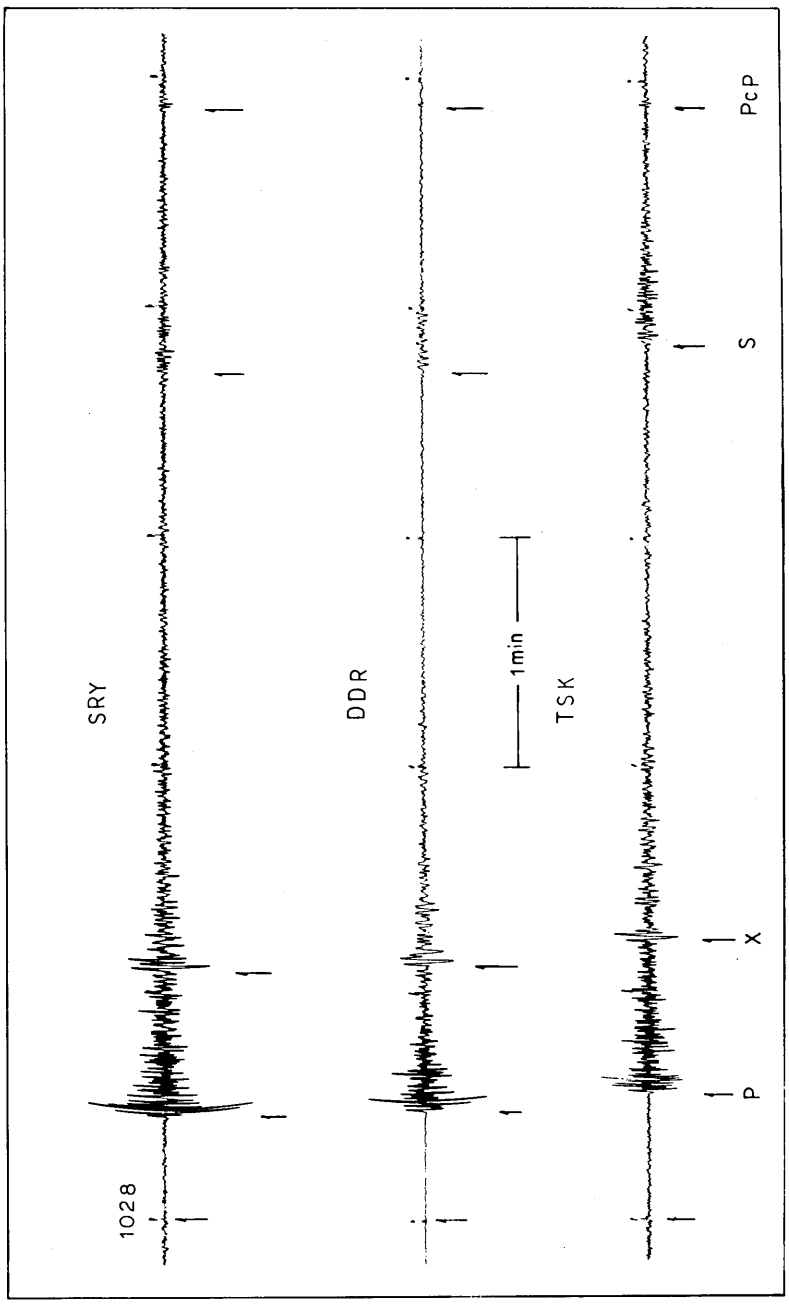

Fig. 16. Seismograms accompanied with *X* phase from Taiwan earthquake. Considering the velocity of *X* phase among the stations, this phase is probably *pP*, although there are no data on *J-B* Table.

17. Character of *PcP* and *ScP* phases

The *PcP* and *ScP* phases are frequently observed for events having a wide range of epicentral distance and source depth, and these phases usually show impulsive waveforms. We examined waveforms of about 50 samples and found that some of them do not show an impulsive wave. Their waves separate into two or three phases. Figure 17 shows seismograms including the *PcP* and *ScP* phases. Although these seismograms randomly arranged, the *PcP* and *ScP* do not show impulsive waveforms, especially for seismograms Nos. 3 and 7. Table 19 shows the focal parameters of these events.

Table 19. Focal parameters by ISC.

No.	Origin Time					Epicenter		*h*	*Mb*	*Δ*	Region
	y		d	h	m s	N, S	E	km		deg	
1	1972	July	7	12	36 15.3	11°.56	126°.27	41	5.5	20.72	Philip.
2	1969	May	13	14	30 20.7	07.22 S	120.90	627	5.6	46.31	Flores-
3	1975	Apr.	13	01	34 37.4	05.66	125.38	235	5.5	32.75	Mindanao
4	1972	Nov.	27	15	17 39.8	05.30 S	126.62	412	5.6	42.5	Banda-
5	1975	July	31	16	24 32.3	05.25 S	152.78	51	5.6	42.96	New Bri.
6	1977	Feb.	13	13	06 55.0	00.08 S	125.11	70	5.7	38.70	Molucca-
7	1980	Apr.	13	05	41 46.4	09.00	126.27	66	5.8	29.25	Mindanao
8	1979	Feb.	7	21	02 04.7	05.23	127.36	114	6.2	32.5	Philip.

Comments ;

1) The *PcP* phase is indicated by an arrow. This phase is identified in *J-B* Table. Some of them consist of two wavelets with a maximum of 4 sec interval. These events are distributed between 20-46 degrees and their source depth of 40-600 km.
2) The time interval of two wavelets of *ScP* (No. 3) is 7.4 sec. Large events frequently occur as multiple shocks. The events presented here are not due to multiple shocks.

The existence of two wavelets of *PcP* and *ScP* with different time intervals suggests that the Core-Mantle boundary is not simple.

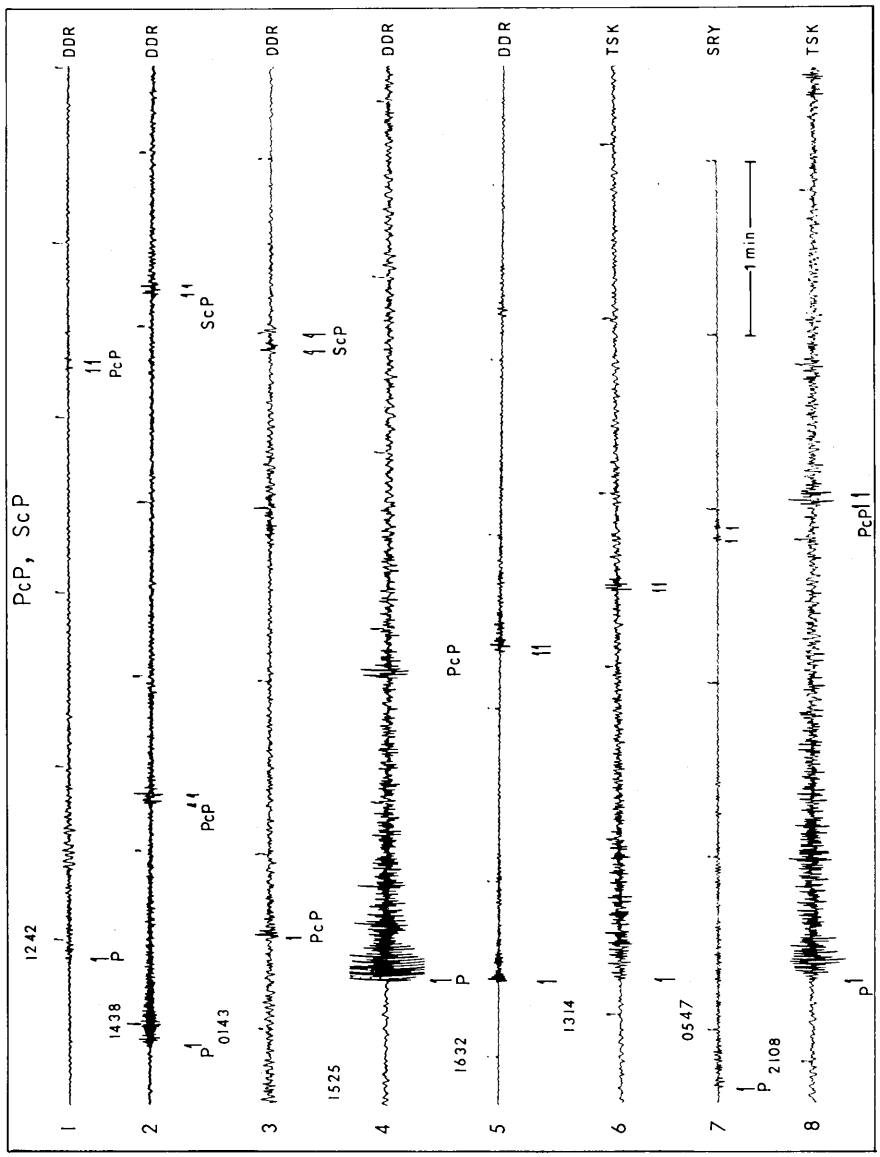

Fig. 17. Example of *PcP* and *ScP* waveform. As indicated by the arrows, some of them are separated into two wavelets. *ScP* of No. 3 and *PcP* of No. 7 seismograms are especially noticeable.

18. Separated waveforms of *ScS* or *ScP* phase

In the previous figure (Fig. 17), it can be seen that the *PcP* and *ScP* waves are not impulsive. They consist of two separated wavelets with time intervals of up to 7.4 sec.

Figure 18 shows that the *ScS* and *ScP* phases also consist of two or three wavelets as indicated by arrows. Table 20 shows the focal parameters of these events.

Table 20. Focal parameters by ISC.

No.	Origin Time					Epicenter		*h*	*Mb*	*Δ*	Region
	y		d	h	m s	N, S	E	km		deg	
1	1980	July	17	19	42 23.0	12°.48 S	166°.06	29	5.6	54.49	Santa-
2	1975	Apr.	13	01	34 37.4	05.66	125.38	235	5.5	32.75	Mindanao
3	1983	Oct.	8	07	45 26.3	44.21	130.74	551	5.6	10.79	E. Russia
4	1983	July	24	23	07 31.8	53.91	158.36	190	5.4	22.20	Kamchatka
5	1970	Feb.	13	03	12 52.8	24.52	141.40	190	5.4	11.60	Volcano
6	1973	Sep.	12	06	59 54.6	73.32	54.97	0	6.8	54.28	Novaya-

Comments ;

1) The *ScP* phase having two wavelets is seen for events of Nos. 2 and 6. The time interval of event No. 2 is 7.4 sec and that of No. 6 is 13.5 sec.
2) The *ScS* phase is also separated into two or three phases as indicated by arrows. The time interval of the first two arrows lies between 4.3 sec and 8.5 sec.
3) In the previous study of this series (TSUJIURA, 1988), similar separated *ScS* waves can be seen. The waveforms are, however, different between both cases. In the previous study, the amplitude of the first arrival is very small compared to that of later arrival, and it may be concluded that the first phase is *ScSp*. Considering the waveform of this case, the existence of two phases is undoubted. A detailed study of these waves will give important information on the Core-Mantle boundary.

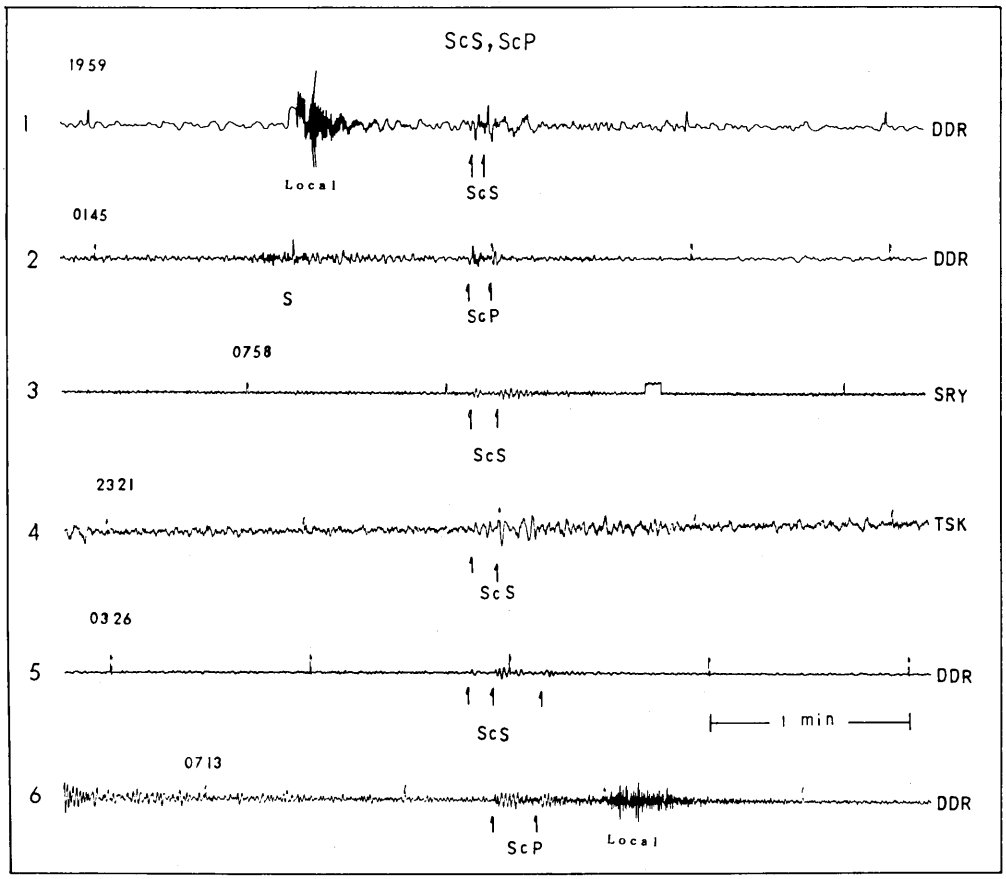

Fig. 18. Seismograms including *ScS* and *ScP* phases. These phases are identified by the *J-B* Table. The separated waveforms of *ScP* and *ScS* are noticeable.

19. *P*-Later phase from deep earthquakes in the three regions

As shown previously, the deep earthquakes from Bonin Is. and Marianas regions are accompanied with the *P*-Later phase, about 18, 39, 48 and 80 sec after *P* wave onset. Such a phase may be related to the underlying discontinuities between station and epicenter.

Another example of *P*-Later phase (*X*) can be seen with events of other seismic regions. Figure 19 shows seismograms from three regions. The top four seismograms (Nos. 1-4) are from Solomon Is., the center six seismograms (Nos. 5-8) are from Fiji and the bottom seismogram is from Southern Italy.

Table 21. Focal parameters by ISC and *X-P* time.

No.	Origin Time					Epicenter		*h*	*Mb*	*Δ*	*X-P*
	y		d	h	m	s	N	E	km		deg	s
1	1978	Nov.	12	08	11	16.0	10°.56	161°.44	75	5.2	50.47	14
2	1971	Feb.	26	04	55	52.1	10.47	161.35	107	5.7	50.36	16.5
3	1972	Jan.	29	08	41	52.3	07.73	158.03	113	5.0	46.59	16
4	1973	Dec.	18	04	09	09.2	05.34	154.28	413	5.2	43.11	22
							S	W				
5	1983	Jan.	25	15	04	10.0	21.96	177.39	274	5.4	70.78	9
6	1978	Sep.	16	23	38	09.6	25.72	177.94	227	5.6	74.46	10
7	1972	July	16	00	29	17.5	20.86	178.75	611	5.3	69.15	10
8	1974	May	26	05	47	37.0	20.72	178.48	565	5.6	68.85	13
							N	E				
9	1978	Dec.	27	17	46	10.4	41.08	13.56	392	5.4	88.80	8.5

Comments ;

1) The *X* phase of the top four seismograms (Solomon Is.) is thought to be the *pP* phase, although source depth and *X-P* time does not agree with *J-B* Table, especially for seismogram No. 4.
2) The middle six seismograms (Nos. 5-8) from Fiji are unknown, at least the *X* phase is not a *PcP* or *pP* phase.
3) The *X* phase of seismogram No. 9 (Italy) is not a *PcP* phase. The *PcP* phase should be arrived after about 3 sec of *P*.

Considering *X-P* time and source depth, it is expected that the *X* phases are neither *pP* or *PcP* nor the local phase.

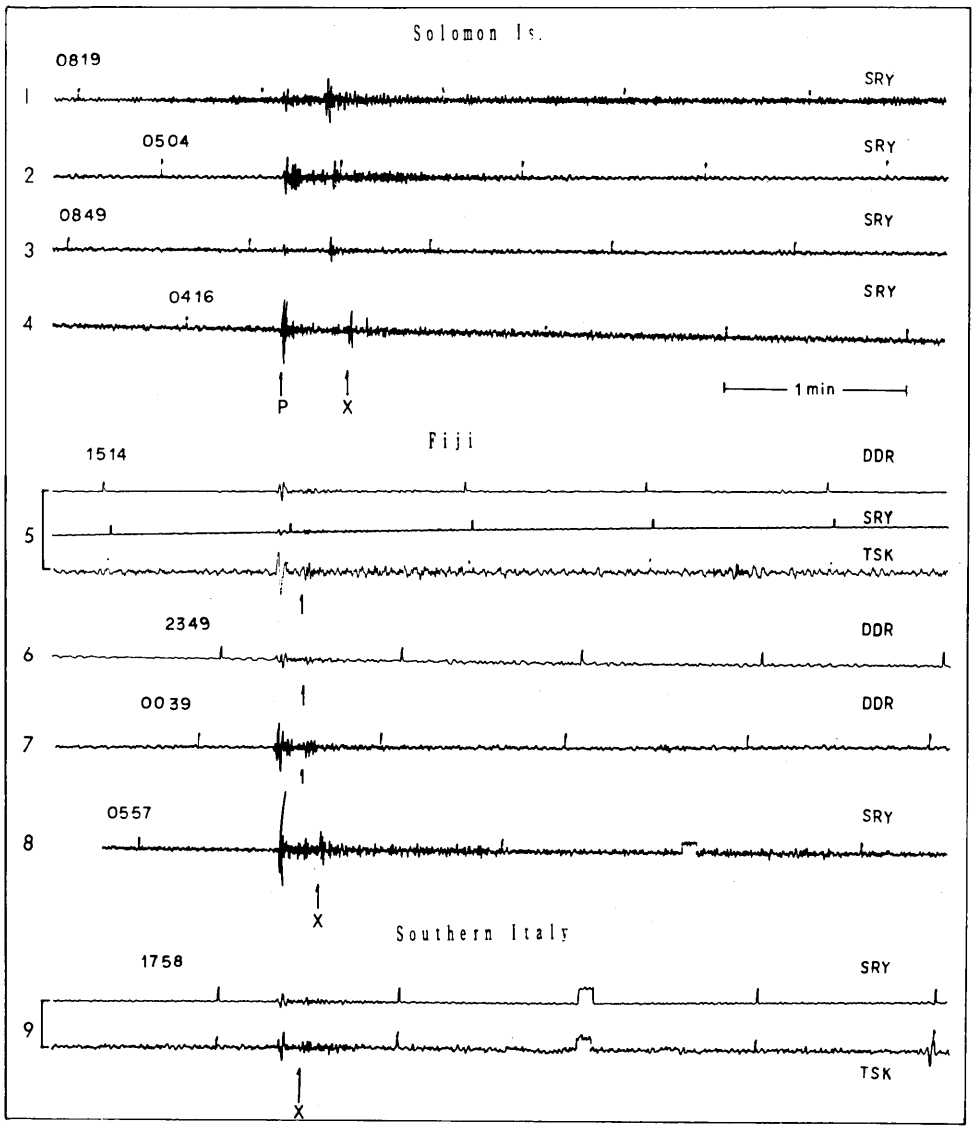

Fig. 19. Seismograms accompanied with *X* phase from events in three regions (Solomon, Fiji and S. Italy). The *X* phase is distributed over wide ranges of epicentral distance and source depth.

20. *X* phase between *P* and *PcP* from deep earthquakes in the Fiji region

In the previous figure (Fig. 19), the *P*-Later phase about 10 sec after *P* wave onset is found for deep earthquakes in the Fiji region. Among these seismograms, however, no *PcP* phase was found.

Figure 20 shows the seismograms from Fiji region obtained at SRY station. The *PcP* phase is clearly seen for all seismograms. Moreover, one or two phases, as indicated by *X* or a broken line, seems to exist between *P* and *PcP*.

Table 22. Focal parameters by ISC and *PcP*–*X* time.

No.	Origin Time					Epicenter		*h*	*Mb*	*Δ*	*PcP*–*X*
	y	d	h	m	s	N	E	km		deg	s
1	1972 May	9	12	20	22.3	17°.83	178°.79	565	5.8	66.36	11.3
2	1973 Feb.	13	15	22	54.8	17.63	178.47	543	5.7	66.38	10.4
3	1976 Apr.	10	17	12	08.3	17.70	178.46	548	5.7	66.44	11.3
4	1977 Apr.	14	04	05	32.1	17.70	178.67	546	5.2	66.32	11.4
5	1972 Mar.	17	00	21	26.2	24.83	179.63	415	5.5	72.28	10.7

Comments ;

Usually, there is no phase between *P* and *PcP* in these epicentral distances, however, one or two phases with a small amplitude, as indicated by *X*, seem to exist there.

1) The *PcP*–*X* times are about 11 sec. One more phase indicated by a broken line is seen with events Nos. 1, 3 and 4. The time interval of this phase and *PcP* is about 5 sec.
2) A similar phase with a small amplitude preceding *PcP* can be seen with the events at New Ireland (Mar. 4, 1978) and Solomon Is. regions (Nov. 28, 1968).
3) There is a possibility that the *X* phase preceding the *PcP* is the *PdP* wave reflected at the upper plane of layer D".

Recently, the study of the Core-Mantle boundary, e.g., the existence of layer D", has been one of the most important problems. A detailed study of the preceding phase of *PcP* will give clues to this problem.

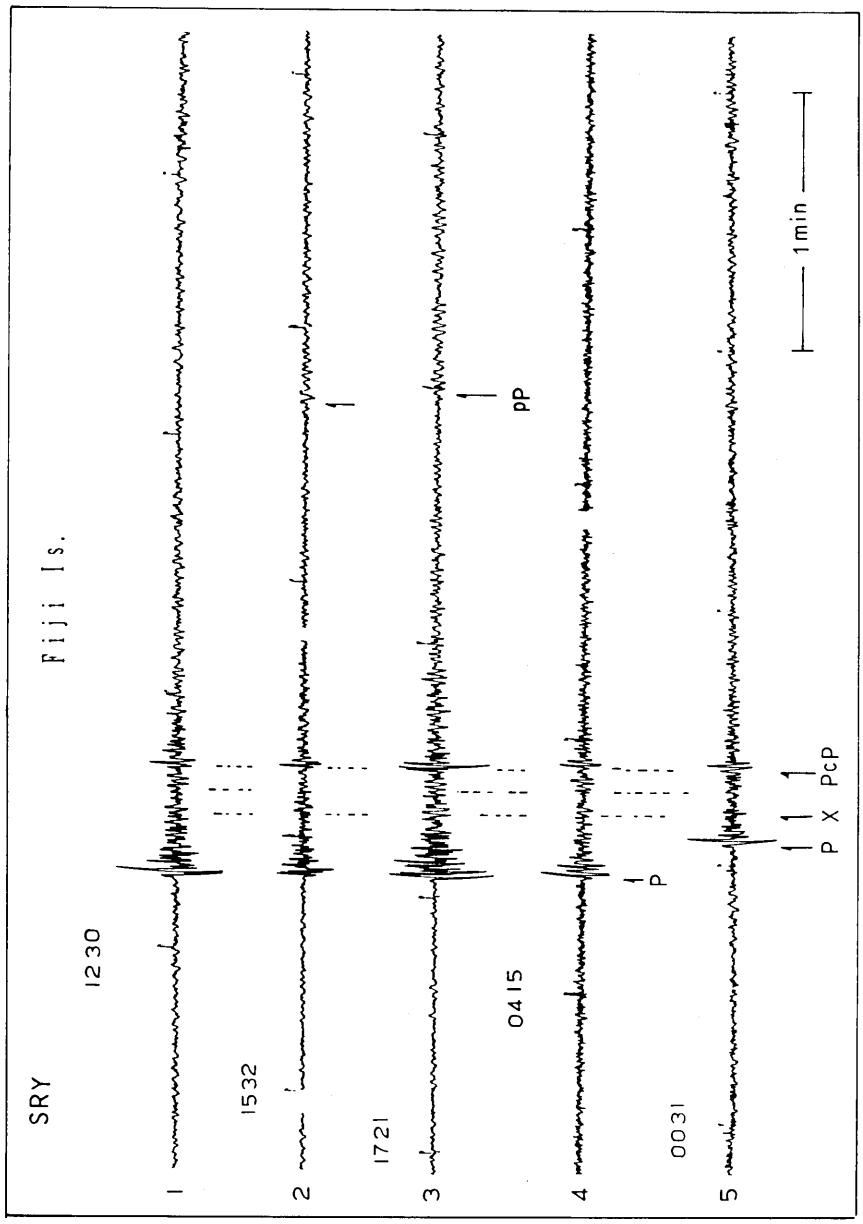

Fig. 20. Seismograms obtained at SRY for deep events from Fiji Islands region. One or two phases indicated by *X* or a broken line seems to exist between *P* and *PcP* phases, which is probably related to CMB.

21. *pP* phase of earthquakes from the Alaska region

During the interpretation of the seismogram from Alaska Peninsula a clear phase can be found after *P* wave arrival. Figure 21 shows five seismograms obtained at DDR station. Table 23 shows the focal parameters by ISC and the time between *P* and later phase (ΔT).

Table 23. Focal parameters by ISC and ΔT.

No.	Origin Time					Epicenter		*h*	*Mb*	Δ	ΔT
	y		d	h	m	s	N	E	km		deg	s
1	1969	Dec.	26	00	18	19.0	55°.18	160°.44	10	5.3	44.82	15.2
2	1974	Apr.	6	03	55	57.1	55.05	160.51	6	6.0	44.78	16.5
3	1975	July	25	10	40	23.0	55.04	160.41	1	5.6	44.84	15.2
4	1980	Aug.	23	00	45	54.1	54.09	160.48	34	5.3	44.80	15.6
5	1983	Feb.	14	08	10	04.3	54.99	159.24	37	6.0	45.51	13.2

Comments ;

1) A clear phase is seen about 15 sec after *P* wave onset. Considering the epicentral distance, this phase may be the *pP*.
2) The time intervals of *P* and *pP* phases are 15–16 sec as indicated by ΔT, except for event No. 5, whose location is different from those of the others.
3) The source depth varied from 1 to 37 km, though the *pP*-*P* time (ΔT) is almost the same. The ΔT = 16.5 sec corresponds to 65 km source depth.

If our interpretation of *pP* is correct, the source depth of ISC is too shallow.

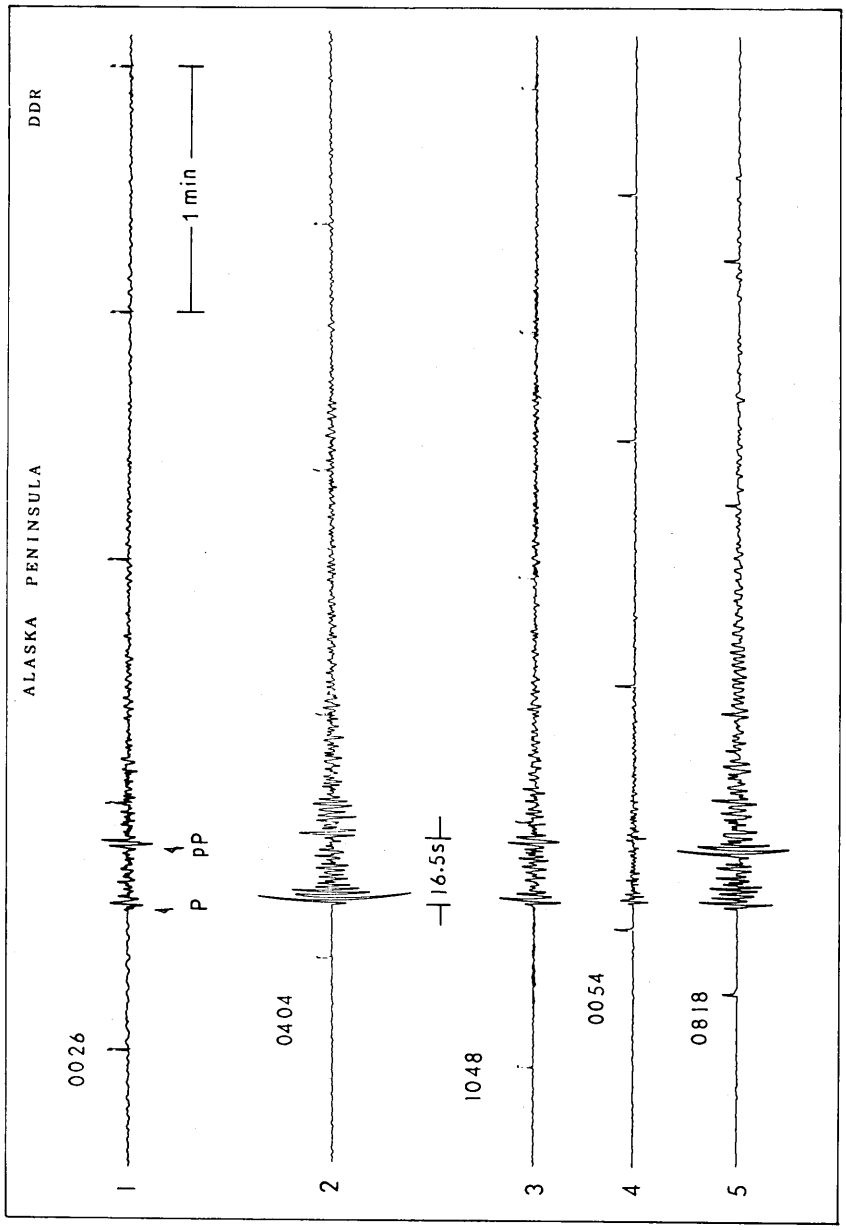

Fig. 21. Seismograms obtained at DDR for events in Alaska region. Clear *pP* phase can be seen for all seismograms, but it time does not agree with the depth of ISC.

22. Double phases of *pP* from deep earthquakes —Fiji Is.—

The Fiji Is. is one of the most active regions of deep earthquake occurrence. The epicentral distances from our stations are about 60 degrees. It is, therefore, very convenient to study *pP* due to the lack of contamination of the other phases. Usually, the *pP* phase has an impulsive waveform. Double or triple phases of *pP* can be seen frequently, but not always, on seismograms from this region.

Figure 22 shows seismograms including *pP* phase from deep earthquakes in the Fiji Islands region. Seven seismograms are selected for the present study.

Table 24. Focal parameters by ISC.

No.	Origin Time					Epicenter		*h*	*Mb*	*Δ*
	y		d	h	m s	N	E	km		deg
1	1979	Apr.	24	01	45 08.7	20°.82	178°.67	596	5.9	68.82
2	1977	Jan.	21	06	11 05.3	18.06	178.37	601	5.7	66.75
3	1981	Oct.	7	03	02 12.7	20.07	178.65	606	5.9	68.74
4	1977	Jan.	21	06	11 05.3	18.06	178.37	601	5.7	67.11
5	1970	Jan.	28	23	06 01.4	20.69	178.79	603	5.6	68.99
6	1977	July	6	11	28 31.5	21.00	178.58	592	5.6	69.35
7	1981	Oct.	7	03	02 12.7	20.70	178.65	606	5.9	68.74

Comments ;

1) The *pP* phase consisting of multiple phases are events with a source depth of about 600 km.
2) The first arrow of each seismogram corresponds to *pP*.
3) The time intervals of first and second arrows vary between 7.5 s and 11 s, and that of first and third arrows is about 16 s.

The *pP* phase comprises reflected waves at the sea bottom. The second wavelets of *pP* phase, therefore, may be the reflected wave at the free surface. This phase is, therefore, called as the *pwP*. Similar *pwP* waves are observed with deep events (390–450 km) in the Bonin Islands (BARLEY *et al.*, 1982). The existence of three phases may be related to a sedimentary layer.

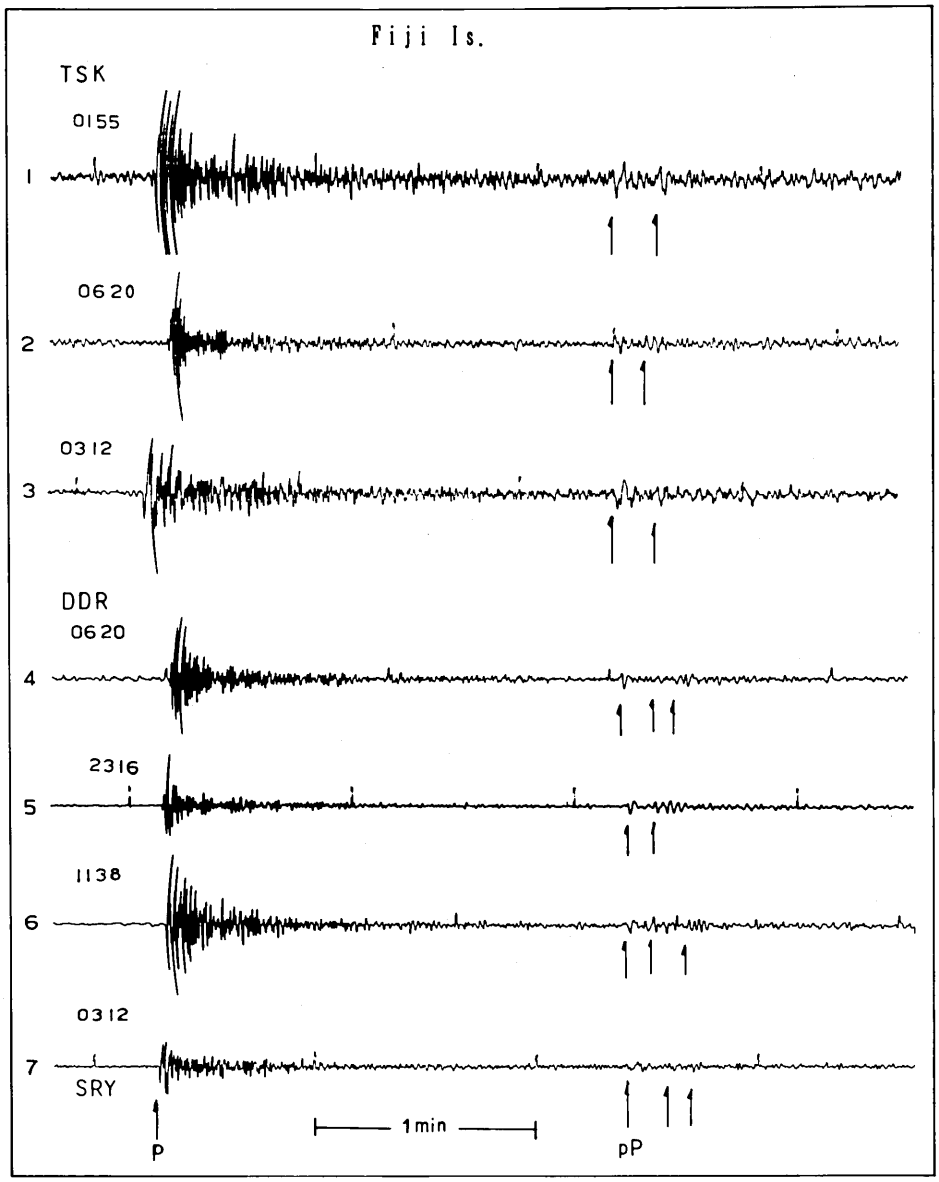

Fig. 22. Seismograms showing the *pwP* phase obtained at TSK, DDR and SRY for the deep events of Fiji Islands region. The first arrow shows the *pP* phase, and the 2nd arrow shows the *pwP* phase. Moreover, the 3rd phase seems to exist there (Nos. 4, 6, 7). In this case, the 2nd phase may be a reflected wave at the sedimentary layer. But, the separation of each phase is not clear.

23. Double phases of *pP* from earthquakes of three regions

In the previous figure, the double phases of *pP* can be seen on the seismograms from deep earthquakes (600 km) of Fiji Islands region. The *pP* consisting of double phases can be seen also in the other seismic regions.

Figure 23 shows the *pP* phase consisting of double phases for earthquakes from three regions. The seismograms of Nos. 1-3 are from south of Fiji Is., No. 4 is from south of Kermadec Is. and No. 5 is from Fiji Is. region, respectively. It is noted that the source depths are located at between 189-618 km.

Table 25. Focal parameters by ISC.

No.	Origin Time					Epicenter		*h*	*Mb*	*Δ*
	y		d	h	m	s			km		deg
1	1970	Feb.	16	21	36	22.4	25°.27 S	178°.44 E	585	5.3	71.32
2	1969	Feb.	3	07	51	24.9	25.87 S	178.23 E	618	5.3	71.37
3	1974	Mar.	23	14	54	07.7	23.91 S	179.01 E	531	5.5	70.80
4	1970	Jan.	8	17	12	40.6	34.85 S	178.79 E	189	6.1	79.57
5	1970	Feb.	18	15	23	31.5	20.83 S	176.71 W	240	5.7	70.25

Comments ;

1) The source depths of Nos. 4 and 5 are shallower than the other events.
2) The *pP* consisting of two wavelets is shown by two arrows.
3) The time interval of two arrows is 4-5 sec, except for event No. 3, and these values are shorter than those of previous figure (Fig. 22).
4) The *pP-P* time of event No. 3 is 142 sec. This value is about 30 sec later than the expected value of *J-B* Table. The arrival time of *PP* by *J-B* Table is 15 h 08 m 47.7 s, but, there is no phase for the corresponding time.

If 2 nd phase is the reflected wave at the sea surface (*pwP*), the water depths at the reflected point of seismograms Nos. 4 and 5 are shallower than the previous ones. If we assume that the average velocity of *P* wave is 1.5 km/s, the time interval of 5 s corresponds to an ocean depth of 3.75 km.

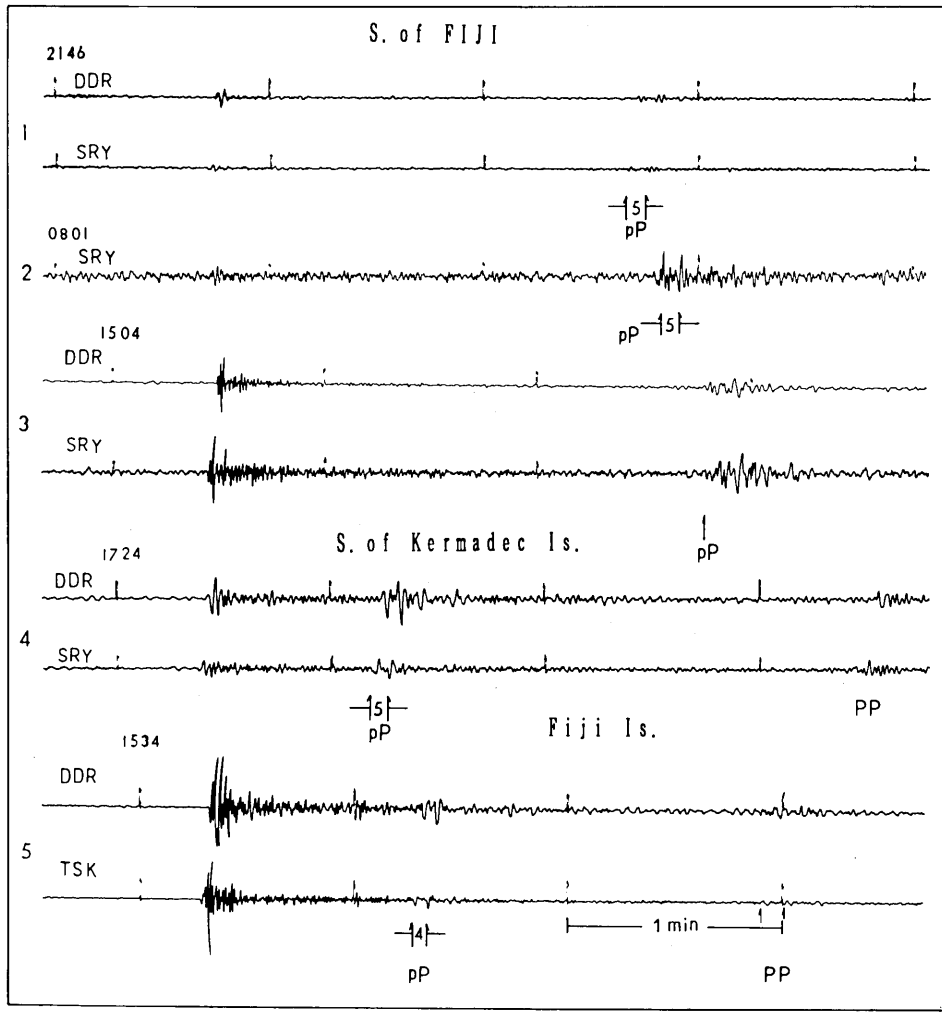

Fig. 23. Seismograms showing the multiple phases of *pP* for the events in three regions. Note that the time interval of two wavelets is shorter than that shown in Fig. 22.

24. *P3KP* from Near and Regional Earthquakes

The *P'P'* phase is frequently observed with large earthquakes having an epicentral distance of 60–70 degrees. This may be due to the reflecting point being located at about 145 degrees from the epicenter where the seismic waves focus. A similar phase is rarely observed with near earthquakes.

Figure 24 shows reflected waves from near and regional earthquakes obtained at DDR and TSK in which it corresponds to *P'P'* wave of a teleseismic event. Although the onset of this phase is not clear as indicated by arrows, the waveforms are like the *P'P'* waves of a teleseismic event. The focal parameters of the events following the reflected waves are shown in Table 26.

Table 26. Focal parameters by ISC.

No.	Origin Time					Epicenter		*h*	*Mb*	*Δ*	Region
	y		d	h	m s	N	E	km		deg	
1	1978	Jun.	12	08	14 24.4	38°.23	142°.02	48	6.7	3.17	N. Honshu
2	1971	Aug.	2	07	24 56.0	41.37	143.44	45	6.5	6.31	Hokkaido
3	1978	Dec.	6	14	02 04.5	44.55	146.67	118	6.3	10.27	Kurile Is.
4	1971	Nov.	25	19	35 28.5	52.85	159.22	99	6.4	21.98	Kamchatka
5	1979	Aug.	27	14	31 25.8	19.04	122.12	43	6.0	22.62	Philip.

Comments ;

1) The shortest epicentral distance for the appearance of a reflected phase is 3.17 degrees. Over this distance, the path length of *PKPPKP* (*P'P'*) phase is about 357 degrees, and its time travel is about 44 min from the origin time.
2) As connected by a broken line, the arrival time of event No. 1 is 39 m 21 s, and that of event No. 5 is 38 m 40 s. These times are too fast for the arrival time of *P'P'* phase.
3) The occurrence of another event during one hour for each event was examined. However, there is no event on the ISC.

Considering arrival times and their epicentral distances, this phase probably will be the *P3KP*.

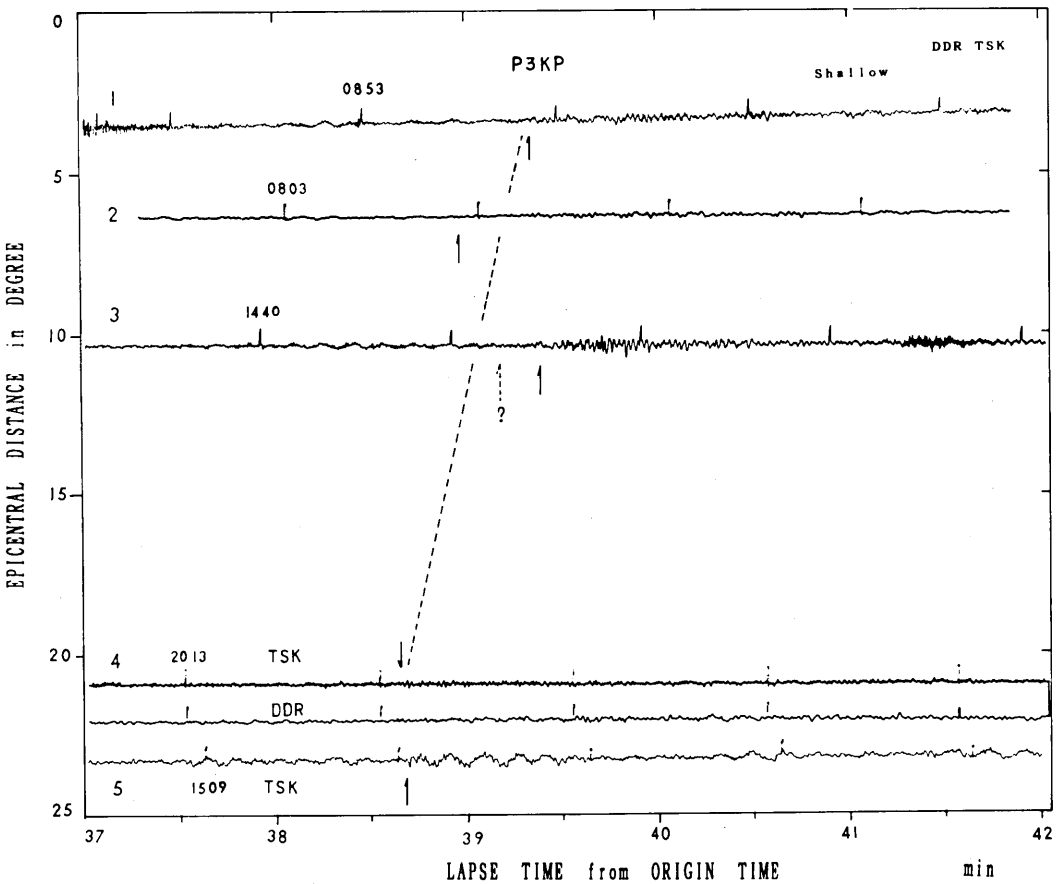

Fig. 24. *P3KP* waves from near and regional events. Broken line and arrows show onset of their waves.

25. *P3KP* and *P'P'* from deep earthquakes

The previous figure (Fig. 24) shows *P3KP* waves from near earthquakes with a source depth shallower than about 100 km. In this section, the *P3KP* phase from deep earthquakes is examined.

Figure 25 shows *P3KP* waves from deep earthquakes ($h>400$ km) obtained at DDR. Table 27 shows focal parameters of these events and their regions.

Table 27. Focal parameters by ISC.

No.	Origin Time					Epicenter		h	Mb	Δ	Region
	y		d	h	m s	N, S	E	km		deg	
1	1978	Mar.	7	02	48 47.6	31°.99	137°.61	441	6.5	4.51	S. Honshu
2	1975	Jun.	29	10	37 40.6	38.79	130.09	549	6.1	7.76	Japan Sea
3	1982	Jun.	22	04	18 40.3	07.33 S	126.08	449	6.3	44.82	Banda Sea
4	1973	Dec.	28	05	31 03.8	23.88 S	180.00	517	6.2	70.96	S. Fuji
5	1972	Mar.	30	05	34 50.4	25.69 S	179.58	479	6.1	72.24	S. Fuji

Comments ;

1) Small, but clear phases are seen for events Nos. 1 and 2 as indicated by *X*. The arrival times of these phases are 38 m 28 s and 38 m 26 s, respectively. Comparing event No. 1 in the Fig. 24, the arrival time of this phase is about 53 sec earlier than the previous one. Such a difference is due to the difference of source depth. The *X* phase of events Nos. 1 and 2 is, therefore, the *P3KP* as in the previous figure.
2) The *X* phase of event No. 3 is different from the with other one. This phase has a *PKHKP* branch (see Fig. 29 a), but onset of this phase is not clear.
3) The arrival times of *X* phase indicated by arrows on seismograms Nos. 4 and 5 are 38 m 15 s. This value almost agrees with the *J-B* Table as *PKPPKP* (*P'P'*).

The *X* phases shown in this figure, therefore, are *P3KP* for a short distance and *P'P'* waves for a large distance.

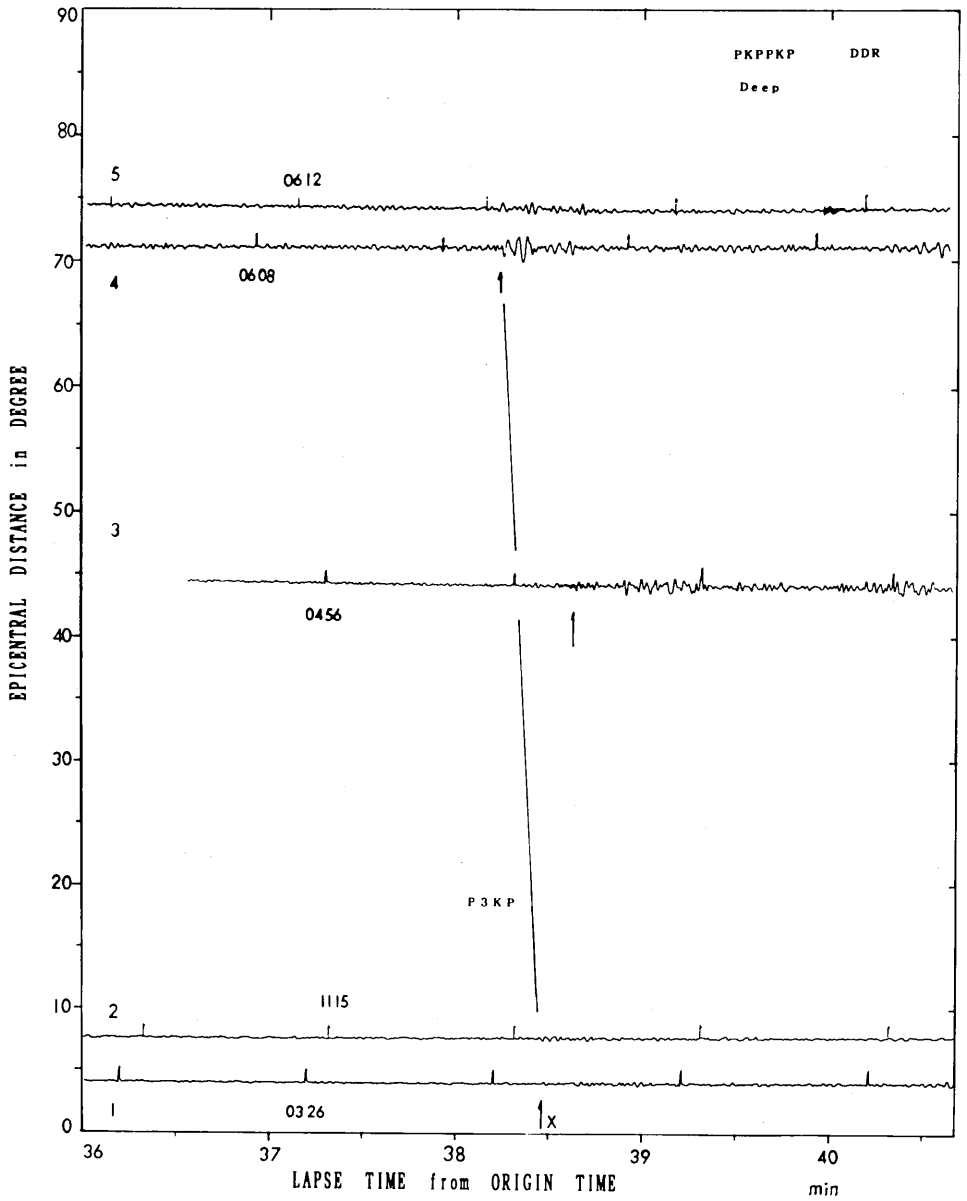

Fig. 25. Seismograms showing the *P3KP* wave from near, regional earthquakes and *P'P'* wave from teleseismic events with deep focus. The onset of each phase is shown by an arrow.

26. *P'P'* wave from teleseismic events

In the previous figures (Figs. 24, 25), the *P3KP* waves from near earthquakes are explained. In this section, ordinary *PKPPKP* (*P'P'*) waves are investigated.

Figure 26 shows *P'P'* waves for events with epicentral distance of 45–70 degrees obtained at DDR.

Table 28. Focal parameters of events by ISC.

No.	Origin Time					Epicenter		*h*	*Mb*	*Δ*	Region
	y	d	h	m	s	N, S	E, W	km		deg	
1	1975	July 20	14	37	40.6	06°.64	155°.09	54	6.5	44.96	Solomon
2	1983	Apr. 4	02	51	34.5	05.71 N	94.72	82	6.5	50.68	Sumatra
3	1977	Aug. 19	05	08	54.8	11.16	118.41	78	6.8	50.84	Sumbawa
4	1971	Oct. 27	17	58	37.9	15.57	167.24	49	6.3	57.74	Hebrides
5	1979	May 1	13	03	37.6	21.22	167.72	77	6.2	63.82	Loyalty
6	1976	Aug. 2	10	55	25.2	20.59	169.31	43	6.0	63.09	Hebrides
7	1975	Mar. 13	18	45	29.9	21.75	170.53	86	6.0	66.10	Loyalty
8	1977	Mar. 21	21	18	53.6	27.59 N	56.38	24	6.2	68.92	S. Iran
9	1975	Dec. 26	15	56	39.1	16.22	172.47 W	33	6.3	69.18	Samoa

Comments ;

1) The *P'P'* waves indicated by a broken line are in good agreement with the *J-B* Table, except for event No. 2, which occurred at N. Sumatra.
2) The precursors preceding the *P'P'* waves indicated by a solid line are somewhat uncertain, except for Nos. 1 and 6. The time interval of precursor and *P'P'* waves of event No. 1 is about 33 sec.
3) The precursor of the *P'P'* wave, such as the reflected wave from mantle discontinuity, cannot be found from these seismograms.

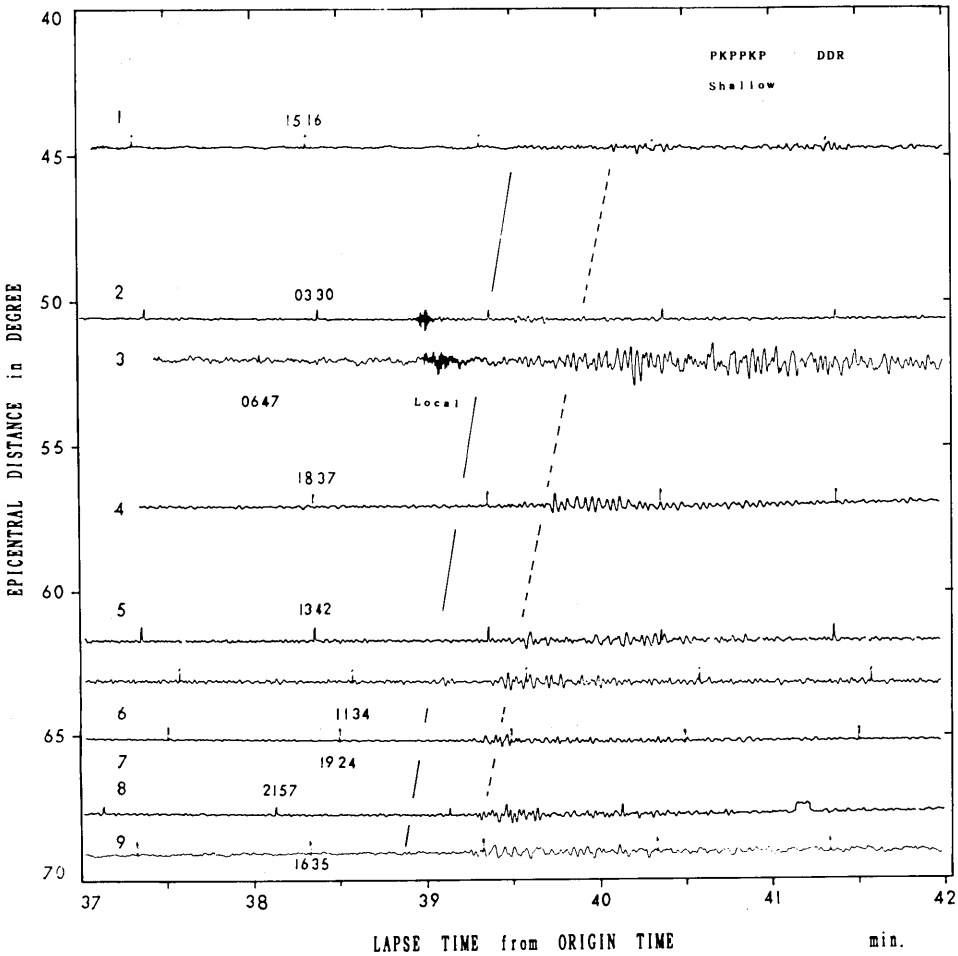

Fig. 26. Arrangement of *P'P'* wave along the epicentral distance. The ordinate shows the epicentral distance in degrees, and the abscissa shows the lapse time measured from the origin time. Broken line shows the onset of *P'P'* wave, and solid line shows the precursor of *P'P'*, but their onsets are not clear.

27. *X* phase from near and regional earthquakes

During the re-examination of seismograms, an unknown phase (*X*) is found on the near and regional seismograms.

Figure 27 shows three seismograms with this phase. The onset of each phase is indicated by arrow.

Table 29. Focal parameters of events by ISC.

No.	Origin Time					Epicenter		*h*	*Mb*	*Δ*	Region
	y	d	h	m	s	N	E	km		deg	
1	1972	Apr. 25	19	30	08.0	13°.38	120°.24	38	6.4	28.19	Mindanao
2	1978	Dec. 6	14	02	04.5	44.55	146.67	118	6.3	10.27	Kurile
3	1978	Jun. 12	08	14	24.4	38.23	142.02	48	6.7	3.17	E. Honshu

Comments ;

1) A small, but clear phase is seen on the seismogram, and this phase is neither that of aftershock nor another event as inferred from ISC.
2) The seismogram of event No. 2 is the same for event No. 3 in Fig. 24 where the *P3KP* phase is observed.
3) The arrival time of this phase lies between 50 m 51 s and 49 m 12 s for the epicentral distance of 3.17 and 28.19 degrees, respectively.
4) The nearest phase on this seismogram is *P4KP*. *P4KP*, however, does not appear at the epicentral distance less than 40 degrees (J Array Seismograms, 1994).

Although the nature of this phase cannot be explained, the phase undoubtedly exists.

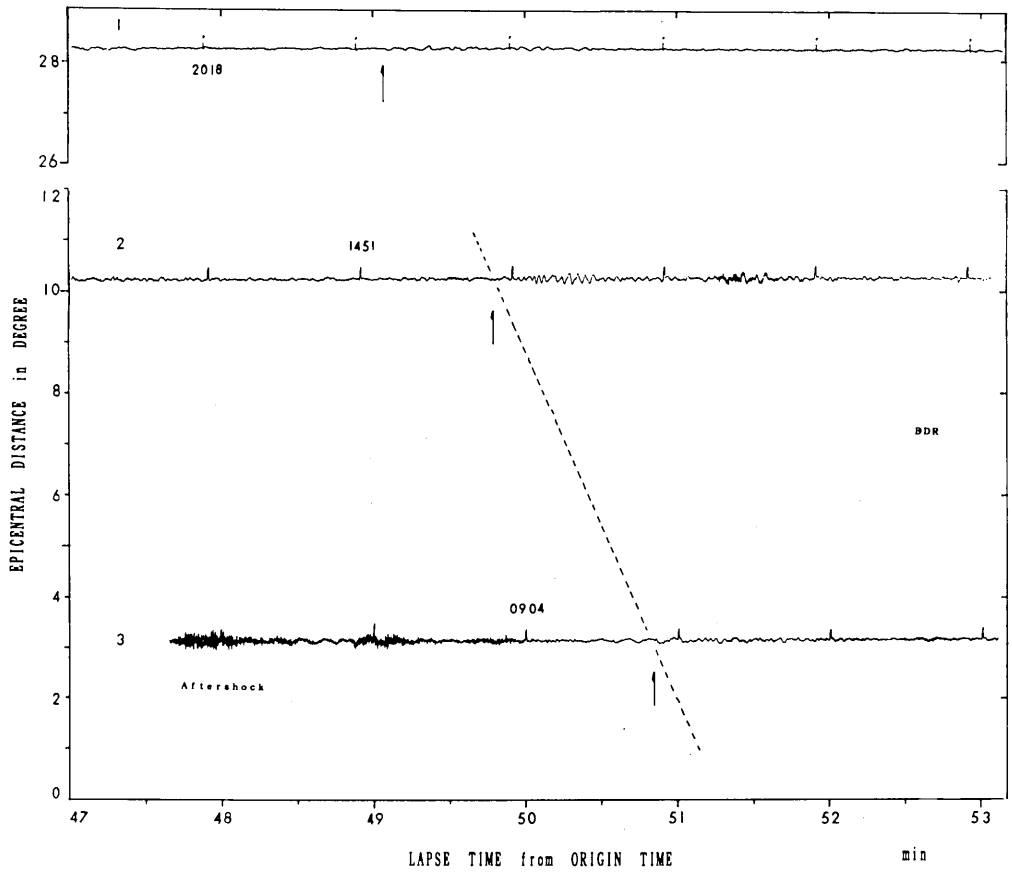

Fig. 27. Arrangement of *X* wave from near and regional earthquakes. The ordinate shows the epicentral distance in degrees, and the abscissa shows the lapse time measured from origin time. These phases, however, cannot be found from *J-B* Table.

28. *X* phase from Banda Sea earthquake

In the previous figure (Fig. 27), it was found that the unknown phase (*X*) exists about 50 min after the origin time for events with a distance of 3-28 degrees. A similar phase is also found for the event of Banda Sea.

Figure 28 shows seismograms for the time from 04 h 55 m to 05 h 12 m. These seismograms are separated into three traces, and the lapse time measured from the origin time is also shown under each seismogram.

Table 30. Focal parameters of event by ISC.

Origin Time						Epicenter		*h*	*Mb*	*Δ*
y		d	h	m	s	N	E	km		deg
1982	June	22	04	18	40.3	07°.33	126°.08	449	6.3	44.82

Comments ;

1) The onset of DF branch of *P'P'* is somewhat uncertain, but that of the AB branch is clearly seen. The DF and AB branches are shown later (see Fig. 29 a).
2) There are two phases on the middle seismogram. The arrival time of the first phase measured from the origin time is 44 m 14 s, and that of another phase is 47 m 37 s. The nearest phase of this travel time is *P4KP*. The theoretical travel time of this phase is 46 min for the event with a 197 km source depth and distance of 45 degrees (J Array Seismograms, 1994).
   The two phases presented here therefore do not belong to *P4KP* phase, even considering the difference of depth.
3) There seems to be one more phase there as indicated by an arrow (top seismogram). The arrival time of this phase is 50 m 35 s similar to that in the previous figure (Fig. 27). However, these phases cannot be found in *J-B* Table.

There are three phases after *P'P'* wave with times of 44 m 12 s, 47 m 37 s and 50 m 35 s. For a better comparison of the two phases the seismograms of the 2 nd phase is superimposed on the top seismogram. It is noted that the 3 rd phase (50 min later) appears with four events including the events in Fig. 27.

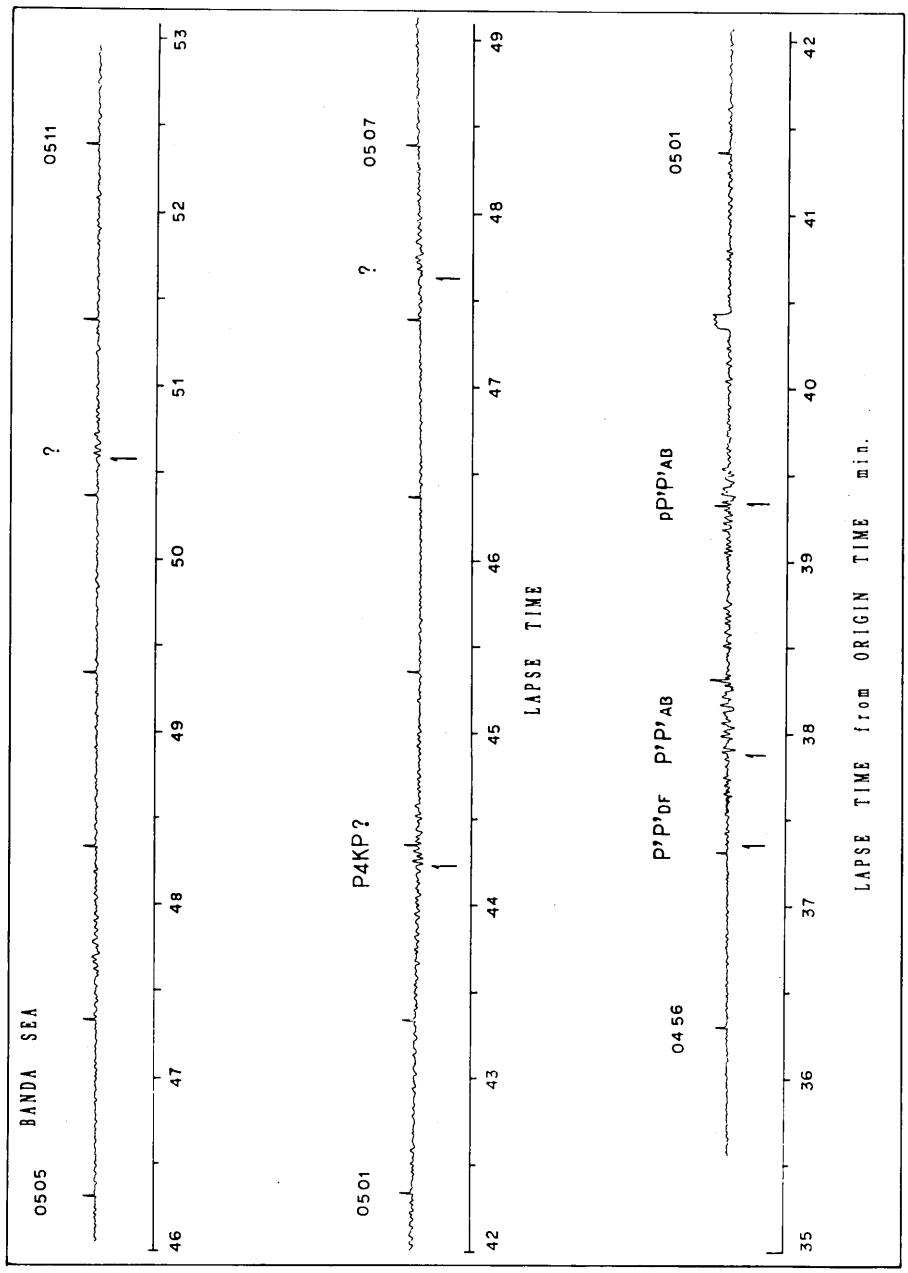

Fig. 28. The seismogram after *P'P'* wave from Banda Sea event. The seismogram is separated into three parts. The abscissa of each seismogram shows the lapse time measured from origin time, respectively. Three phases seem to exist after *P'P'* wave as indicated by ? marks. The 2nd phase (05 h 03 m) is superimposed on the top seismogram to get a better comparison of pair phases. These phases, however, cannot be found from *J-B* Table.

29. Arrangement of *PKP* waves
—Δ=129°-146°—

The precursor of *PKIKP* (*P"*), which was called *PKHKP* (BOLT, 1964), is one of the most important problems studied in relation to the Core-Mantle boundary (CMB). In this section, we examine the range where the precursor appeared and it time interval preceding the *P"* waves. Fig. 29 shows an arrangement of *PKP* waves for the epicentral range of 129 and 146 degrees. The broken line shows the onset of the *P"* wave where the residual of travel time is zero as inferred from *J-B* Table, and the arrow shows the GH branch of the *PKP* wave. Figs. 29a and 29b show the travel time curves of *PKP* wave by BOLT (1964) and HADDON (1982), respectively as a supplement.

Table 31. Focal parameters of events by ISC and Δt.

	Origin Time				Epicenter		h	Mb	Δ	Δt
y	d	h	m	s	N, S	W, E	km		deg	s
1968 Sep.	20	06	00	33.0	10°.76 N	62°.70 W	103	6.2	129.11	+ 2.2
1980 Nov.	11	10	36	57.7	51.49 S	28.98 E	0	6.1	129.19	− 0.4
1970 Dec.	10	04	34	38.0	03.97 S	80.66 W	15	6.3	131.40	− 2.1
1971 May	17	11	04	06.9	01.59 S	77.69 W	172	5.7	131.65	+ 0.9
1983 Apr.	12	12	07	54.4	04.84 S	78.09 W	102	6.4	133.78	− 8.7
1975 Mar.	19	17	21	24.7	04.26 S	77.01 W	111	6.2	134.09	− 8.2
1970 May	31	20	23	28.4	09.15 S	78.83 W	48	6.4	135.57	−10.9
1974 Dec.	5	11	57	31.1	07.65 S	74.46 W	156	6.0	138.29	− 7.3
1978 Jul.	11	12	17	07.7	07.86 S	71.35 W	643	5.6	139.77	− 8.4
1971 Oct.	14	22	36	34.8	54.4 S	02.5 E	25	5.2	145.05	− 2.9
1977 Dec.	31	07	53	13.9	15.37 S	71.71 W	125	6.0	145.63	+ 1.4

Δt ; travel time residual of initial phase. Seismograms beyond 147° have already been published (see TSUJIURA, 1988).

Comments ;

1) The *PKP* (GH) branch is scattered waves at the Core-Mantle boundary (KING *et al.*, 1973).
2) The travel time residual of *PKP* (GH) wave is systematically changed between the range of 129-145 degrees, although the data at 143 degrees are insufficient. The earlist arrival of observed *PKHKP* is 11 s earlier than that expected from *J-B* Table, and its epicentral distance is 135.5 degrees.

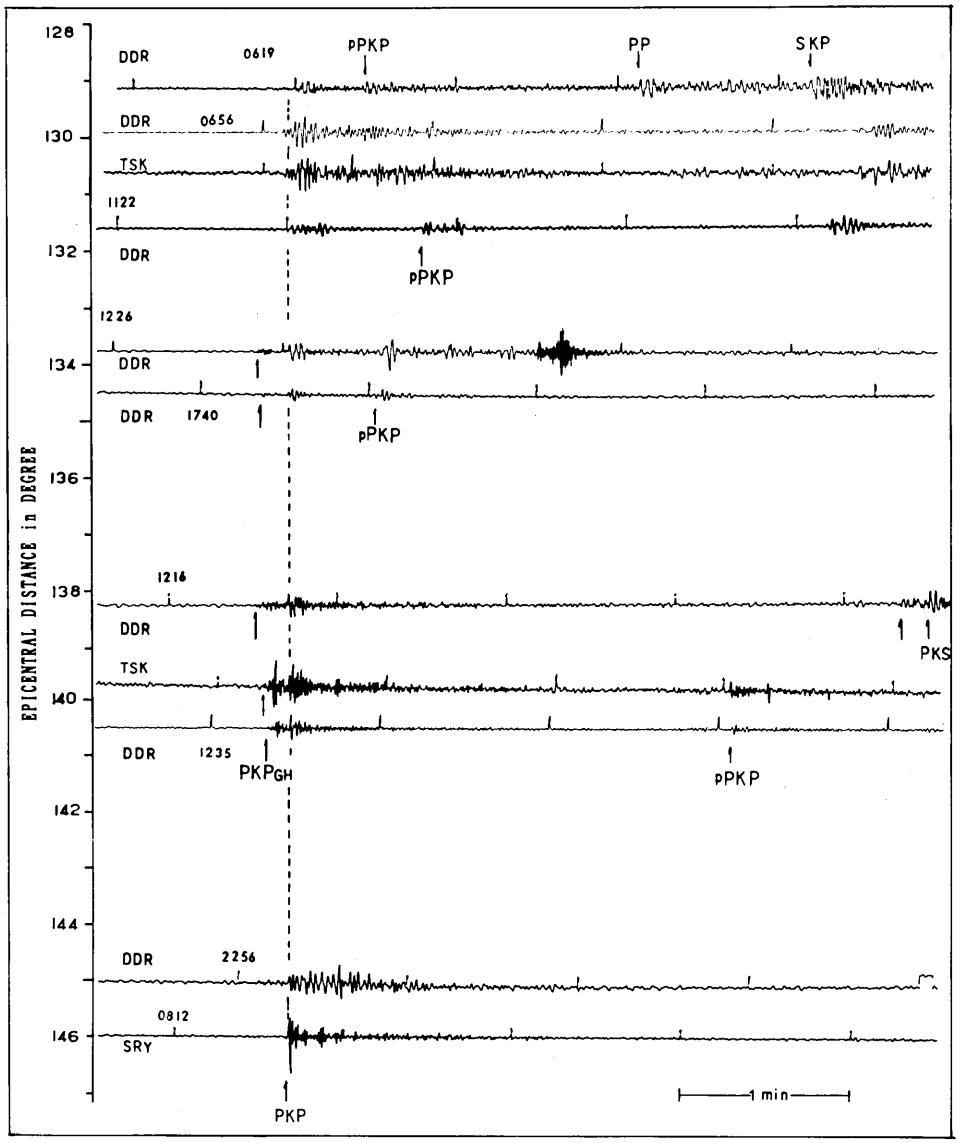

Fig. 29. The *PKP* waves for the events with epicentral distance from 129 to 146 degrees. The *PKP* waves beyond 147 degrees are already shown in the previous study (TSUJIURA, 1988). The GH branch of *PKP* waves (see Fig. 29 a) are clearly seen for the seismograms between 134 and 141 degrees.

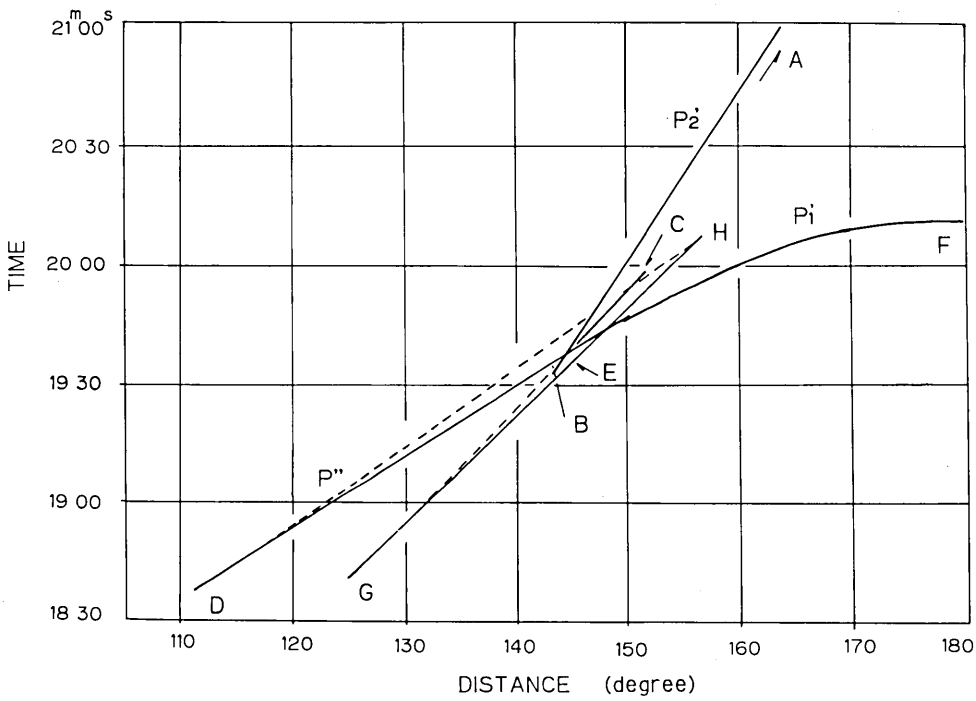

Fig. 29a. The travel time curve of *PKP* wave by BOLT (1964). P_1', *P"* waves correspond to *PKIKP*, and GH branch corresponds to *PKHKP* wave, respectively.

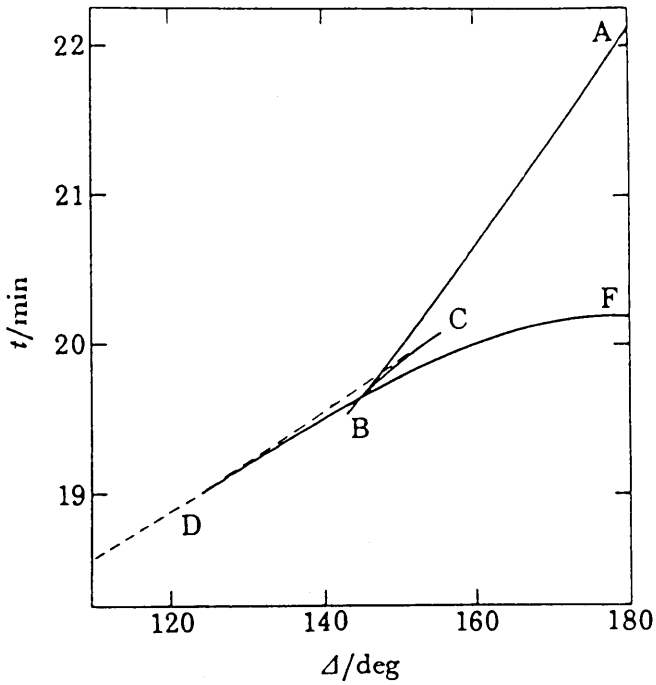

Fig. 29 b. Travel time branches for core phases in a two-layer model. The branch DF corresponds to the phase *PKIKP*, and the branch of CD corresponds to *PKiKP* (After HADDON, 1982).

30. *PKP* waves from deep Colombia earthquake

Seismograms of this earthquake obtained by medium- and long-period seismographs have already been published in the previous study of this series (TSUJIURA, 1988).

Figure 30 shows seismograms obtain by short-period seismograph (SP-Z) at TSK and DDR stations. This figure consists of two events indicated by E 1 and E 2, although event E 2 is not available on the ISC Bulletin. The abscissa therefore shows the lapse time measured from origin time of E 1.

Table 32. Focal parameters of E1 by ISC.

Origin Time					Epicenter		h	Mb	Δ	Δt^*
y	d	h	m	s	S	W	km		deg	s
1970 July	31	17	08	05.4	01°.46	72°.56	653	6.5	134.75	−13.8

Δt^* ; residual at TSK, and −12.3 s at DDR.

Comments ;

1) The GH branch of *PKP* (*PKHKP* by BOLT, 1964) is clearly demonstrated. Moreover, the clear phase indicated by "*i*" can be seen 12.5 sec after the *PKP* (DF) branch (*PKIKP*) on the DDR seismogram.
2) The E 2 seismograms similar to E 1, except for *PKHKP*, are observed about 54 min after E 1. Although there are no data available on the ISC, a small, but clear *i* phase can also be seen as in E 1.
3) Considering the waveforms of E 1 and E 2, the E 2 is probably an aftershock of E 1.
4) The *i* phase can be seen more clearly with an isolated waveform on the MP seismogram as shown previously.
5) The onset of *PKP* (GH) at TSK is 13.8 sec earlier than the value expected from *J-B* Table, and this is the maximum value for the present study.

If our interpretation of the *i* phase corresponding to *PKiKP* in Fig. 29b is correct, the *i* phase will give new information in CMB.

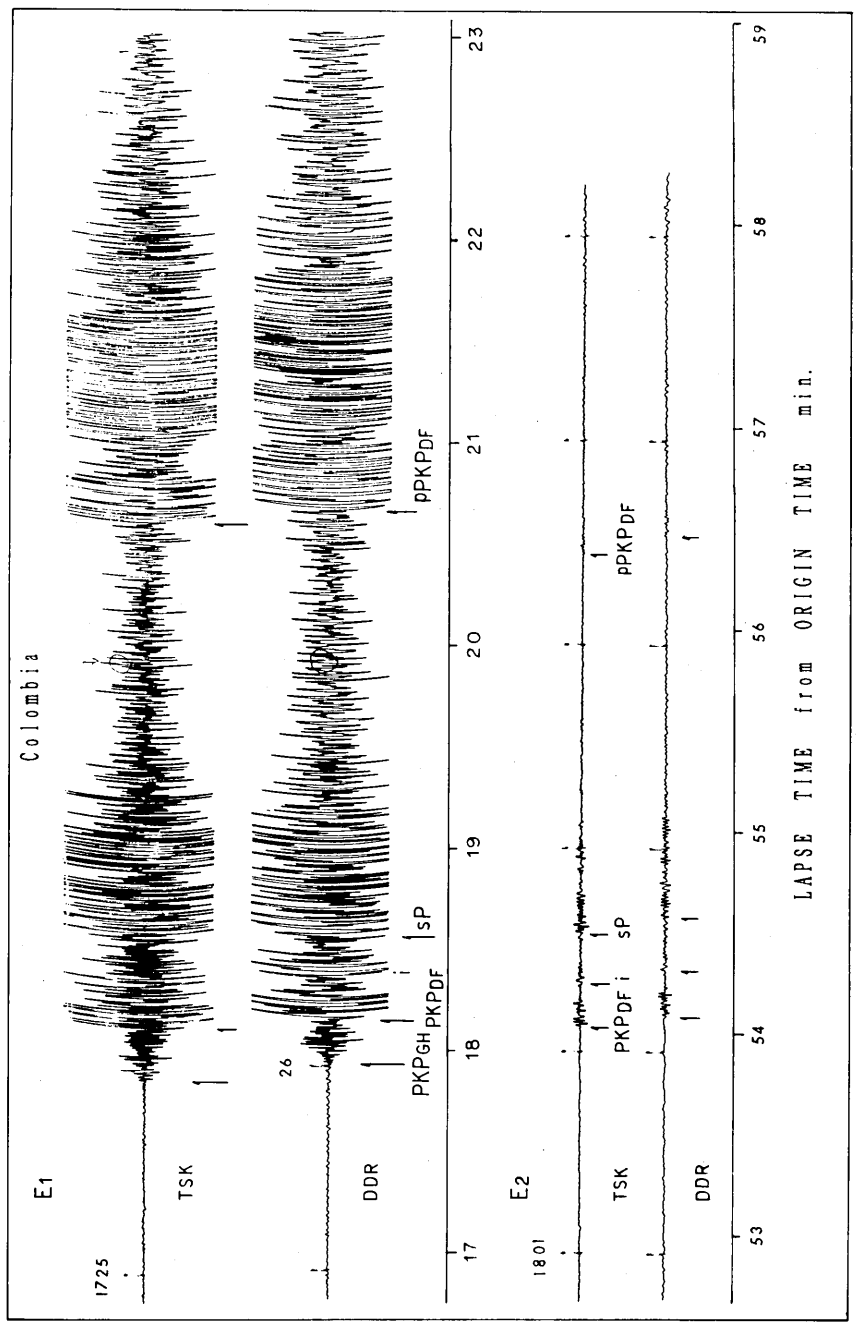

Fig. 30. Seismograms from deep Colombia earthquakes. This figure consists of two events: E1 and E2, although data on E2 are not available on the ISC. The abscissa therefore shows the lapse time from origin time. The *i* phase corresponding to *PKiKP* is cleary demonstrated.

31. Character of *P* waveforms of a large earthquake (1) —in the relation to aftershock activity—

When the event began to appear on a seismogram, it is important to judge whether this earthquake is growing into a large one or finish as a small one. Here we examine the *P* waveform of large earthquakes.

Figure 31 shows eight seismograms with a body-wave magnitude (*Mb*) greater than 6.2. In this selection, seismograms with appropriate amplitudes (no saturation) are used, because the magnification is different among the stations (TSUJIURA, 1983 a).

Table 33. Focal parameters of events by ISC.

No.	Origin Time					Epicenter		*h*	*Mb*	*Ms*	*Δ*	NA
	y	d	h	m	s	N, S	E, W	km			deg	
1	1975 Jul.	20	14	37	40.6	06°64 S	155°09 E	54	6.5	7.9	44.96	54
2	1975 Dec.	26	15	56	39.1	16.22 S	172.47 W	33	6.3	7.8	68.07	14
3	1976 Jun.	25	19	18	57.5	04.58 S	140.14 E	33	6.3	7.1	39.56	17
4	1981 Jul.	6	03	08	34.1	22.29 S	171.44 E	114	6.3	7.0	65.10	3
5	1977 Mar.	18	21	43	53.0	16.73 N	122.29 E	40	6.2	7.0	23.98	38
6	1977 Aug.	19	06	08	54.8	11.16 S	118.41 E	78	6.8	7.9	50.49	36
7	1977 Aug.	27	07	12	20	08.10 S	125.38 E	4	6.2	6.8	45.75	8
8	1978 Jul.	23	14	42	39.5	21.19 N	121.42 E	34	6.4	7.4	20.88	54

Ms ; Surface-wave magnitude, NA ; Number of aftershocks during 24 hours taken from ISC.

Comments ;

1) The initial motion of each seismogram is small when comparing the amplitude of the later arrival, and the time interval of first and later phases does not depend on *Mb* or *Ms*.
2) The number of aftershocks also does not depend on *Ms*, although its number depends on the geometry of the observatory around the epicenter.
3) The duration time having a large amplitude on the *P* wave group is related to the number of aftershocks, e.g., the amplitude of the *P* wave of event No. 4 is rapidly degreasing in contrast with that of event No. 5, and there is a correlation between the duration and number of aftershocks.

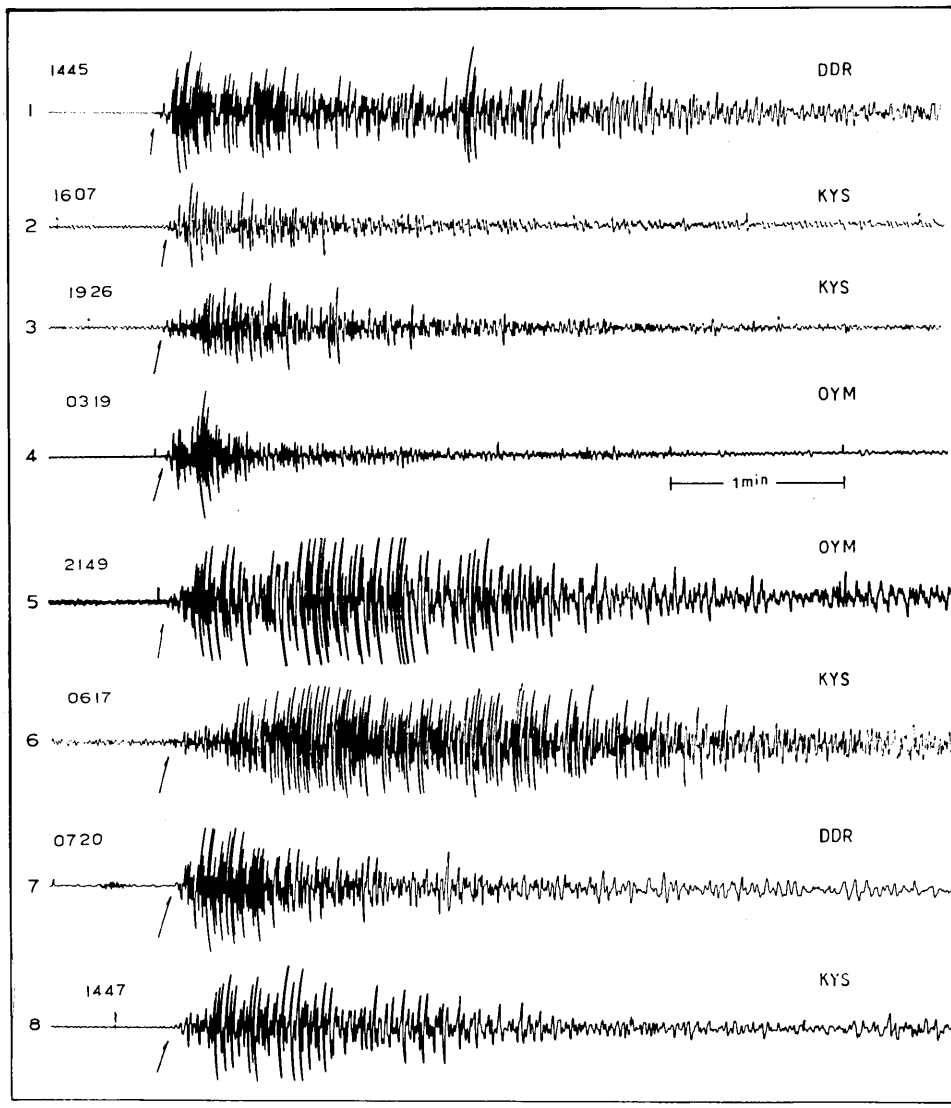

Fig. 31. Arrangement of large earthquakes ($Mb > 6.2$). Small amplitudes are commonly observed for all events, and large amplitudes are followed a few seconds after P wave onset. Note that the duration time with large amplitudes is different by event.

32. Character of *P* waveforms of large earthquake (2) —Solomon Is.—

Large earthquakes ($Mb>6$) occur frequently in the Solomon Islands region. The *P* waveforms of large earthquakes are examined, and compared to small ones in the area.

Figure 32 shows four seismograms including large and small events which occurred in almost the same area.

Table 34. Focal parameters of events by ISC.

No.	Origin Time					Epicenter		*h*	*Mb*	*Ms*	Δ
	y		d	h	m s	S	E	km			deg
1	1977	Apr.	20	23	13 12.3	09°.99	160°.44	49	6.3	6.7	49.85
2	1977	Apr.	20	23	42 53.0	09.94	160.48	33	6.1	7.5	49.90
3	1977	Apr.	21	00	44 36.0	09.90	159.40	33	5.6	5.9	49.47
4	1977	Apr.	21	04	24 09.0	11.00	160.77	31	6.4	7.5	50.07

Ms ; from NEIS.

Comments ;

1) Four earthquakes with $Mb>5.6$ occur within five hours. Among these earthquakes the magnitude (*Mb*) of three events are greater than 6.1.
2) The initial motion of four events is almost the same within a factor of two, although *Ms* is different by more than a factor of 1.5.
3) *P* waveforms of large events are complex. They consist of three phases as indicated by *P*, X_1 and X_2.
4) The times of X_1-*P* and X_2-*P* differ from event to event, and that of event No. 1 is shorter than those of events No. 2 and No. 4, although magnitude (*Mb*) is greater than No. 2.
5) The *P* waves of event No. 1 abound in high-frequency components than the others, but its amplitude rapidly decreases.

Event No. 1 with a short duration time and with a high-frequency component suggests that the stress concentration was higher than in later events.

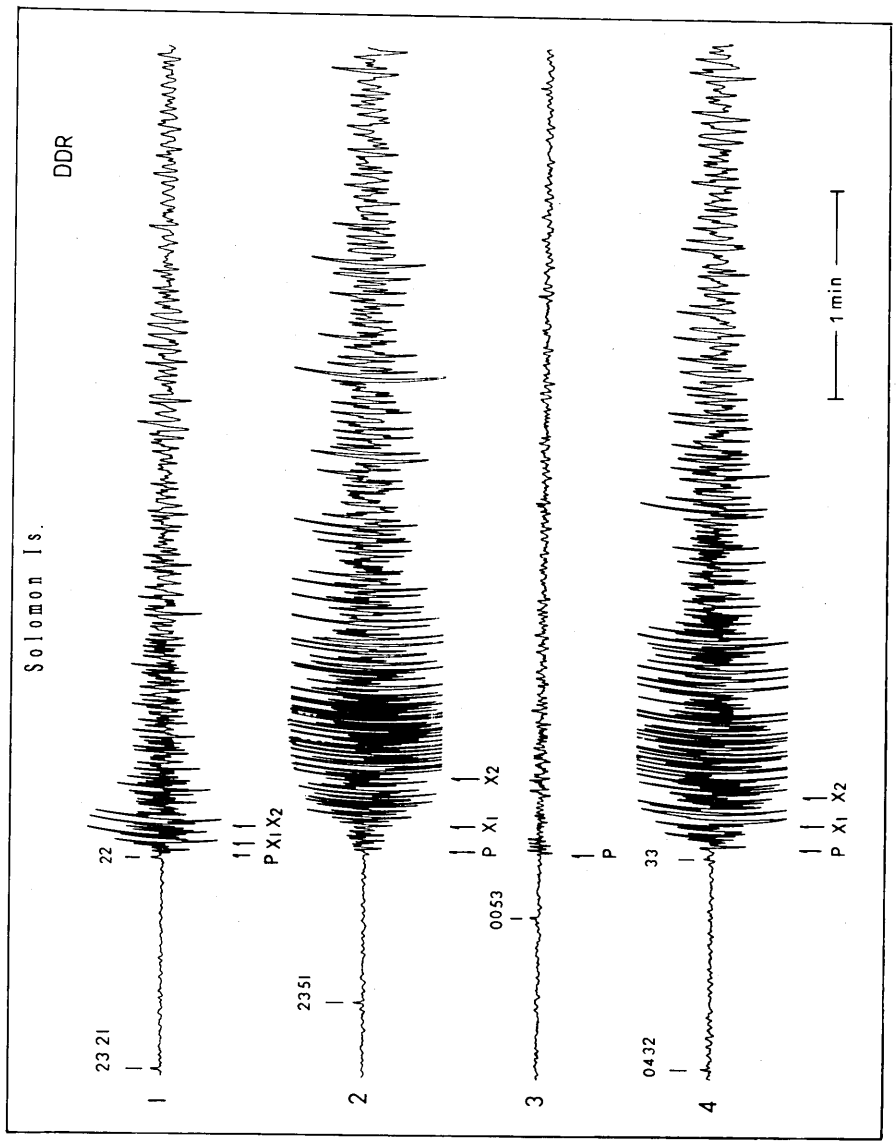

Fig. 32. Seismograms of large earthquakes ($Mb>6.1$) which occurred in the Solomon Islands region during five hours. Note that the difference of time intervals of X_1-P and X_2-P among the events.

33. Character of *P* waveforms of moderate-size earthquakes

As shown in the previous figures (Figs. 31 and 32), the initial motion of large earthquake is small and large later phases follow after about few seconds of *P* wave arrival. These complex *P* waveforms are seen frequently even in the moderate-size earthquakes.

Figure 33 shows typical examples of seismograms with complex *P* waveforms. As indicated by the arrows, two or three phases exist on the *P* wave group.

Table 35. Focal parameters by ISC and X_1-*P* time.

No.	Origin Time						Epicenter		*h*	*Mb*	*Ms*	Δ	X_1-*P*
	y		d	h	m	s	N, S	E, W	km			deg	s
1	1971	Jan.	25	00	18	25.2	09°.65 S	151°.40 E	31	5.9	—	46.84	10
2	1972	Sep.	5	18	11	12.5	11.78 S	166.31 E	64	6.1	6.8**	53.98	4
3	1975	Dec.	27	15	56	39.1	16.22 S	172.47 W	33	6.3	7.8*	68.07	5
4	1978	July	22	11	51	47.3	04.20 S	152.84 E	45	5.8	6.0	41.98	6
5	1978	Nov.	1	19	48	24.0	39.34 N	72.56 E	7	5.9	6.8	51.77	8
6	1982	Feb.	15	05	50	08.8	03.48 S	177.49 E	10	5.7	5.6	53.13	5
7	1969	Oct.	13	06	56	01.6	18.78 S	169.31 E	244	5.7	—	61.49	4

*; NEIS, **; MOS.

Comments;

1) The magnitude (*Ms*) is distributed over 5.6 and 7.8, and X_1-*P* time is also distributed between 4 and 10 sec. However, there is no relation between *Ms* and *X*-*P* time.
2) As shown in seismogram No. 7, even in the intermediate-depth event (244 km), there is a later phase about 4 s after *P* wave onset. A similar later phase can be seen for the intermediate-depth event (h=126 km) of the Alaska region (Aug. 22, 1976).

UMEDA (1990) suggested that the time interval *P* and later phase is proportional to earthquake size. Our results including the results in Figs. 31 and 32 show that the time interval does not depend on earthquake size. It must be noted that the *X*-*P* time varies from event to event.

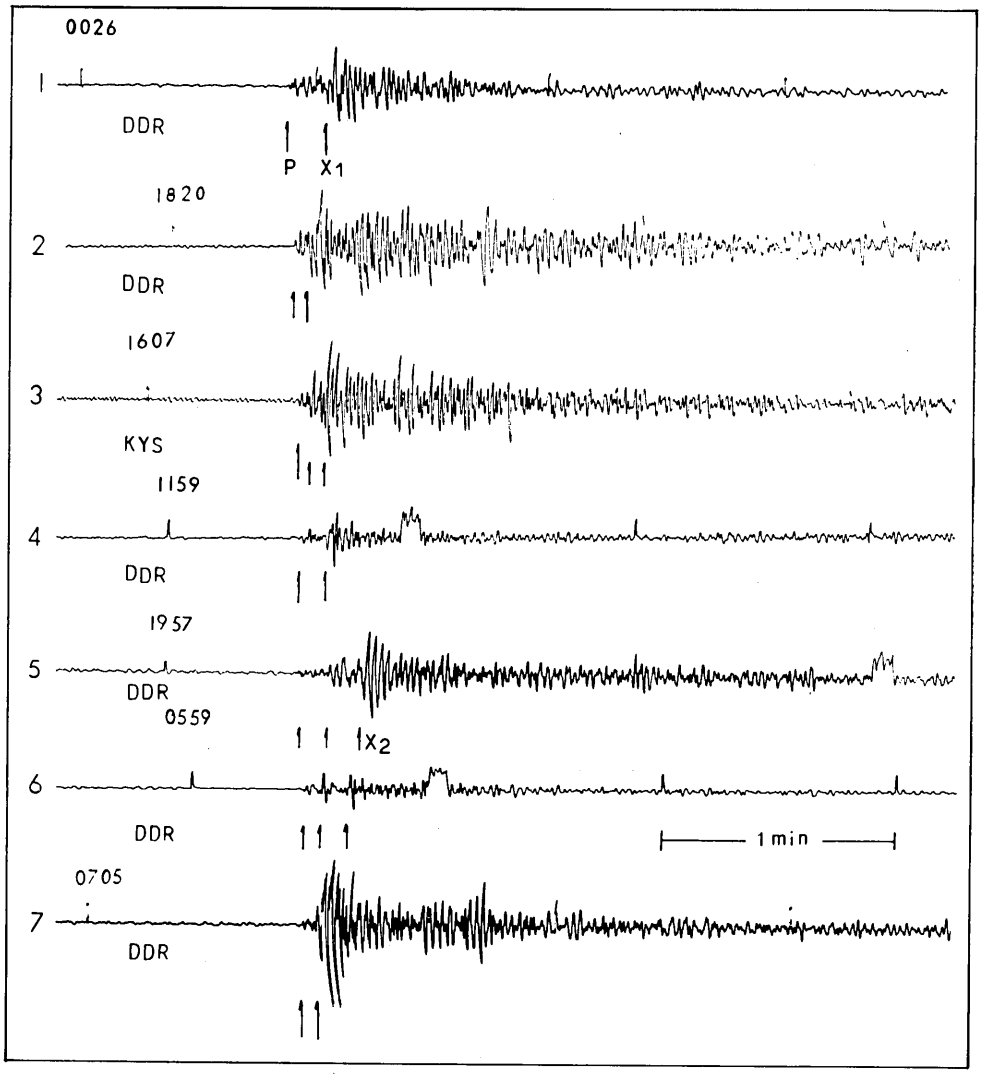

Fig. 33. Comparison of P waveforms for events of a moderate size (Ms=5.6-7.8) earthquakes. There is no special relation between the time interval of X-P and earthquake size.

34. Character of *P* waveforms of moderate-size earthquakes —Soft and Barrier earthquakes—

The previous figures (Figs. 31-33), show complex *P* waveforms. In this section, another example of a *P* waveform is shown.

Figure 34 shows seismograms from various regions. There are two kinds of *P* waveform as indicated by A and B.

Table 36. Focal parameters by ISC and P_2-P_1 time.

No.		Origin Time				Epicenter		*h*	*Mb*	*Ms*	*Δ*	P_2-P_1
	y	d	h	m	s	N, S	E, W	km			deg	s
	1 1972	Apr. 24	09	57	21.2	23°.60 N	121°.55 E	29	6.1	6.9*	19.47	6.5
A	2 1975	Jul. 21	02	38	57.8	06.84 S	155.41 E	63	6.2	6.7**	44.87	4.5
	3 1976	Sep. 30	23	34	11	30.30 S	177.65 W	31	5.7	6.5*	77.42	4.5
	4 1973	Jan. 1	03	46	09.2	09.29 S	150.73 E	41	5.6**	—	46.5	4
B	5 1972	Sep. 24	20	09	36.2	06.22 S	131.15 E	33	6.0	6.9*	42.30	2.6
	6 1976	Aug. 2	10	55	25.2	20.59 S	169.31 E	43	6.0	6.9*	62.72	5.0

*; by NEIS, **; by MOS.

Comments;

1) Seismograms are separated into two groups, A and B, by character of *P* waveforms. In group A, the rupture starts slowly, and after a few seconds (see P_2-P_1) a large rupture suddenly occurs. This is clearly seen in frequency and amplitude. We tentatively call this a Soft earthquake.

2) Unlike group A, the *P* waveform of group B can be separated clearly into the two wavelets P_1 and P_2. As shown previously (Figs. 31-33), an initial motion is very small compared to the amplitude of the later arrival. In this seismogram, however, the amplitude of initial motion (P_1) is similar to that of the later arrival within a factor of two. Moreover, the MP seismograms show that the waveforms of P_1 and P_2 consist of an impulsive form (see Fig. 64, TSUJIURA, 1988). these seismograms suggest that there exist strong barriers. We call tentatively this a Barrier earthquake.

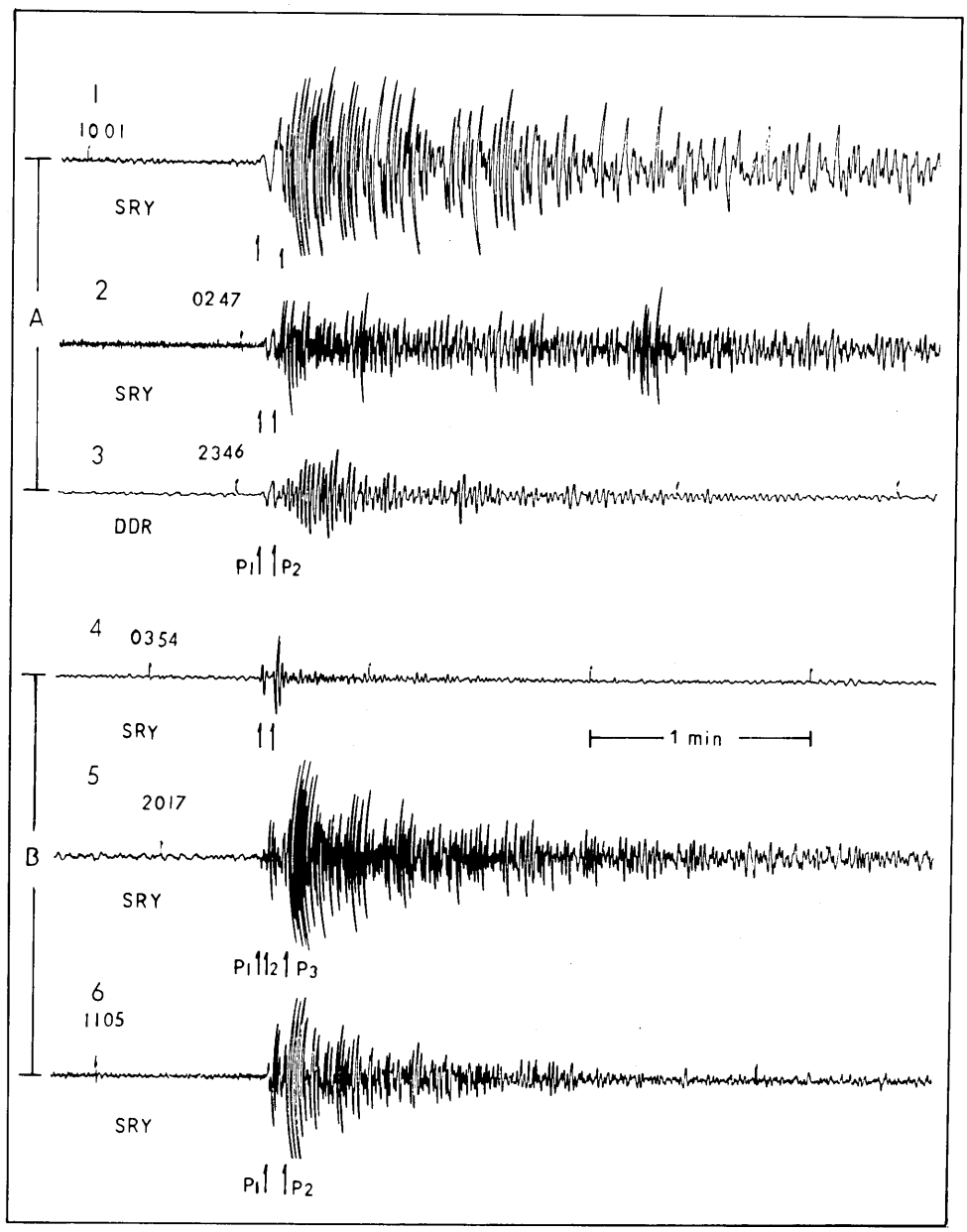

Fig. 34. Differences in rupture process of the earthquake occurrence. The rupture process is divided into two groups : A and B. The difference in the rupture process can be seen from the difference of frequency components of initial motion.

35. Recurrent occurrence of family earthquakes —Evidence from 1982 Miyakejima earthquake—

The earthquake swarm occurring in a short time, e.g., one hour mainly consists of events with similar waveforms called a "earthquake family" (TSUJIURA, 1979). We examined the waveform for the earthquake sequence of the 1982 Miyakejima earthquake. The magnitude of the main shock was 6.4. It was accompanied by many foreshocks and aftershocks including the 2nd largest event with $M=5.9$. This sequence is, therefore, a swarm activity.

This sequence mainly consists of six families, except for the immediate aftershocks of M6.4 and M5.9 events.

Figure 35 shows seismograms belonging to one family, which were obtained at OYM locating at about 220 km from the epicenters. The amplitude of each trace is adjusted using high (H) and low (L) magnification seismographs that differ by a factor of 10.

Table 37. Focal parameters of two large events by JMA.

Origin Time					Epicenter		h	M
	d	h	m	s	N	E	km	
Dec.	28	15	37	42.0	33°.52	139°.27	20	6.4
Dec.	29	16	02	30.5	33.46	139.22	20	5.9

Comments ;

1) One family occurred repeatedly. The number of seismograms in each period was limited in order to easy comparison.
2) After the activity of one family finished, its activity moved to the adjacent area, and formed another family.
3) After the activity of several families finished, its activity returned to the origin. Three groups of the same family were found during an eight-days period.

The re-occurrence of the same family will be due to tectonic stress concentrated repeatedly over the same fault plane, and the difference in earthquake size may be caused by the difference in the amount of slip over the same fault plane (TSUJIURA, 1983 b).

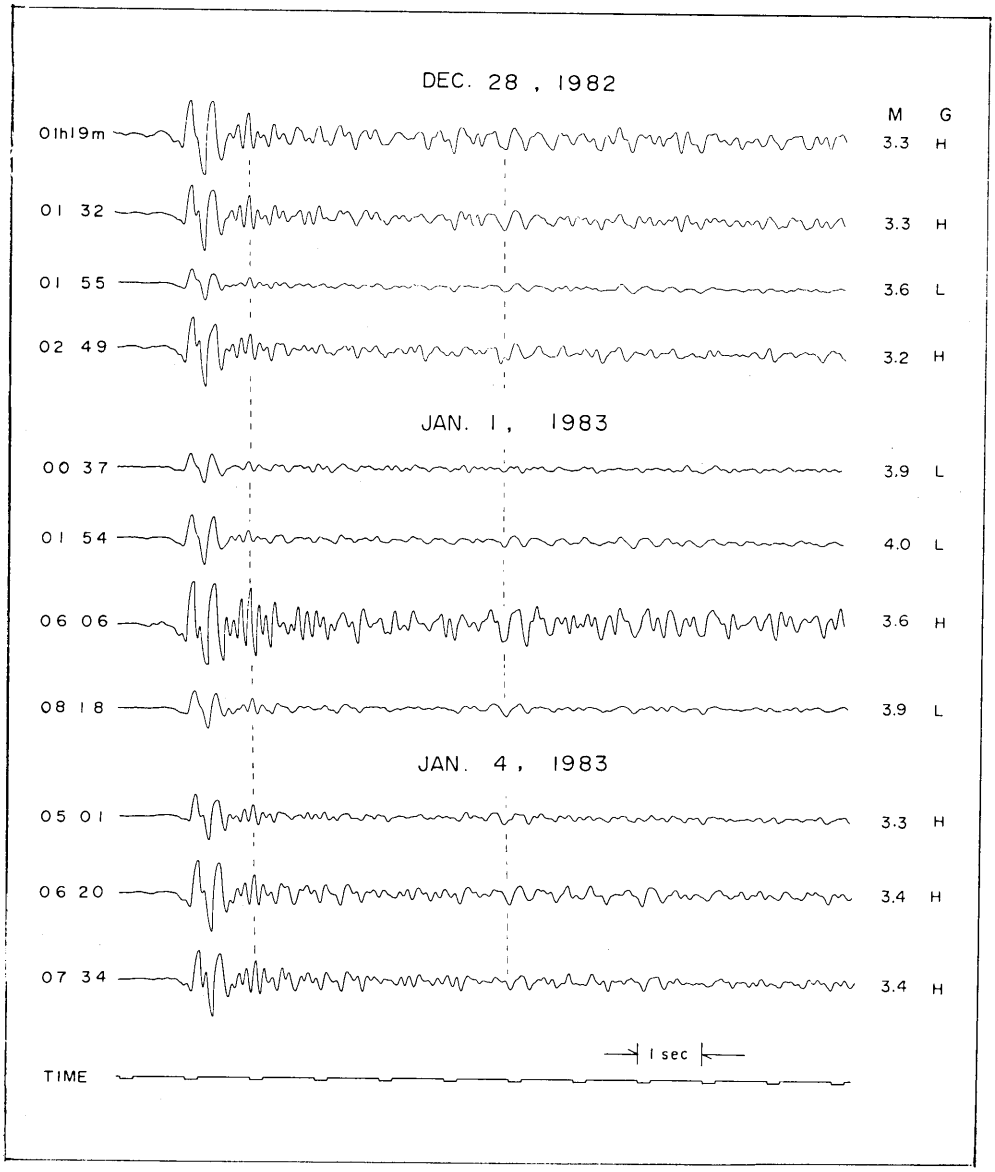

Fig. 35. Recurrent occurrence of "earthquake family" obtained from the 1982 Miyakejima earthquake. Three groups consisting by similar waveforms are found during eight-days. The symbol G shows high (H) and low (L) magnification seismographs differing by a factor of 10.

36. Characteristic frequencies of earthquake families

Swarms of earthquakes occurring in a short time consist mainly of events with similar waveforms called as an "earthquake family", and many families are observed during a swarm sequence (TSUJIURA, 1979).

The source spectra of an earthquake family share the same corner frequency, even though their low-frequency levels may differ by a factor as great as 100-1,000. We tentatively called this corner frequency the characteristic frequency.

Figure 36 shows seismogramms belonging to one family obtained at Uchino-komori, Ashio, Tochigi Prefecture (UKM). The magnitude of these events lies between -0.3 and 3.0.

Symbols of H and L in this figure show high- and low- magnification seismographs differing by a factor of 50, and G shows the relative difference of magnifications.

The similarity of waveforms is clearly seen from P wave onset until coda waves, except for the $M3.0$ event (23 h 19 m). The largest event with the same corner frequency is $M=2.5$. When the magnitude exceeds this value events may occur as multiple type events, and the half-period of the initial motion is two times greater than those of other events. Because the earthquake family occurs repeatedly in a small area enclosed by a strong barrier. The difference in earthquake size may be due to a difference in the amount of slip in each event, and the maximum slip is limited by the size of that area (TSUJIURA, 1983 b).

Local variations of characteristic frequency within a factor of 25 are found among earthquake swarms in the Kanto District (TSUJIURA, 1983 a). These observations suggest the existence of a characteristic fault length, and its length may be responsible for the size of the largest event in the family (TSUJIURA, 1983 b).

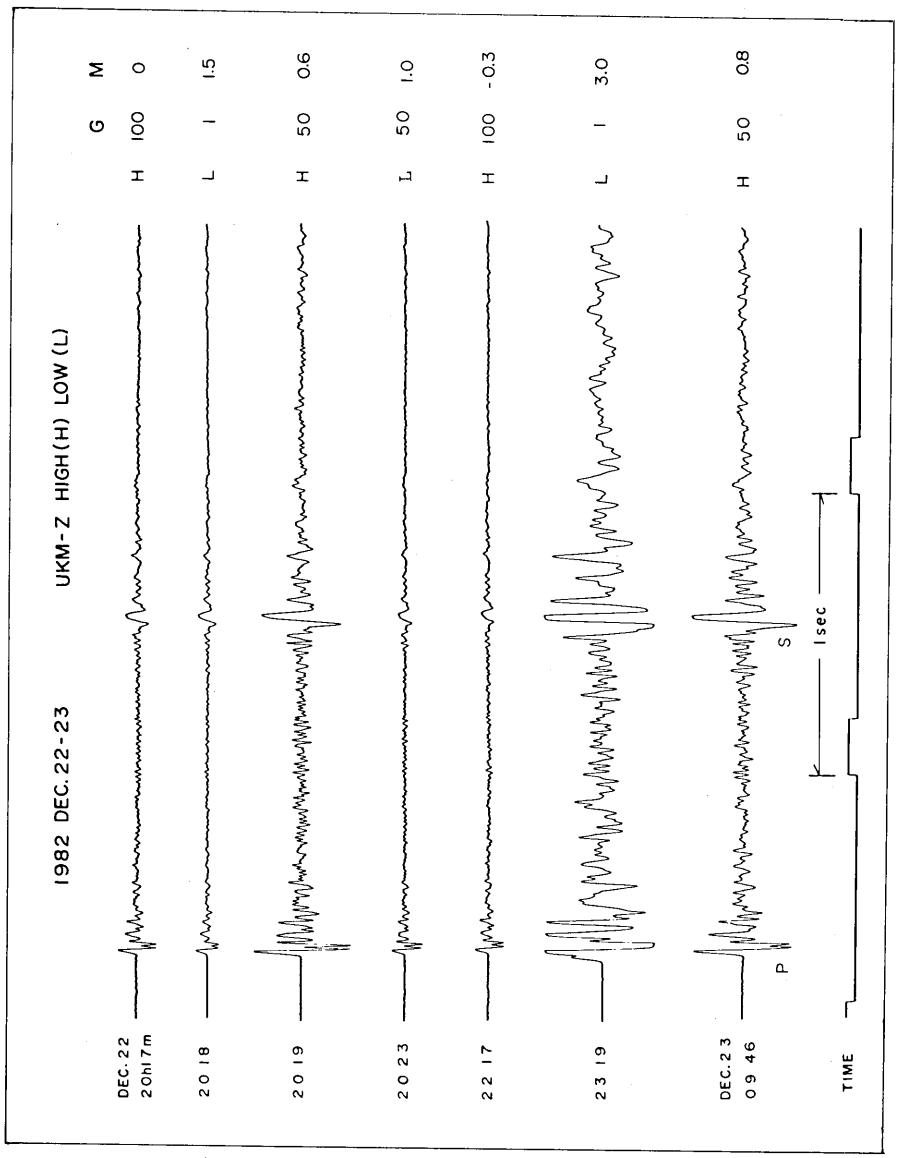

Fig. 36. Seismograms with similar waveforms, except for the largest event ($M=3.0$). H and L are high-and low-magnification seismographs differing by a factor of 50, and G shows the relative difference of magnifications.
Note that the half period of the initial motion of the largest event is two times greater than the others.

37. Spectral features of foreshocks

To obtain the spectral features of foreshocks in comparison with other events, a spectral analysis of some foreshocks-main shock-aftershocks sequences were performed, and the results were shown by TSUJIURA (1977, 1978, 1983 a). In these studies, however, the spectral analysis of ordinary seismic activity was insufficient. It is, therefore, very difficult to obtain the spectral features of foreshocks.

Here, a similar analysis is performed for the 1982 Off Ibaraki Prefecture earthquake, M 7.0. This earthquake was accompanied with many foreshocks during about 32 hours preceding the main shock. The seismic activity in this area is high. The spectral comparison, therefore, can be made for events of an ordinary seismic activity. Figure 37 shows foreshocks $M>4.5$ obtained by MP-Z at DDR. The length of bars at the end of seismogram shows relative differences of magnification.

Table 38. Focal parameters of foreshocks by JMA.

Origin Time				Epicenter		h	M
d	h	m	s	N	E	km	
22	15	22	38.6	36°.22	142°.03	30	4.5
22	19	57	51.7	36.17	141.98	40	5.0
23	02	32	30.3	36.22	142.05	30	5.4
23	03	17	18.0	36.22	141.87	60	5.0
23	05	24	07.2	36.18	141.98	30	4.7
23	20	25	00.8	36.18	141.92	50	5.0
23	23	23	50.9	38.18	141.95	30	7.0

Comments ;

1) High-frequency components, about 3 Hz, differ from event to event.
2) The amplitude of high-frequency components increases with time, and the foreshock immediately before the main shock shows the maximim value.
3) Clear phase indicated by a dotted line is commonly observed. Although immediate foreshocks abound in high-frequency components, it is very difficult to predict a M 7.0 event.

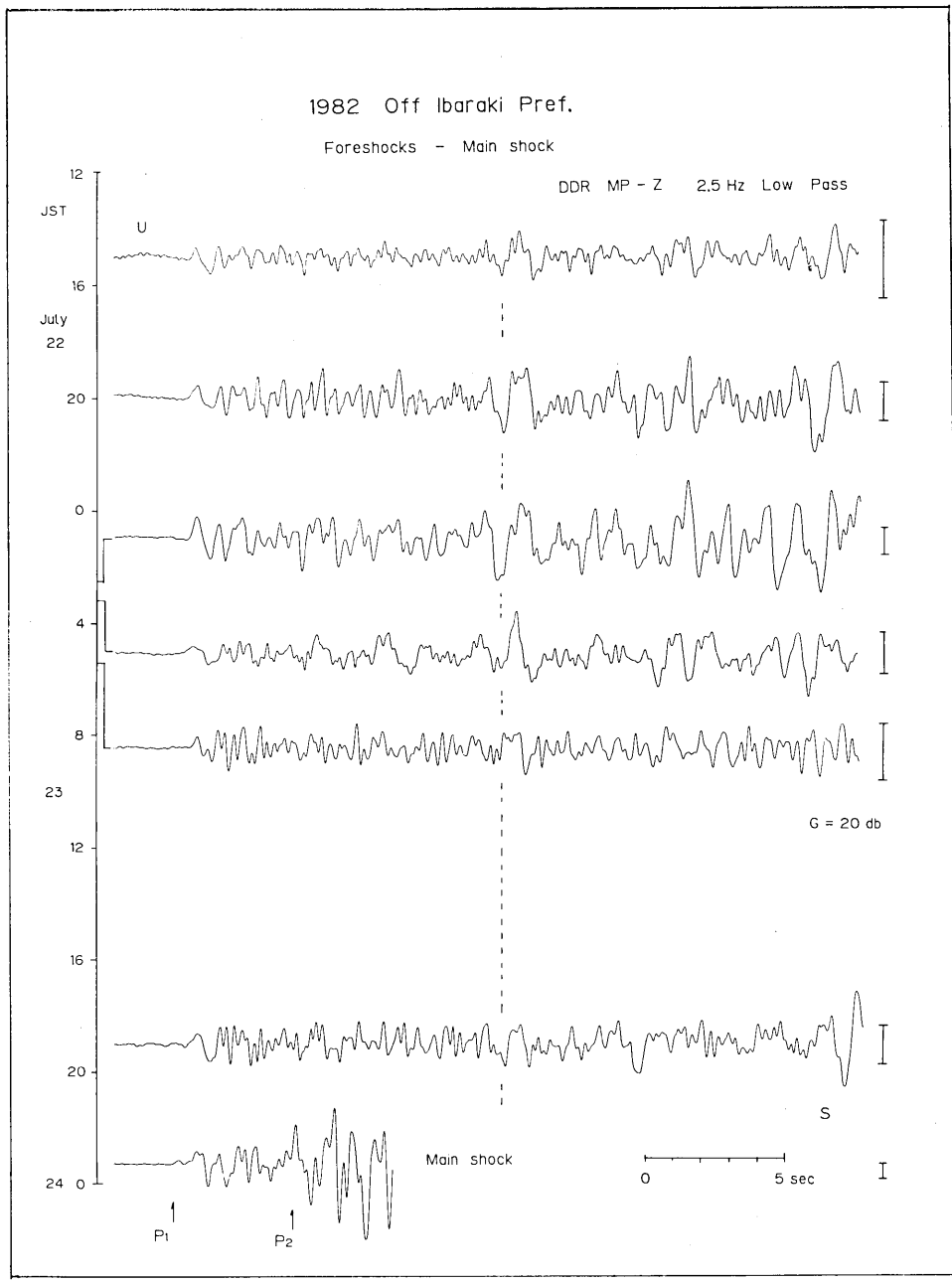

Fig. 37. Seismograms of foreshocks preceding the 1982 Off Ibaraki Prefecture earthquake with M 7.0. The length of bar to the right shows the relative differences of magnification. The seismogram of the main shock is presented for comparison. Note that the foreshock immediately before the main shock abounds in high-frequency components.

38. Seismograms of ordinary seismic activity —Off Ibaraki Prefecture—

In the previous figure, the spectral features of foreshocks Off Ibaraki Prefecture earthquake (M7.0) are shown. Here, the seismograms and spectral features in an ordinary seismic activity are examined.

Figure 38 shows seismograms obtained by a MP-Z seismograph at DDR for events which occurred during the period from 1974 to 1981 Off Ibaraki Prefecture. The symbol G shows relative differences of magnification of the seismograph, and numerals at the beginning of each trace show origin time and magnitude by JMA.

There is a variety in waveforms and spectra, and there is no relation between waveform including frequency component and earthquake size. The comparison of foreshocks shown in the previous figure is another important item of this study. There is also no special differences in frequency component.

Through figures for 37 and 38, it can be suggested that the immediately before the foreshock abounds in high-frequency components. However, such a difference does not give a clue for predicting a large earthquake (M7.0). Foreshock activity, however, is different from ordinary activity. The combined data of spectrum and seismic activity, therefore, will be more useful for earthquake prediction.

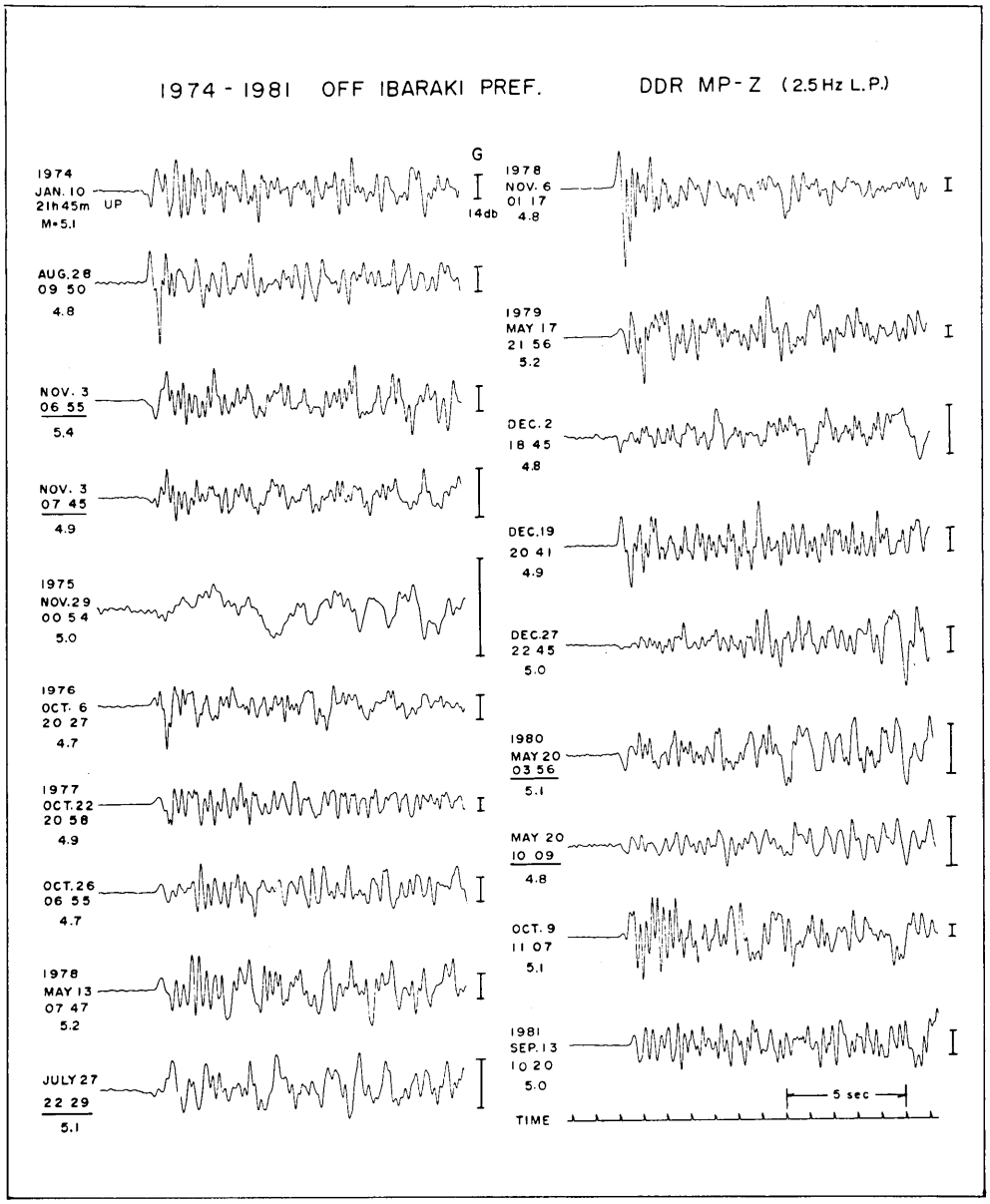

Fig. 38. Seismograms obtained during the period from 1974 to 1981 in the Off Ibaraki Prefecture region. Numerals to the left show date, arrival time and magnitude, respectively. G shows the relative differences of magnification.

4. Conclusion

In order to demonstrate discontinuities of the Earth's interior, seismic phases are investigated, and in a later section, seismogram behavior relating to earthquake occurrence is presented using data from DDR and its satellite stations. The data corrected during the period between 1968 and 1984 were used in the present study.

Thirty-eight samples of phase including a few characteristic seismograms were collected through the local and tele-seismic events. Among these phases, some of them are already well known, however, there are still some new phases included, especially as shown in Fig. 13, the X phase of 80 s after the P wave onset, which was obtained from Marianas deep events is thought to be a new phase. It is interesting to note that the time between P and X phase differs by regions (see Fig. 14). Moreover, a clear *PKiKP* (Fig. 30) is another interesting phase of the study of CMB.

Waveform features shown after Fig. 31 are another important item relating to the rupture process of large earthquakes, foreshocks, aftershocks and earthquake swarms.

Although our interpretation of each sample is somewhat uncertain, a detailed investigation of each set gives new information on the discontinuity of the Earth's interior and is also useful for obtaining a better understanding of earthquake phenomena.

Acknowledgments

The author was employed at Earthquake Research Institute (ERI), the University of Tokyo, and retired in 1988. To commemorate his retirement, a collection of seismograms called "Characteristic Seismograms" was published in 1988.

I have received many letters of thanks from domestic and oversea seismologists for this seismogram collection. The author wishes to express his thanks to them.

After retiring from ERI, the author re-examined the seismograms which were not sufficiently examined during his period at ERI, and the result is the 2nd seismogram collection.

The author wishes to express his thanks to Prof. Y. Fukao, Director of Earthquake Research Institute and to Prof. M. Mizoue for permission to use the seismograms. Copies of original seismograms were made at Earthquake Observation Center and the Library of ERI, and data of ISC were obtained at DDR and JMA. Gratitude is expressed to their staff.

Prof. Y. Morita gave me the data to obtain the deepest point, which were very useful for the interpretation of seismic phase.

Finally, the helpful comments by anonymous reviewers are greatly appreciated.

References

BARLEY, B.J., J.A. HADSON and A. DOUGLAS, 1982, *S* to *P* scattering at the 650 km discontinuity, *Geophys. J. R. Astr. Soc.*, **69**, 159–172.

BOCK, G. and J. HA, 1984, Short-period *S*–*P* conversion in the mantle at a depth near 700 km, *Geophys. J. R. Astr. Soc.*, **77**, 593–615.

BOLT, B.A., 1964, The velocity of seismic waves near the earth center, *Bull. Seismol. Soc. Am.*, **54**, 191–208.

FLINN, E.A. and E.R. ENGDAHL, 1965, A proposed basis for geographical and seismic regionalization, *Review of Geophysics*, **3**, 123–149.

FUKAO, Y., K. KANJO and S. HORI,1988, Seismic reflecter near the leading edge of a subducting slab, *Programme Abs., Seism. Soc. Japan*, 1988, No. 2 82 (in Japanese).

HADDON R.A.W., 1982, Evidence for inhomogeneities near the core–mantle boundary, *Phil. Trans. R. Soc. Lond. A*, **306**, 61–70.

IIDAKA, T., I. NAKAMURA and M. MIZOUE, 1989, The upper boundary of the Pacific plate beneath the Kanto region estimated from *P S* converted waves, *Bull. Earthq. Res. Inst., Univ. Tokyo*, **64**, 37–50 (in Japanese).

ISHIDA, M., 1992, Geometry and relative motion of the Philippine Sea plate and Pacific plate beneath the Kanto-Tokai District, Japan, *J. Geophys. Res.*, **97**, 489–513.

J Array Group, 1994, *J Array Seismograms*, Editor Y. MORITA, pp. 140 (in Japanese).

JEFFREYS, H. and K.E. BULLEN, 1967, *Seismological Tables*, British Association for Advancement of Seiences, London, pp. 50.

KATSUMATA, M., T. YOKOTA and S. KASHIWABARA, 1983, *S*–*P* converted waves reflected at the lower boundary of plate, *Programme Abs., Seism. Soc. Japan*, 1983, No. 1 65 (in Japanese).

KAWAKATSU, H. and F. NIU, 1994, Seismic evidence for a 920 km discontinuity in the mantle, *Nature*, **371**, 301–305.

KING, D.W., R.A.W. HADDON and J.R. CLEARLY, 1973, Evidence for seismic wave scattering in the D" layer, *Earth Planet. Sci. Lett.*, **20**, 353–356.

MATSU'URA, R.S., I. KARAKAMA and K. TSUMURA, 1988, *List of Earthquakes in the Kanto Area and its Vicinity*, Earthq. Res. Inst., Univ. Tokyo, Japan (in Japanese).

MATSUZAWA, T., 1989, Seismic-wave velocity structure of the subducting plate boundary estimated from later phases, *Zisin*, **42**, 526–536 (in Japanese).

OBARA, K., 1989, Regional extent of the *S* wave reflector beneath the Kanto District, Japan, *Geophys. Res. Lett.*, **16**, 839–842.

OBARA, K.,1996, Reflective zone for *S* wave around the subducting slab surface, *Programme Abs., Seism. Soc. Japan*, 1996, No. 2 C 33 (in Japanese).

TSUJIURA, M., 1977, Spectral features of foreshocks, *Bull. Earthq. Res. Inst., Univ. Tokyo*, **52**, 357–371.

TSUJIURA, M., 1978, Spectral analysis of seismic waves for a sequence of fore-

shocks, main shock and aftershocks : the Izu-Oshima-kinkai earthquake of 1978, *Bull. Earthq. Res. Inst., Univ. Tokyo,* **53**, 741-759 (in Japanese).

TSUJIURA, M., 1979, Mechanism of the earthquake swarm activity in the Kawanazaki-oki, Izu Peninsula, as inferred from the analysis of seismic waveforms, *Bull. Earthq. Res. Inst., Univ. Tokyo*, **54**, 441-462.

TSUJIURA, M., 1983 a, Waveform and spectral features of earthquake swarms and foreshocks —in special reference to earthquake prediction— *Bull. Earthq. Res. Inst., Univ. Tokyo,* **58**, 65-134.

TSUJIURA, M., 1983 b, Characteristic frequencies for earthquake families and their tectonic implications : Evidence from earthquake swarms in the Kanto District, Japan, *Pure Appl. Geophys.*, **121**, 573-600.

TSUJIURA, M., 1988, Characteristic Seismograms, *Bull. Earthq. Res. Inst., Univ. Tokyo, Suppl.* **5**, pp. 212.

UMEDA, Y., 1990, High-amplitude seismic waves radiated from the bright spot of an earthquake, *Tectonophysics*, **175**, 81-92.

WIELANDT, E. and G. STRECKEISEN, 1982, The Leaf-Spring seismometer : design and performance, *Bull. Seismol. Soc. Am.*, **72**, 2349-2367.

(Received March 21, 1997)
(Accepted November 13, 1997)

地震記象集

—第二輯—

辻浦　賢

一般に，ある観測所で記録される地震記象は，発震機構，震源の深さ，伝播経路等の影響を受け，又プレートの存在，地殻，マントル，マントルーコアー境界等の不均質のため多様な気象形態を示す．

先に，堂平観測所の広帯域地震計の磁気テープ記録を用い，近地地震から遠地地震に至る特徴ある波形を集め“Characteristic Seismograms”として100例の記象集を出版した（TSUJIURA, 1988）．

今回，更に記象集の充実を計るため，堂平観測所並びにその衛星観測所の短周期地震計で記録した15年余りの記録を用い，特に，「位相」を中心に“Characteristic Seismograms”第二輯の編集を試みた．今回集めた記録の中には，地球の不均質に起因する数々の位相が見出され，中には今回初めてみる位相も含まれる．更に記象集の特徴を高めるため，短周期からみた大地震の特徴，群発地震，或いは前震のもつ波形並びにスペクトル的特徴をも加え，合計38枚の図として編集し，簡単な解説をも加えた．

本資料は，最近展開されつつある新型の地震計の記録と相まって，教材の補足として，又新しい研究対象の1因ともなれば誠に幸である．

地震記象は局地的な構造の影響，ストレスの集中度によっても変化する．更に資料の蓄積をまって，より充実した記象集の完成を希望する次第である．